

# Multimodality and multi-parametric imaging in abdominal oncology

Citation for published version (APA):

Min, L. A. (2022). *Multimodality and multi-parametric imaging in abdominal oncology: current and future strategies to harnessing the complementary value of PET/CT and MRI*. [Doctoral Thesis, Maastricht University]. Ipskamp Drukkers B.V., Enschede. <https://doi.org/10.26481/dis.20220607lm>

## Document status and date:

Published: 01/01/2022

## DOI:

[10.26481/dis.20220607lm](https://doi.org/10.26481/dis.20220607lm)

## Document Version:

Publisher's PDF, also known as Version of record

## Please check the document version of this publication:

- A submitted manuscript is the version of the article upon submission and before peer-review. There can be important differences between the submitted version and the official published version of record. People interested in the research are advised to contact the author for the final version of the publication, or visit the DOI to the publisher's website.
- The final author version and the galley proof are versions of the publication after peer review.
- The final published version features the final layout of the paper including the volume, issue and page numbers.

[Link to publication](#)

## General rights

Copyright and moral rights for the publications made accessible in the public portal are retained by the authors and/or other copyright owners and it is a condition of accessing publications that users recognise and abide by the legal requirements associated with these rights.

- Users may download and print one copy of any publication from the public portal for the purpose of private study or research.
- You may not further distribute the material or use it for any profit-making activity or commercial gain
- You may freely distribute the URL identifying the publication in the public portal.

If the publication is distributed under the terms of Article 25fa of the Dutch Copyright Act, indicated by the "Taverne" license above, please follow below link for the End User Agreement:

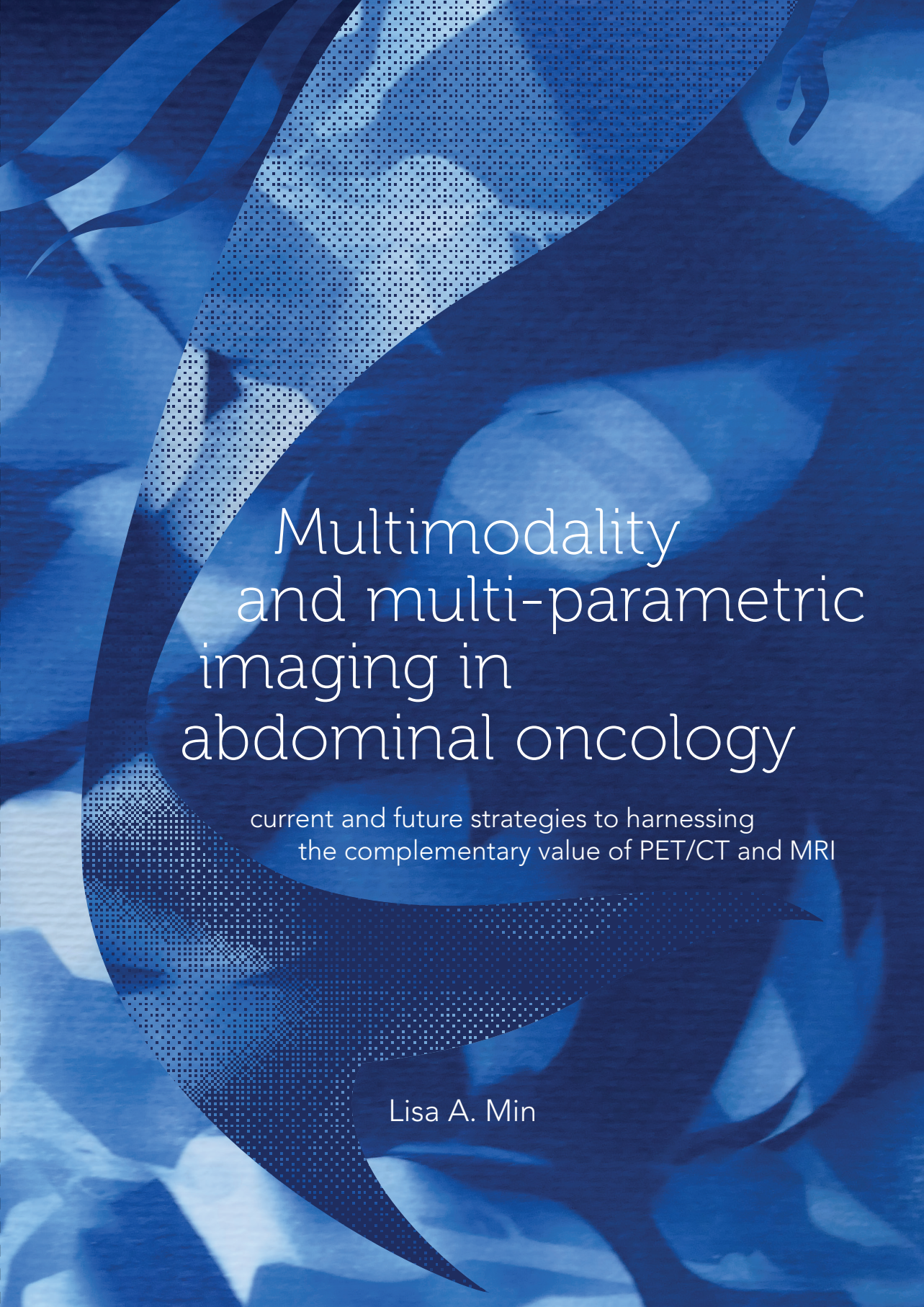
[www.umlib.nl/taverne-license](http://www.umlib.nl/taverne-license)

## Take down policy

If you believe that this document breaches copyright please contact us at:

[repository@maastrichtuniversity.nl](mailto:repository@maastrichtuniversity.nl)

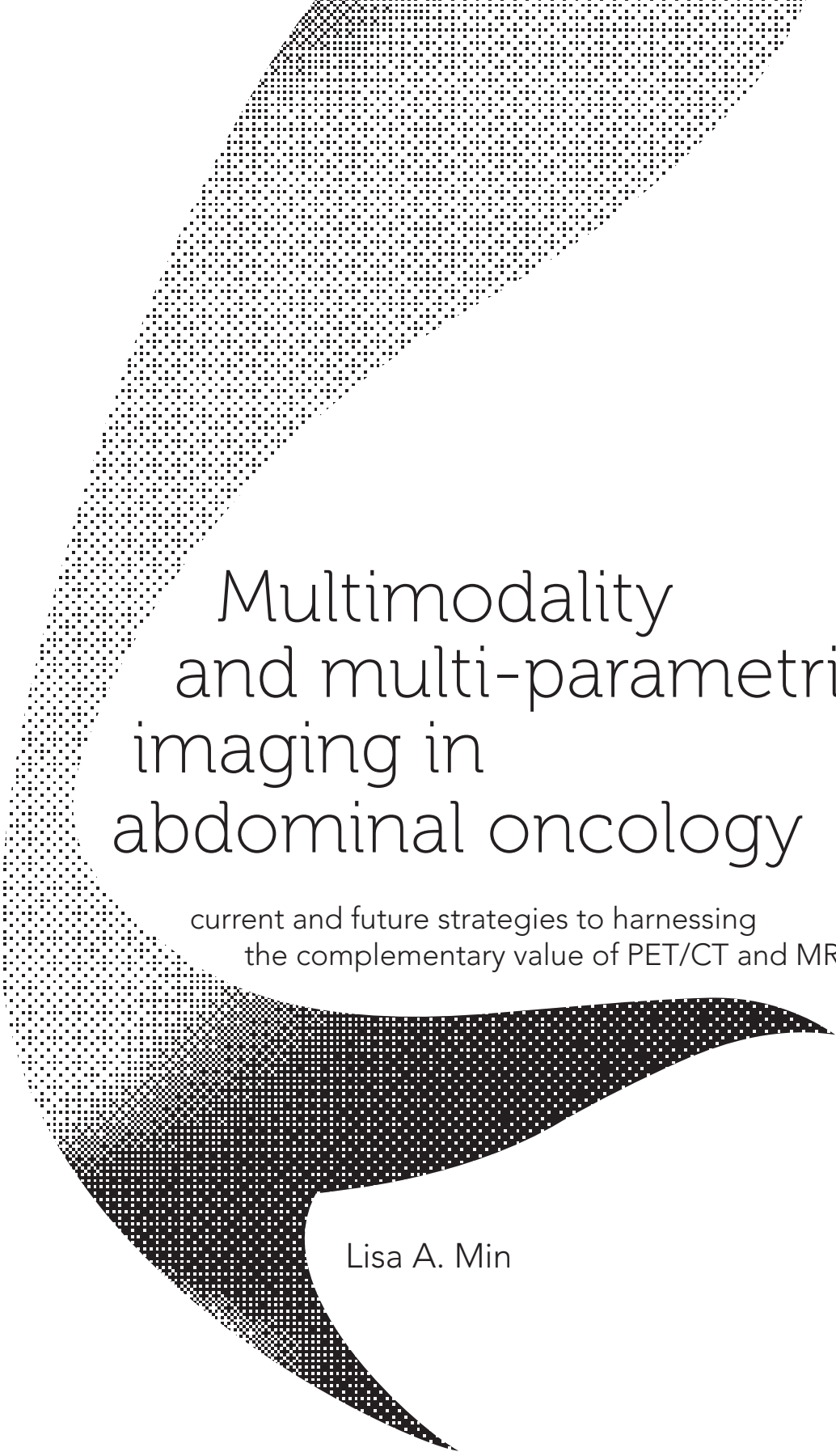
providing details and we will investigate your claim.



# Multimodality and multi-parametric imaging in abdominal oncology

current and future strategies to harnessing  
the complementary value of PET/CT and MRI

Lisa A. Min



# Multimodality and multi-parametric imaging in abdominal oncology

current and future strategies to harnessing  
the complementary value of PET/CT and MRI

Lisa A. Min

ISBN: 978-94-6421-729-2

Cover design, Artwork (cyanotype) & lay-out: Esther Beekman ([www.estherontwerpt.nl](http://www.estherontwerpt.nl))

Printed by: Ipskamp printing, Enschede

Publication of this thesis was financially supported by Maastricht University.

©2022 Lisa Anna Min

All rights reserved. No parts of this publication may be reproduced, stored, or transmitted in any form or by any means without permission of the author. The copyrights of published articles have been transferred to the respective journals.



# Multimodality and multi-parametric imaging in abdominal oncology

current and future strategies to harnessing  
the complementary value of PET/CT and MRI

PROEFSCHRIFT

ter verkrijging van de graad van doctor aan de Universiteit Maastricht,  
op gezag van de Rector Magnificus, Prof. dr. Pamela Habibović  
volgens het besluit van het College van Decanen,  
in het openbaar te verdedigen  
op dinsdag 7 juni 2022 om 13:00 uur

door

Lisa Anna Min

**Promotor**

Prof. dr. R.G.H. Beets-Tan (Universiteit Maastricht / Antoni van Leeuwenhoek, Amsterdam)

**Co-promotor**

Dr. D.M.J. Lambregts (Antoni van Leeuwenhoek, Amsterdam)

**Beoordelingscommissie**

Prof. dr. Roy F.P.M. Kruitwagen (voorzitter)

Prof. dr. Lioo-Fee de Geus-Oei (LUMC)

Prof. dr. Corrie Marijnen (LUMC)

Prof. dr. Felix Mottaghy

Prof. dr. Simon G.F. Robben



The background is a deep blue with a complex, layered design. A large, white, circular graphic is centered, featuring a halftone dot pattern. The overall aesthetic is modern and professional.

# Contents

Chapter 1	General Introduction, aim and outline of the thesis	9
Chapter 2	A decade of multimodality PET and MR imaging in abdominal oncology <i>Lisa A. Min et al. BJR. 2021; 94:20201351. doi: 10.1259/bjr.20201351</i>	19
Chapter 3	Integrated versus separate reading of F-18 FDG-PET/CT and MRI for abdominal malignancies – effect on staging outcomes and diagnostic confidence <i>Lisa A. Min et al. Eur Radiol. 2019;29(12):6900-6910. doi: 10.1007/s00330-019-06253-1</i>	55
Chapter 4	Value of combined multiparametric MRI and FDG-PET/CT to identify well-responding rectal cancer patients before the start of neoadjuvant chemoradiation <i>Niels W. Schurink, Lisa A. Min et al. Eur Radiol. 2020;30(5):2945-2954. doi: 10.1007/s00330-019-06638-2 (shared first authorship)</i>	83
Chapter 5	Pre-treatment prediction of early response to chemoradiotherapy by quantitative analysis of baseline staging FDG-PET/CT and MRI in locally advanced cervical cancer <i>Lisa A. Min et al. Acta Radiol. 2021 Jul;62(7):940-948. doi: 10.1177/0284185120943046</i>	107
Chapter 6	Pre-treatment FDG-PET, clinical and high-risk human papillomavirus biomarkers in anal cancer: which can best predict locoregional treatment failure after chemoradiotherapy? <i>Lisa A. Min et al. In submission</i>	125
Chapter 7	General Discussion	147
Chapter 8	Impact Paragraph	160
	Summary	164
	Samenvatting	166
	List of publications	170
	Dankwoord	172
	Curriculum Vitae	176



The background is a vibrant blue with a complex, organic pattern. It features several overlapping, rounded shapes that resemble stylized leaves or petals. A prominent feature is a large, curved band that contains a fine halftone dot pattern, creating a textured effect. The overall composition is dynamic and modern.

# Chapter 1

GENERAL INTRODUCTION,  
AIM AND OUTLINE OF  
THE THESIS

# GENERAL INTRODUCTION, AIM AND OUTLINE OF THE THESIS

Cross-sectional medical imaging is an integral part of the staging process for virtually all abdominal malignancies and plays a crucial role in disease management and treatment decision making of oncologic patients. In many tumour types, computed tomography (CT) is used as a first line staging modality, since it is relatively widely accessible and allows fast acquisition of a large field of view. On account of its superior soft-tissue contrast, magnetic resonance imaging (MRI) is mainly used for detailed local tumour staging, for example in pelvic malignancies such as rectal, anal and gynaecological cancers. Recent advances in MRI technology, including the introduction of diffusion-weighted imaging (DWI) for improved lesion detection<sup>1-3</sup> and use of liver-specific (hepatobiliary) contrast agents for detection and characterization of even very small liver lesions,<sup>4</sup> have further contributed to the diagnostic value of MRI. Positron Emission Tomography (PET), most commonly acquired using fluorodeoxyglucose (FDG) as a tracer and combined with a CT-scan for anatomical correlation and attenuation correction (FDG-PET/CT), can complement staging in several ways. FDG-PET/CT is a form of functional medical imaging based on the accumulation of a labelled glucose analogue within metabolically hyper-active tissues such as malignant tumour. The main strong suits of PET/CT are its high sensitivity and lesion-to-background ratio to detect lesions, combined with a large (whole body) coverage. Because of these advantages, PET/CT has acquired a place in the routine staging workup of several primary abdominal cancer types, including anal and gynaecological cancers, primarily aimed at the detection of lymph node and distant metastasis.<sup>5-8</sup> In other tumour types, PET/CT is employed as a problem solver in specific situations, for example for detection of recurrent or extrahepatic disease in patients with colorectal cancer.<sup>9</sup>

To date, oncological imaging is increasingly becoming a multimodality approach, where different cross-sectional imaging techniques – and their respective strengths – are combined in one diagnostic workup to offer a more comprehensive diagnostic evaluation of the patient. Within the spectrum of multimodality imaging, a special role is reserved for hybrid acquisition techniques that combine different imaging modalities within one examination performed on a single machine. Hybrid PET/CT, which combines PET with either a non-enhanced (low dose) or fully diagnostic contrast-enhanced CT, was first introduced in clinics in 2001 and is now part of the standard array of clinically available imaging techniques in many developed countries. More recently, hybrid PET/MRI machines were introduced, and have become available for clinical

use in 2011. Since then, many reports have been published on the first experiences with this new modality, for staging as well as for more experimental applications such as (semi-)quantitative analysis and prognostic modelling. In contrast to PET/CT, to date hybrid PET/MRI remains mostly employed within the research domain, and its potential advantages for daily clinical practice have not yet been fully crystallized.

### **Multimodality imaging in clinical practice**

In various clinical guidelines, multimodality combinations of different imaging techniques are now routinely advised for the diagnostic workup of oncology patients.<sup>5,6,8,10</sup> In common clinical practice, CT and MRI examinations are typically acquired at the Radiology department and reported by radiologists, while PET (or PET/CT) imaging is within the domain of Nuclear Medicine. In case of hybrid PET/CT acquisition – especially when PET is combined with a fully diagnostic contrast-enhanced CT – integrated reporting by a team consisting of a radiologist and nuclear medicine physician has become customary for an increasing number of centers worldwide. In some practices, integrated reporting is even done by dedicated “hybrid” diagnosticians experienced in both radiological and nuclear imaging. In the Netherlands, the radiology and nuclear medicine residency training programs have been fused into one curriculum as of 2015, which is currently rendering the first officially certified ‘nuclear radiologists’. These developments will likely boost integrated assessment and reporting of multimodality imaging by dually-trained specialists and may eventually lead to the further integration of Radiology and Nuclear Medicine. Integrated reporting can have several benefits, such as improved consistency in reporting, avoidance of discrepant findings and provide a single comprehensive oncologic staging report to serve as a solid basis for multidisciplinary team discussions. For the multimodality combination of PET(/CT) and MRI, integrated diagnostic assessment and reporting is much less common practice, which is probably largely related to the limited clinical availability of hybrid PET/MRI systems at this time. Though evidence is limited, in research settings it has been suggested that integrated assessment of PET(/CT) combined with MRI – even when acquired separately – can result in improved early detection of locally recurrent cervical cancer after curative-intent chemoradiotherapy<sup>11</sup> and improved assessment of tumour stage and residual pelvic lymph node metastases after preoperative chemoradiotherapy in rectal cancer.<sup>12-14</sup> Also, there have been some reports demonstrating that in patients with metastatic disease who are considered for curative (local) treatment, combined use of PET/CT and MRI can impact treatment planning by improving the overall detection of disease localisations.<sup>15-18</sup> In daily clinical practice PET and MRI examinations are rarely reported together. As part of this thesis,

we therefore investigated the potential impact of integrated assessment and reporting of PET/CT and MRI in a clinical setting, focusing on patients presenting with abdominal malignancies.

### **Quantitative multimodality imaging and imaging biomarkers**

In addition to visual (qualitative) interpretation of medical imaging, there has in recent years been a growing interest in more quantitative approaches to image assessment. Some of the more basic and widely used examples of quantitative imaging evaluation include tumour size or volume measurements that can be derived directly from images using simple annotation tools. In addition, the distribution of greyscale values within an image can be used to calculate parameters reflecting the underlying tissue architecture and heterogeneity, a process called image "texture analysis". Finally, functional imaging techniques including PET, DWI, and dynamic contrast enhanced imaging can render various (semi-)quantitative parameters describing biological properties like cellularity, metabolism, perfusion or receptor expression levels of a tissue or tumour. These size, texture and functional parameters may serve as 'imaging biomarkers' that can be linked to other tumour properties (e.g. histology, immunohistochemistry) or used to predict clinical outcomes such as treatment response or survival. A number of studies have indicated a potential prognostic value for imaging biomarkers derived from PET/CT or MRI in different abdominal tumour types, for example to predict treatment response in cervical cancer, and survival in esophageal or anal cancer.<sup>19-23</sup> Evidence on the value of combining imaging biomarkers derived from different imaging techniques in a multimodality study setting is, however, limited to a few reports.<sup>24-27</sup> For example, a combination of DWI and PET parameters acquired during and after neo-adjuvant chemoradiotherapy, together with histology, has been found to be predictive for complete pathological response in esophageal cancer.<sup>24</sup> In cervical cancer, it has been suggested that locoregional control after definitive chemoradiotherapy may be predicted by a combination of texture parameters derived from PET and MRI.<sup>27</sup> For patients with rectal cancer, a small study showed potential for the combination of pre-therapy PET and MRI derived parameters as predictors of response to neoadjuvant treatment.<sup>28</sup> Little is known about how parameters from PET and MRI should best be combined with other types of parameters, such as clinical disease stage, laboratory findings and histopathology, to build the best possible clinical prediction models. This is an interesting research field for further exploration, as it may be expected that combining the information from different imaging techniques and clinical modalities will render more valuable information than any single modality on its own. Hence, the second part of this thesis focuses on exploring the complementary value of quantitative parameters from PET and MRI combined with various clinical



parameters as pre-therapy predictors of treatment response in three different types of primary pelvic malignancies.

### **Aim of this thesis**

The overall aim of this thesis is to investigate the current status and possible future applications of multimodality imaging in abdominal oncology, with a specific focus on the combination of PET and MRI, both from a visual (qualitative) and quantitative perspective.

### **The main study questions addressed in this thesis are:**

1. How has the role of multimodality PET/CT + MR imaging in abdominal oncological imaging evolved during the last decade?
2. What is the value of integrated PET/CT + MRI assessment for clinical staging of abdominal malignancies?
3. Can (semi-)quantitative assessment of PET/CT and MRI contribute to the prediction of treatment outcomes in patients with primary abdominal malignancies?

### **Thesis Outline**

**Chapter 2** reviews the evolution of multimodality imaging in abdominal oncology during the last decade, from the perspective of our own European comprehensive cancer center, as well as the published scientific literature.

In **Chapter 3** the effects of integrated assessment of FDG-PET/CT and MRI on clinical diagnostic staging outcomes and staging confidence in abdominal malignancies are investigated.

**Chapters 4 and 5** focus on quantitative imaging and explore the value of combining imaging biomarkers derived from pre-treatment FDG-PET/CT, T2-weighted and diffusion-weighted MRI with clinical parameters for prediction of treatment response to chemoradiotherapy in locally-advanced rectal cancer and cervical cancer patients, respectively.

**Chapter 6** studies the individual and complementary value of pre-treatment FDG-PET/CT, high-risk human papillomavirus (HPV) status and clinical biomarkers as predictors of locoregional treatment failure in anal cancer.

## REFERENCES

1. Engbersen MP, van' t Sant I, Lok C, Lambregts DMJ, Sonke GS, Beets-Tan RGH, et al. MRI with diffusion-weighted imaging to predict feasibility of complete cytoreduction with the peritoneal cancer index (PCI) in advanced stage ovarian cancer patients. *Eur J Radiol.* 2019;114:146–51. doi:10.1016/j.ejrad.2019.03.007
2. Lambregts DMJ, Lahaye MJ, Heijnen LA, Martens MH, Maas M, Beets GL, et al. MRI and diffusion-weighted MRI to diagnose a local tumour regrowth during long-term follow-up of rectal cancer patients treated with organ preservation after chemoradiotherapy. *Eur Radiol.* 2016;26(7):2118–25. doi:10.1007/s00330-015-4062-z
3. Exner M, Kühn A, Stumpp P, Höckel M, Horn L-C, Kahn T, et al. Value of diffusion-weighted MRI in diagnosis of uterine cervical cancer: A prospective study evaluating the benefits of DWI compared to conventional MR sequences in a 3T environment. *Acta radiol.* 2016;57(7):869–77. doi:10.1177/0284185115602146
4. Granata V, Fusco R, de Lutio di Castelguidone E, Avallone A, Palaia R, Delrio P, et al. Diagnostic performance of gadoxetic acid-enhanced liver MRI versus multidetector CT in the assessment of colorectal liver metastases compared to hepatic resection. *BMC Gastroenterol.* 2019;19(1):129. doi:10.1186/s12876-019-1036-7
5. Glynne-Jones R, Nilsson PJ, Aschele C, Goh V, Peiffert D, Cervantes A, et al. Anal cancer: ESMO-ESSO-ESTRO clinical practice guidelines for diagnosis, treatment and follow-up. *Radiother Oncol.* 2014;111(3):330–9. doi:10.1016/j.radonc.2014.04.013
6. Cibula D, Pötter R, Planchamp F, Avall-Lundqvist E, Fischerova D, Haie Meder C, et al. The European Society of Gynaecological Oncology/European Society for Radiotherapy and Oncology/European Society of Pathology Guidelines for the Management of Patients With Cervical Cancer. *Int J Gynecol Cancer.* 2018;28(4):641–55. doi: 10.1016/j.radonc.2018.03.003
7. Concin N, Matias-Guiu X, Vergote I, Cibula D, Mirza MR, Marnitz S, et al. ESGO/ESTRO/ESP guidelines for the management of patients with endometrial carcinoma. *Int J Gynecol Cancer.* 2021;31(1):12–39. doi:10.1136/ijgc-2020-002230
8. Lordick F, Mariette C, Haustermans K, Obermannová R, Arnold D, on behalf of the ESMO Guidelines Committee. Oesophageal cancer: ESMO clinical practice guidelines for diagnosis, treatment and follow-up. *Ann Oncol.* 2016;27:v50–7. doi:10.1093/annonc/mdw329

9. Van Cutsem E, Cervantes A, Nordlinger B, Arnold D, on behalf of the ESMO Guidelines Working Group. Metastatic colorectal cancer: ESMO clinical practice guidelines for diagnosis, treatment and follow-up. *Ann Oncol.* 2014;25:iii1–9. doi:10.1093/annonc/mdu260
10. Öberg K, Knigge U, Kwekkeboom D, Perren A. Neuroendocrine gastro-entero-pancreatic tumors: ESMO clinical practice guidelines for diagnosis, treatment and follow-up. *Ann Oncol.* 2012;23(SUPPL. 7):vii124–30. doi:10.1093/annonc/mds295
11. Kalash R, Glaser SM, Rangaswamy B, Horne ZD, Kim H, Houser C, et al. Use of Functional Magnetic Resonance Imaging in Cervical Cancer Patients With Incomplete Response on Positron Emission Tomography/Computed Tomography After Image-Based High-Dose-Rate Brachytherapy. *Int J Radiat Oncol Biol Phys.* 2018 Nov;102(4):1008–13. doi:10.1016/j.ijrobp.2018.01.092
12. Schneider DA, Akhurst TJ, Ngan SY, Warriar SK, Michael M, Lynch AC, et al. Relative Value of Restaging MRI, CT, and FDG-PET Scan After Preoperative Chemoradiation for Rectal Cancer. *Dis Colon Rectum.* 2016;59(3):179–86. doi:10.1097/DCR.0000000000000557
13. Cho YB, Chun HK, Kim MJ, Choi JY, Park CM, Kim BT, et al. Accuracy of MRI and 18F-FDG PET/CT for restaging after preoperative concurrent chemoradiotherapy for rectal cancer. *World J Surg.* 2009;33(12):2688–94. doi:10.1007/s00268-009-0248-3
14. Ishihara S, Kawai K, Tanaka T, Kiyomatsu T, Hata K, Nozawa H, et al. Diagnostic value of FDG-PET/CT for lateral pelvic lymph node metastasis in rectal cancer treated with preoperative chemoradiotherapy. *Tech Coloproctol.* 2018;22(5):347–54. doi:10.1007/s10151-018-1779-0
15. Wang W, Tan GHC, Chia CS, Skanthakumar T, Soo KC, Teo MCC. Are positron emission tomography-computed tomography (PET-CT) scans useful in preoperative assessment of patients with peritoneal disease before cytoreductive surgery (CRS) and hyperthermic intraperitoneal chemotherapy (HIPEC)? *Int J Hyperth.* 2018;34(5):524–31. doi:10.1080/02656736.2017.1366554
16. Viganò L, Lopci E, Costa G, Rodari M, Poretti D, Pedicini V, et al. Positron Emission Tomography-Computed Tomography for Patients with Recurrent Colorectal Liver Metastases: Impact on Restaging and Treatment Planning. *Ann Surg Oncol.* 2017;24(4):1029–36. doi:10.1245/s10434-016-5644-y
17. Georgakopoulos A, Pianou N, Kelekis N, Chatziioannou S. Impact of 18F-FDG PET/CT on therapeutic decisions in patients with colorectal cancer and liver metastases. *Clin Imaging.* 2013;37(3):536–41. doi:10.1016/j.clinimag.2012.09.011

18. Schmidt GP, Paprottka P, Jakobs TF, Hoffmann RT, Baur-Melnyk A, Haug A, et al. FDG-PET-CT and whole-body MRI for triage in patients planned for radioembolisation therapy. *Eur J Radiol.* 2012;81(3):e269-76. doi:10.1016/j.ejrad.2011.02.018
19. Staal FCR, van der Reijnd DJ, Taghavi M, Lambregts DMJ, Beets-Tan RGH, Maas M. Radiomics for the Prediction of Treatment Outcome and Survival in Patients With Colorectal Cancer: A Systematic Review. *Clin Colorectal Cancer.* 2021;20(1):52–71. doi:10.1016/j.clcc.2020.11.001
20. Leccisotti L, Manfrida S, Barone R, Ripani D, Tagliaferri L, Masiello V, et al. The prognostic role of FDG PET/CT before combined radio-chemotherapy in anal cancer patients. *Ann Nucl Med.* 2020;34(1):65–73. doi:10.1007/s12149-019-01416-y
21. Desbordes P, Ruan S, Modzelewski R, Pineau P, Vauclin S, Gouel P, et al. Predictive value of initial FDG-PET features for treatment response and survival in esophageal cancer patients treated with chemo-radiation therapy using a random forest classifier. *PLoS One.* 2017;12(3):e0173208. doi:10.1371/journal.pone.0173208
22. Mongula JE, Slangen BFM, Lambregts DMJ, Cellini F, Bakers FCH, Lutgens LCHW, et al. Consecutive magnetic resonance imaging during brachytherapy for cervical carcinoma: predictive value of volume measurements with respect to persistent disease and prognosis. *Radiat Oncol.* 2015;10(252). doi:10.1186/s13014-015-0559-5
23. Kidd EA, Siegel BA, Dehdashti F, Grigsby PW. The standardized uptake value for F-18 fluorodeoxyglucose is a sensitive predictive biomarker for cervical cancer treatment response and survival. *Cancer.* 2007;110(8):1738–44. doi:10.1002/cncr.22974
24. Borggreve AS, Goense L, Rossum PSN Van, Heethuis SE, Hillegersberg R Van, Lagendijk JJW, et al. Preoperative prediction of pathologic response to neoadjuvant chemoradiotherapy in patients with esophageal cancer using 18F-FDG PET/CT and DW-MRI: a prospective multicenter study. *Int J radiat Oncol Biol Phys.* 2021;106(5):998–1009. doi:10.1016/j.ijrobp.2019.12.038
25. Giannini V, Mazzetti S, Bertotto I, Chiarenza C, Cauda S, Delmastro E, et al. Predicting locally advanced rectal cancer response to neoadjuvant therapy with 18 F-FDG PET and MRI radiomics features. *Eur J Nucl Med Mol Imaging.* 2019;46(4):878–88. doi:10.1007/s00259-018-4250-6
26. Akkus Yildirim B, Onal C, Erbay G, Cem Guler O, Karadeli E, Reyhan M, et al. Prognostic values of ADC mean and SUV max of the primary tumour in cervical cancer patients treated with definitive chemoradiotherapy. *J Obstet Gynaecol (Lahore).* 2019;39(2):224–30. doi:10.1080/01443615.2018.1492528

27. Lucia F, Visvikis D, Desseroit M-C, Miranda O, Malhaire J-P, Robin P, et al. Prediction of outcome using pretreatment 18 F-FDG PET/CT and MRI radiomics in locally advanced cervical cancer treated with chemoradiotherapy. *Eur J Nucl Med Mol Imaging*. 2018;45(5):768–86. doi:10.1007/s00259-017-3898-7
28. Giannini V, Mazzetti S, Bertotto I, Chiarenza C, Cauda S, Delmastro E, et al. Predicting locally advanced rectal cancer response to neoadjuvant therapy with 18 F-FDG PET and MRI radiomics features. *Eur J Nucl Med Mol Imaging*. 2019;46(4):878–88. doi:10.1007/s00259-018-4250-6

1



The background is a vibrant blue with a halftone dot pattern. A dark blue, ribbon-like shape curves across the center, partially overlapping the text. The text 'Chapter 2' is centered within this dark blue area.

## Chapter 2

# A DECADE OF MULTI- MODALITY PET AND MR IMAGING IN ABDOMINAL ONCOLOGY

Lisa A. Min, Francesca Castagnoli, Wouter V. Vogel, Jisk P. Vellenga,  
Joost J.M. van Griethuysen, Max Lahaye, Monique Maas,  
Regina G.H. Beets-Tan, Doenja M.J. Lambregts

*Br J Radiol (2021) 94:20201351 doi: 10.1259/bjr.20201351*

# ABSTRACT

## **Objectives**

To investigate trends observed in a decade of published research on multimodality PET(/CT)+MR imaging in abdominal oncology, and to explore how these trends are reflected by the use of multimodality imaging performed at our institution.

## **Methods**

First, we performed a literature search (2009–2018) including all papers published on the multimodality combination of PET(/CT) and MRI in abdominal oncology. Retrieved papers were categorized according to a structured labelling system, including study design and outcome, cancer and lesion type under investigation and PET-tracer type. Results were analysed using descriptive statistics and evolutions over time were plotted graphically. Second, we performed a descriptive analysis of the numbers of MRI, PET/CT and multimodality PET/CT+MRI combinations (performed within a  $\leq 14$  days interval) performed during a similar time span at our institution.

## **Results**

Published research papers involving multimodality PET(/CT)+MRI combinations showed an impressive increase in numbers, both for retrospective combinations of PET/CT and MRI, as well as hybrid PET/MRI. Main areas of research included new PET-tracers, visual PET(/CT)+MRI assessment for staging, and (semi-)quantitative analysis of PET-parameters compared to or combined with MRI-parameters as predictive biomarkers. In line with literature, we also observed a vast increase in numbers of multimodality PET/CT+MRI imaging in our institutional data.

## **Conclusions**

The tremendous increase in published literature on multimodality imaging, reflected by our institutional data, shows the continuously growing interest in comprehensive multivariable imaging evaluations to guide oncological practice.

Advances in knowledge: The role of multimodality imaging in oncology is rapidly evolving. This paper summarizes the main applications and recent developments in multimodality imaging, with a specific focus on the combination of PET+MRI in abdominal oncology.

# INTRODUCTION

Multimodality imaging in the context of diagnostic medical imaging can be defined as “the use of a combination of imaging techniques or platforms encompassing aspects of anatomical, functional or molecular imaging methods”,<sup>1</sup> and it is often used in clinical practice as a term to describe the use of different imaging modalities to address a single medical problem. In oncology, multimodality imaging can aid in diagnosis, staging and treatment response monitoring by visualizing different tumour properties, thereby providing complementary information on both morphology and physiology. Different imaging modalities can either be combined retrospectively, after separate acquisition (with or without retrospective image registration and/or fusion), or by simultaneous acquisition (commonly referred to as “hybrid” imaging), of which PET/CT and the more recently introduced hybrid PET/MRI systems are the most familiar examples.

Advantages of “hybrid” acquisition include – apart from patient convenience – improved image co-registration and better opportunities to study and correlate dynamic disease processes in vivo, such as perfusion and tracer distribution, and tumour response to pharmacological and interventional treatments.<sup>2,3</sup> PET/CT has already proven to be a valuable tool in the staging of a wide range of malignancies, and its use is recommended in many oncological guidelines.<sup>4–9</sup> Owing to the growing array of tumour-targeted tracers, including prostate cancer radiotracers and tracers for somatostatin receptor imaging in neuroendocrine tumours, its clinical role keeps evolving.<sup>10–13</sup>

Already before the development of hybrid imaging systems, it was recognized that a multimodality combination of PET with anatomical imaging has many potential advantages. Combining PET with MRI offers the specific benefits of the superior soft-tissue contrast and image resolution of MRI, allowing detailed anatomical correlation and local staging.<sup>14</sup> In addition, it allows multiparametric evaluations by combining the metabolic information from PET with functional MR sequences such as diffusion-weighted imaging (DWI) and dynamic contrast-enhanced (DCE) MRI, to allow simultaneous assessment of biological tumour properties such as metabolism, cellularity and perfusion. From a safety perspective, the lack of radiation in MRI is an additional property that makes MRI an attractive modality for repeated longitudinal follow-up and for paediatric imaging. The arrival of the first hybrid PET/MRI systems has further boosted the field of multimodality PET+MRI imaging and research.

# 2

With this paper, we set out to investigate trends in published research on multimodality imaging during the time span of a decade, with a specific focus on the combination of PET(/CT) and MRI in abdominal oncology. Second, we explored how trends observed in literature are reflected by the use of multimodality imaging at our own comprehensive European Cancer Centre.

## METHODS AND MATERIALS

### Literature search

A search strategy was constructed in PubMed (NCBI) to retrieve all English-language original research publications (2009–2018) combining PET/CT and MRI in a multimodality study setting, either acquired as stand-alone modalities (with or without retrospective image registration and/or fusion), or using bed system-combined or fully hybrid PET/MRI systems. The search was restricted to studies focusing on abdominal oncology. Main search terms included “PET” and “MRI” and “abdominal malignancy” as well as terms referring to various abdominal regions, individual organs and specific tumour types (or their respective synonyms/MeSH-terms) in the title and/or abstract. Animal studies were excluded. Further details of the search strategy are provided in **Supplementary Table 1**. All retrieved articles were reviewed by a single reviewer (LAM or FC), based on title and abstract, to assess eligibility for inclusion. In case of doubt, the other reader was consulted to reach consensus. Each included paper was labelled (using the Rayyan QCRI online application)<sup>15</sup> according to the following descriptors:

- (1) Study design: prospective/retrospective, single-centre/ multicentre, combination/ correlation/comparison of PET and MRI; (note: combination = assessing complementary value of PET combined with MRI to predict a clinical outcome; correlation = assessing correlation between PET and MRI parameters (e.g. SUV and ADC), comparison = comparing diagnostic performance of PET to that of MRI);
- (2) Method of multimodality imaging: retrospective combination of stand-alone PET/CT and MRI with or without retrospective image fusion, bed system-combined PET/MRI, hybrid PET/MRI;
- (3) Type of PET-tracer(s);
- (4) Method of image evaluation: visual/qualitative, quantitative, other;
- (5) Study aim: lesion detection, correlation of PET and MRI parameters, response assessment, technical (e.g. sequence development and testing), prognostic (e.g. survival prediction), or other;

- (6) Cancer type;
- (7) Lesion type: primary tumour, nodes, metastases, mixed

### Analysis of literature data

Based on the assigned labels, annual numbers of research papers in each category and subcategory were determined and relative proportions (%) and cumulative effects over time were calculated using descriptive analyses in Microsoft Excel (Microsoft Office 2019, version 16.16.22, Redmond, WA, USA). Trends over time were plotted using Microsoft Excel and GraphPad Prism (GraphPad Software, version 7.03, San Diego, CA, USA).

### Institutional data

Our institute's internal picture archiving and communication system (PACS; Carestream Vue, version 11.4.1.1102, Carestream Health, Rochester, New York, USA) was searched for all MRI and PET/CT studies performed from 2008 to 2017 as part of routine clinical care. Patients who underwent a multimodality combination of both PET/CT and MRI within the same diagnostic workup (arbitrarily defined as studies performed within a time-interval of  $\leq 14$  days) were documented separately. For each individual study, the exam date, modality, PET-tracer used (if applicable), study description (i.e. body part and protocol) and pseudonymized patient identification number were stored. Studies were excluded if they were imported from another hospital or performed solely for protocol optimization (e.g. phantom studies, calibration series) or interventional guidance (e.g. MR-guided biopsy). Annual numbers of MRI, PET/CT and multimodality combinations of MRI+PET/CT were determined, and the relative increase over time compared to the baseline year was calculated and plotted in GraphPad.

## RESULTS

### Main study characteristics

The literature selection process is illustrated schematically in the PRISMA flowchart in **Figure 1**. A total of 443 original research papers combining PET/CT and MRI in a multimodality study setting for abdominal malignancies were retrieved, including a total number of 60,725 patients. The PET-tracer used was 18F-labeled glucose analogue fluorodeoxyglucose ([18F] FDG, or "FDG") in 294/443 studies, 149 studies used other non-FDG tracers (a combination of both FDG and non-FDG tracers was used in 14 studies). Trends over time are shown in **Figure 2**.



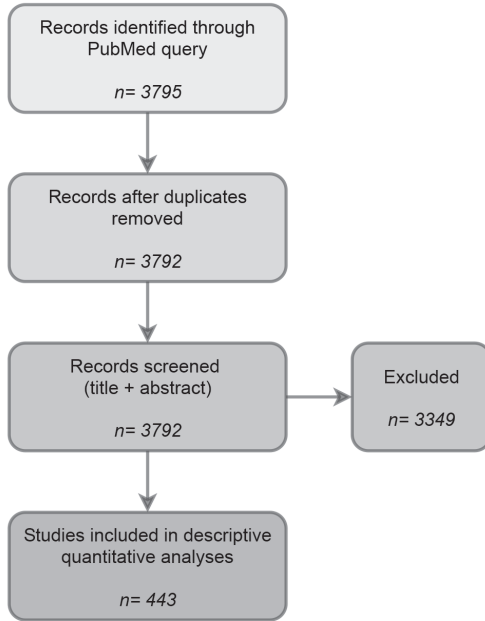


Figure 1. Literature selection process.

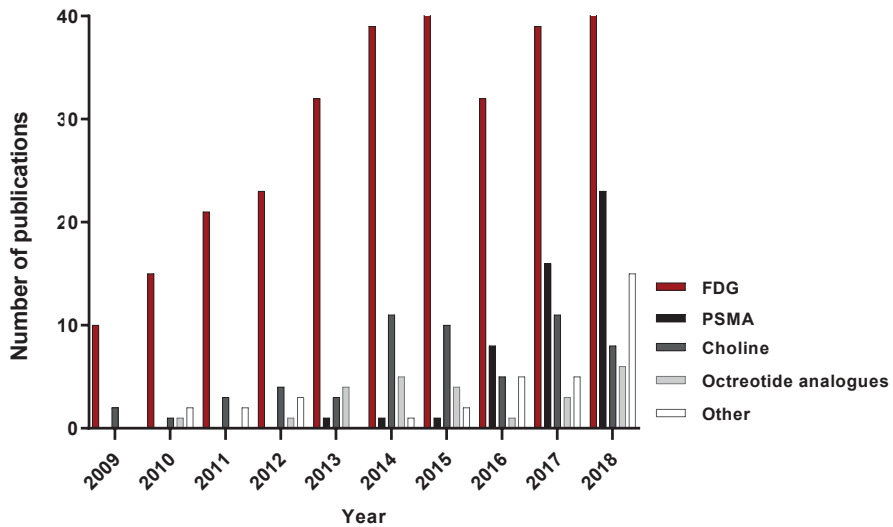


Figure 2. Evolution in the annual numbers of PET studies in published multimodality imaging research, specified for the PET-tracer(s) used. FDG: 18F-fluorodeoxyglucose; PSMA: prostate-specific membrane antigen; octreotide analogues: 68Ga-labelled somatostatin receptor ligands; 'Other tracers' includes tracers used in a single or few of the retrieved studies (e.g. fluciclovine, fluorothymidine (18F-FLT), fluoromisonidazole (18F-FMISO), dihydroxyphenylalanine (18F-DOPA)).

**Table 1.** summarizes the detailed study characteristics for the main group of 294 FDG-PET/(CT)+MRI papers. The majority of these papers (211/294, 72%) retrospectively combined or compared FDG-PET/CT and MRI that were acquired separately, the remaining studies (28%) concerned combined PET/MRI acquisitions using either hybrid or bed system-combined PET/ MRI scanners. Visual image assessment was the most commonly employed method of image evaluation (144/294, 49%), followed by papers focusing on quantitative imaging evaluation (96/294, 33%). The most frequently studied tumour types were gynaecological and colorectal cancer. The largest subgroups of papers focused on assessing the complementary value of PET/(CT) combined with MRI (127/294, 43%) or on comparing the diagnostic (or predictive) value of PET/CT to that of MRI (113/294, 38%).

#### Evolution of PET-tracers used in multimodality imaging studies

As shown in **Figure 2**, FDG was the most frequently reported PET tracer (66%). Other reported tracers included mainly those used for prostate cancer imaging, that is, choline tracers (11C- or 18F-labelled phospholipid precursor)<sup>16,17</sup> or prostate-specific membrane antigen (PSMA)-based tracers (68Ga- or 18F-labelled small-molecule ligands),<sup>18-20</sup> and octreotide-based tracers (68Ga-labelled octreotide analogues targeted at the somatostatin-receptor, overexpressed in many neuro-endocrine tumours).<sup>21-25</sup> After some incidental reports (<10/year) in the first half of the study period, reports on the use of these tumour-specific tracers showed a marked increase during the second half of the study period, with non-FDG tracers constituting a majority (55%) of the total number of multimodality imaging research reports in 2018, the final study year.

#### Evolutions in stand-alone versus hybrid PET/MRI studies

**Figure 3** compares the evolution of research focusing on retrospective combinations of FDG-PET/CT and MRI, versus prospectively combined FDG-PET/MRI acquisition studies. Of the 211 studies that retrospectively combined FDG-PET/CT and MRI, only a small minority or early studies applied image fusion (22/211, 10%). After the introduction of the first commercially available hybrid PET/MRI scanners in 2011, studies with hybrid PET/ MRI started appearing in 2013. There was a steady increase in the following years and a striking peak in 2015, when the number of hybrid FDG-PET/MRI studies even exceeded the number of retrospectively combined multimodality PET/MRI studies. Studies using bed system-combined PET/MRI scans (where the patient is moved between a separate PET/CT and MRI scanner on a single bed, for direct sequential scanning without the need of patient repositioning) were sparse (11/294, 4%), and for this review (focusing on abdominal oncology), the last retrieved report of this system dates from 2016.



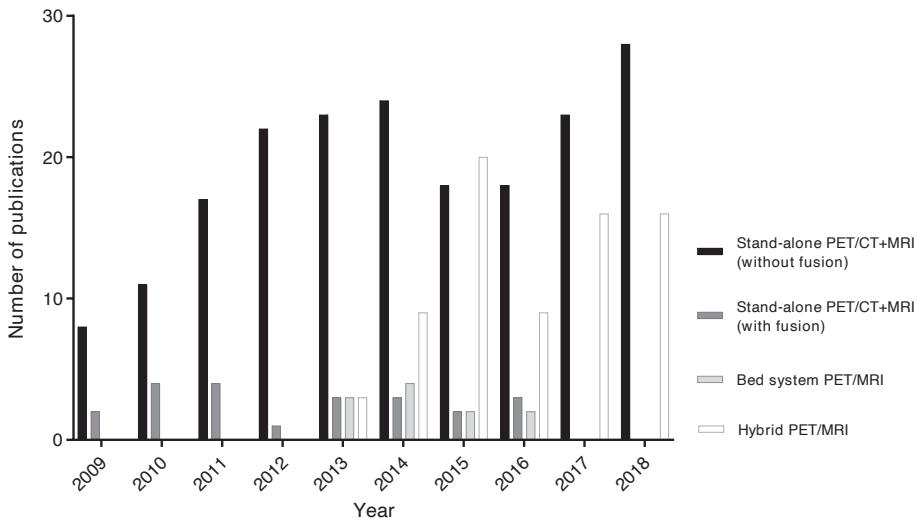


**Figure 3.** Evolution in the annual numbers of original research publications on multimodality combinations of FDG-PET/CT+MRI or PET/MRI in abdominal oncology specified per acquisition approach, i.e. retrospective combination of separately acquired FDG-PET/CT and MRI (with or without retrospective image fusion) versus prospective combination of PET and MRI using either bed system-combined acquisition or fully hybrid acquisition.

**Table 2.** Summary of papers focusing on multimodality combination of PET and MRI for visual lesion detection (for tumour staging)

Tumour type	Total n° of studies (%)	Median number of patients per study (range)
<b>Tumour types/groups with ≥10 available studies</b>		
Gynaecological cancers	43 (36)	43 (12 – 493)
<i>Retrospective combination (separate acquisition)</i>	34 (28)	51.5 (12 – 493)
<i>Combined acquisition (hybrid or bed-system PET/MRI)</i>	9 (8)	27 (18 – 71)
Colorectal cancer	32 (27)	34.5 (12 – 352)
<i>Retrospective combination (separate acquisition)</i>	27 (23)	35 (18 – 352)
<i>Combined acquisition (hybrid or bed-system PET/MRI)</i>	5 (4)	26 (12 – 55)
Mixed tumour types	15 (12)	37 (15 – 237)
<i>Retrospective combination (separate acquisition)</i>	10 (8)	45.5 (15 – 237)
<i>Combined acquisition (hybrid or bed-system PET/MRI)</i>	5 (4)	66 (32 – 173)
<b>Tumour types/groups with ≤10 available studies</b>		
Pancreas	10 (8)	48 (27 – 644)
Urological (prostate, bladder, kidney)	6 (5)	55 (22 – 287)
Anal	5 (4)	43 (11 – 61)
Upper GI (oesophagus, stomach)	4 (3)	46 (19 – 49)
Liver	3 (3)	35 (12 – 111)
Other (GIST, adrenal)	2 (2)	12.5 (9 – 16)

**Table 3.** Overview of papers focusing on multimodality combination of PET and MRI for prediction of treatment response and/or survival, based on (semi-)quantitative image parameters from imaging

Study	n =	Tumour type (+lesion type)	Imaging modalities	Clinical outcome (+outcome definition)	Key findings	Added value of combining PET and MRI?	Combination with non-imaging (clinical) predictors?	Comments
<b>Gynaecological malignancies</b>								
Bowen et al. (2018) <sup>26</sup>	21	cervix (primary tumour)	PET/CT, DWI, DCE-MRI	Response (tumour volume < vs. $\geq 10\%$ of baseline measured 1 month post-treatment)	<p>Predictors of response:</p> <ul style="list-style-type: none"> <li>- pre-therapy SUVmean (AUC 0.81) &amp; SUVmax (AUC 0.81)</li> <li>- after 2 weeks of treatment: <math>\Delta</math>ADCskewness (AUC 0.86)</li> <li>- after 5 weeks of treatment: ADCmean (AUC 0.81), <math>\% \Delta</math>SUVmean (AUC 0.79), <math>\Delta</math>SUVskewness (AUC 0.79)</li> </ul>	Not reported	No	Univariable ROC analysis.
Lucia et al. (2018) <sup>27</sup>	102	cervix (primary tumour)	PET/CT, T2W, DWI, DCE-MRI	Survival & local control (DFS; locoregional control)	<ul style="list-style-type: none"> <li>- DFS independent predictors: ADC Entropy<sub>GLCM</sub>-Q<sub>F</sub> <math>\leq 12.64</math> (HR: 30.95), CE-MRI RUVAR<sub>GLRLM</sub>-Q<sub>L</sub> <math>\leq 0.17</math> (HR: 11.33);</li> <li>- Locoregional control independent predictors: ADC Entropy<sub>GLCM</sub>-Q<sub>F</sub> <math>\leq 12.64</math> (HR: 16.35), PET GLNU<sub>GLRLM</sub>-Q<sub>E</sub> <math>\leq 103.71</math> (HR: 20.01)</li> </ul>	Yes	Yes (age, FIGO, N-stage, BMI, blood cell counts, RTx dose, treatment time)	Uni- & multivariable survival analysis, independent training and testing cohorts
Sarabhai et al. (2018) <sup>28</sup>	8	cervix (primary tumour)	PET/MRI with DWI and DCE-MRI	Response (RECIST+PERCIST CR/ PR vs. SD/PD measured 2-6wk after treatment)	<p>Predictors of response:</p> <ul style="list-style-type: none"> <li>mean <math>\Delta</math>tumour size -60%, <math>\Delta</math>SUVmax -64%, <math>\Delta</math>SUVmean -62%, <math>\Delta</math>ADCmin +38%, <math>\Delta</math>ADCmean +39%, <math>\Delta</math>Ktrans -39%, <math>\Delta</math>Kep -47%, <math>\Delta</math>iAUC -57%</li> </ul>	Not reported	No	Heterogeneous histology and treatments. Descriptive analysis only, only 1 non-responder.
Rahman et al. (2016) <sup>29</sup>	90	cervix (primary + nodes)	PET/CT, T2W	Survival (PFS; OS)	<ul style="list-style-type: none"> <li>- PFS independent predictors: SUVmax <math>\leq 10.7</math> (HR: 2.87) and MTV <math>\leq 26.5</math> (HR: 7.58) or TLG <math>\leq 231</math> (HR: 4.54) in scc; SUVmax <math>\leq 13.4</math> (HR: 12.9) in nsc; <ul style="list-style-type: none"> <li>- OS independent predictors: MTV <math>\leq 30.4</math> (HR: 10.6) or TLG <math>\leq 231</math> (HR 11.6) in scc; SUVmax <math>\leq 14.1</math> (HR: 6.98) in nsc</li> </ul> </li> </ul>	No	Yes (age, FIGO, N+ stage, surgery)	Uni- and multivariable survival analysis. Results stratified for scc vs. nsc histology.

table 3 (continued, 2/5)

Ho et al. (2017) <sup>30</sup>	69	cervix (primary tumour)	PET/CT, DWI	Survival (DFS; OS; central/locoregional/distant recurrence free survival (RFS))	- DFS independent predictors: ADCmean (>0.940x10 <sup>-3</sup> ; HR: 0.36), FIGO-stage I/II (HR: 2.4), nsc (HR: 0.23); - OS, central RFS and locoregional RFS: no significant predictors; - Distant RFS independent predictor: nsc (HR: 0.12)	No	Yes (age, FIGO, histology scc/hcc, differentiation grade, N0 vs N+ disease)	Uni- & multivariable survival analysis.
Ueno et al. (2017) <sup>31</sup>	21	cervix (primary tumour)	PET/CT, DWI	Response & survival (RECIST/PERCIST CR/PR vs. SD/PD; event-free survival (EFS))	- Associated with response: TLG (AUC: 0.84, optimal cut-off ≥679.69 g), MTV (AUC: 0.78, optimal cut-off ≥71.47 ml); - EFS negative prognostic factors: MTV ≥71.47 ml (HR: 4.73), TLG ≥679.69 g (HR: 4.73), ADC10% ≥0.86 x10 <sup>-3</sup> mm <sup>2</sup> /s (HR: 5.21)	Yes	No	Response: univariable ROC analysis; EFS: uni- & multivariable survival analysis.
Micco et al. (2014) <sup>32</sup>	49	cervix (primary tumour)	PET/CT, DWI, DCE-MRI	Survival (DFS; OS)	- DFS predictors: FIGO-stage IB/IIA (HR: 3.89), LN-neg (HR 6.15), max. tumour diameter (HR: 1.47), ADCmean (HR: 1.56), MTV (HR: 1.31), TLG (HR: 1.03) - OS predictors: FIGO-stage IB/IIA (HR: 6.45), LN-neg (HR: 7.8), ADCmean (HR: 0.46), MTV (HR: 1.42)	Not reported	Yes (FIGO, N-stage, histology scc/ nsc, grade, tumour size)	Univariable survival analysis.
Nakamura et al. (2014) <sup>33</sup>	80	cervix (lymph nodes)	PET/CT, DWI	Survival (DFS; OS)	- DFS independent predictors: LN SUVmax ≤2.10 (HR: 6.65); - OS independent predictors: LN SUVmax ≤2.225 (HR: 3.05)	No	No	Univariable ROC analysis, uni- & multivariable survival analysis.
Nakamura et al. (2012) <sup>34</sup>	66	cervix (primary tumour)	PET/CT, DWI	Survival (DFS; OS)	- DFS independent predictors: FIGO-stage IB/ IIA (HR: 5.265), LN-neg (HR: 4.124), SUVmax ≤15.55 + ADCmin ≥0.61 (HR: 8.779); - OS independent predictors: FIGO-stage IB/ IIA (HR: 11.922), LN-neg (HR: 8.659), SUVmax ≤15.55 + ADCmin ≥0.61 (HR: 8.449)	Yes	Yes (FIGO, pelvic N+ disease, histology scc/ nsc, tumour size)	Uni- & multivariable survival analysis.
Nakamura et al. (2013) <sup>35</sup>	131	endometrium (primary tumour)	PET/CT, DWI	Survival (DFS; OS)	- DFS independent predictors: FIGO-stage I/II (HR: 11.49), SUVmax ≤17.70 (HR: 13.33); - OS independent predictors: FIGO stage I/II (HR: 15.15), SUVmax ≤18.42 (HR: 15.63)	No	Yes (age, FIGO, histology, N-stage, lymphovascular invasion, ovarian M+, peritoneal cytology)	Univariable ROC analysis, Uni- & multivariable survival analysis.



table 3 (continued, 3/5)

Rectal cancer											
Joye et al. (2017) <sup>36</sup>	85	rectum (primary tumour)	PET/CT, T2W, DWI	Response (yPTO-1N0 vs. other yPTN)	- Predictors in optimal model: SUVpeak, post-CRT, ADC post-CRT, ADC ratio pre-CRT/post-CRT, diameter sphere post-CRT, $\Delta\%$ diameter sphere post-CRT (0.46). - Model AUC 0.83, sensitivity: 75%, specificity 94%	Yes	Yes (cytokines, gene expression profiles)	Multivariable analysis; cross-validated.			
Nishimura et al. (2016) <sup>37</sup>	15	rectum (primary tumour)	PET/CT, T2W	Response (TRG1-2 vs. TRG3)	Significant results: - Responders on MRI: smaller tumour size post-CRT, larger decrease in size post-CRT - Responders on PET: lower SUVmax during and post-CRT, larger decrease in SUVmax during and after CRT	Not reported	Yes (age, sex, tumour size, chemotherapy regimen, histology)	Fishers exact test.			
Heijnen et al. (2015) <sup>38</sup>	39	rectum (liver metastasis)	PET/CT, DWI, T2*	Survival and response (PFS; OS; size change)	- PFS predictors: pre-chemo ADCmean (HR: 0.749 /0.1x10 <sup>-3</sup> mm <sup>2</sup> /s); - OS predictors: pre-chemo SUVmax (HR: 1.125), TLG (HR: 1.047 /100g), and ADCmean (HR 0.667 /0.1x10 <sup>-3</sup> mm <sup>2</sup> /s), T2* (HR: 1.118 / ms); - No significant predictors for response	Yes, but effect not specified	No	Univariable survival analysis. (No detailed results for multivariable and response analysis).			
Ippolito et al. (2015) <sup>39</sup>	31	rectum (primary tumour)	PET/CT, DWI	Response (TRG1-2 vs. TRG3-5)	Predictors of response: SUVmax post-CRT (AUC: 0.889, optimal cut-off: 4.4), ADCmean post-CRT (AUC: 0.815, optimal cut-off: 1.294 10 <sup>-3</sup> mm <sup>2</sup> /s)	Not reported	No	Univariable ROC analysis.			
Ippolito et al. (2012) <sup>40</sup>	30	rectum (primary tumour)	PET/CT, DWI	Response (TRG1-2 vs. TRG3-5)	Predictors of response: SUVmax post-CRT <4.4, ADCmean post-CRT >1.294 x10 <sup>-3</sup> mm <sup>2</sup> /s	Yes, but effect not specified	No	Univariable regression analysis. (No detailed results for multivariable analysis)			
Herrmann et al. (2011) <sup>41</sup>	28	rectum (primary tumour)	PET/CT, T2W	Response (<10% residual tumour cells vs. $\geq$ 10%)	- Predictors of response, during CRT: $\Delta\%$ SUVmean (AUC: 0.70 - 0.75); - Predictors of response, post-CRT: $\Delta\%$ SUVmean (AUC: 0.75 - 0.76), $\Delta\%$ PETvolume (AUC: 0.73 - 0.76),	Not reported	No	Univariable ROC analysis.			

table 3 (continued, 4/5)

Lambrecht et al. (2010) <sup>42</sup>	22	rectum (primary tumour)	PET/CT, DWI	Response (pCR vs. non-pCR)	<ul style="list-style-type: none"> <li>- Pre-CRT predictors: ADCmean (&lt;1.06 x10<sup>-3</sup> mm<sup>2</sup>/s, sens: 1.0, spec: 0.88)</li> <li>- During CRT predictors: Δ%SUVmax (&gt;-40%, sens: 1.0, spec: 0.75), ADCmean pre-CRT &lt;1.06 x10<sup>-3</sup> mm<sup>2</sup>/s + Δ%SUVmax during CRT &gt;-40% (sens: 1.0, spec: 0.94)</li> <li>- Post-CRT predictors: Δ%SUVmax (&gt;-76%, sens: 1.0, spec: 0.75), ADCmean pre-CRT &lt;1.06 + Δ%SUVmax post-CRT &gt;-76% (sens: 1.0, spec: 1.0), Δ%SUVmax during CRT &gt;-40% + Δ%SUVmax post-CRT &gt;-76% (sens: 1.0, spec: 0.94)</li> </ul>	Yes	No	Univariable ROC analysis.	
<b>Other tumour types</b>									
Fang et al. (2018) <sup>43</sup>	20	oesophagus (primary tumour)	PET/CT, DWI	Response (TRG1 vs. TRG2-5)	<ul style="list-style-type: none"> <li>- Predictors of response during CRT: Δ%ADCmean (AUC: 1.0), Δ%ADCmedian (AUC: 0.99), Δ%ADC10% (AUC: 1.0), Δ%ADC25% (AUC: 1.0), Δ%ADC75% (AUC: 0.97), Δ%TLG (AUC: 0.95)</li> <li>- No predictors of response pre- and post-CRT</li> </ul>	Not reported	No	Univariable ROC analysis.	
Lee et al. (2016) <sup>44</sup>	11	stomach (primary tumour)	PET/MRI with DWI and DCE-MRI	Response (RECIST CR+PR vs. SD+PD)	<ul style="list-style-type: none"> <li>- Predictors of response: Ktrans mean (AUC: 0.917), iAUC mean (AUC: 0.867)</li> </ul>	No	No	Univariable ROC analysis.	
Weber et al. (2013) <sup>45</sup>	15	oesophagus and oesophagogastric (primary tumour)	PET/CT, DWI	Response (PET response; clinical response vs. non-response; histopathological regression grade 1+2 vs. grade 3)	<ul style="list-style-type: none"> <li>- Significant results: <ul style="list-style-type: none"> <li>- PET response: larger Δ%ADCmean and Δ%SUVmean during chemo</li> <li>- Clinical response: no significant results</li> <li>- Histopathological response: higher ADCmean pre-chemo in grade 1+2 vs. grade 3</li> </ul> </li> </ul>	No	No	Student's T-test.	
Hong et al. (2017) <sup>46</sup>	52	HCC (primary tumour)	PET/CT, DWI	Survival (Disease Specific Survival (DSS))	<ul style="list-style-type: none"> <li>- Predictors of impaired DSS: SUVmax tumour/SUVmean normal liver ≥2 (HR: 2.46), T-stage (HR: 3.01), PIVKA-II ≥100 mAU/ml (HR: 5.11), surgery as initial treatment (HR: 0.04)</li> </ul>	No	Yes (age, sex, Edmondson grade, Child-Pugh, MELD score, AFP, PIVKA-II, lesion n°, T-stage, surgery)	Multivariable survival analysis. Cut-offs based on literature.	

table 3 (continued, 5/5)

Han et al. (2014) <sup>47</sup>	298	HCC (primary tumour)	PET/CT, CE-MRI	Survival (clinical+radiological recurrence; OS)	- Recurrence independent predictors: SUV >3.5 (HR: 2.025), male (HR: 2.192), AFP >100 ng/ml (HR: 1.888); - Impaired OS predictors: SUV >3.5 (HR: 7.331), AFP >100 ng/ml (HR: 3.061)	No	Yes (age, sex, platelets, bilirubin, Indocyanin green, Child-Pugh, MELD, AFP, PIVKA-II, lesion size/n°)	Multivariable survival analysis.
Chen et al. (2018) <sup>48</sup>	63	pancreas (primary tumour)	PET/MRI with DWI, DCE-MRI and MR spectroscopy	Survival (OS, time to progression (TTP))	- OS independent predictors: TLG/peak (<11.81, HR: 4.610), ADCmin (>0.844 x10 <sup>-3</sup> mm <sup>2</sup> /s, HR: 0.999); - TTP: TLG/peak (<11.81, HR: 2.130), TLG (<33 g, HR: 1.004)	Yes	Yes (age, sex, TNM-stage)	Multivariate survival analysis.
Wang et al. (2018) <sup>49</sup>	13	pancreas (primary + metastasis)	PET/MRI with DWI	Response & survival (PFS; OS; RECIST PR vs. SD+PD)	- Predictors of response during chemo: Δ%MTV (≥60%, AUC: 0.95), Δ%TLG (≥65%, AUC: 0.95), Δ%ADCmean (≥+20%, AUC: 0.91), Δ%ADCmin (≥+20%, AUC: 0.86) - Predictors of PFS and OS: Δ%MTV ≥60%, %TLG ≥65%, Δ%ADCmean ≥+20%	Not reported	No	Univariable ROC and survival analysis.
Chen et al. (2016) <sup>50</sup>	60	pancreas/periampullar (primary tumour)	PET/MRI with DWI, MR spectroscopy	Survival (PFS)	PFS negative independent predictor: MTV/ADCmin ratio (HR: 1.036)	Yes	Yes (age, sex, tumour size, TNM-stage)	Multivariable survival analysis.

ADC: apparent diffusion coefficient (DWI), ADC Entropy<sub>GLCM</sub>-Q<sub>i</sub>: gray-level co-occurrence texture parameter from the ADC map AFP: alpha-fetoprotein, CE-MRI RUVAR<sub>GLIM</sub>-Q<sub>i</sub>: gray-level run-length matrix texture parameter from the contrast-enhanced MRI image, CR: complete response (RECIST), CRt: chemoradiotherapy, chemo: chemotherapy, DCE-MRI: dynamic contrast-enhanced magnetic resonance imaging, DFS: disease-free survival, DSS: disease-specific survival, DWI: diffusion-weighted magnetic resonance imaging, EFS: event-free survival, FIGO: International Federation of Gynecology and Obstetrics, PET GLNU<sub>GLIM</sub>-Q<sub>i</sub>: gray-level run-length matrix texture parameter from the PET image, HCC: hepatocellular carcinoma, iAUC: initial (60 seconds) area under the gadolinium concentration curve (DCE-MRI), Kep: reverse reflux rate constant (DCE-MRI), Ktrans: volume transfer coefficient (DCE-MRI), LN: lymph node, MR: magnetic resonance, MTV: metabolic tumour volume (PET), nsc: non-squamous cell carcinoma, OS: overall survival, pCR: pathological complete response, PD: progressive disease (RECIST), PERCIST: PET response criteria in solid tumours, PET/Ct: positron-emission tomography/computed tomography, PFS: progression-free survival, PIVKA-II: prothrombin induced by vitamin K absence-II, PR: partial response (RECIST), RECIST: response evaluation criteria in solid tumours, RFS: recurrence-free survival, ROC: receiver operating curve, scc: squamous cell carcinoma, SD: stable disease (RECIST), sens: sensitivity, spec: specificity, SUV: standardized uptake value (PET), T2\*: susceptibility-weighted MRI, T2W: T2-weighted magnetic resonance imaging, TLG: total lesion glycolysis (PET), TRG: tumour regression grade, TTP: time to progression, wk: weeks, yPT: pathological treatment response

**Image evaluation approaches**

As shown in **Figure 4**, approximately half of the papers combining FDG-PET/CT and MRI (144/294, 49%) focused on visual (qualitative) image assessment (mainly lesion detection for primary tumour staging), with more or less consistent numbers of reports over time. The main tumour types under investigation are detailed in **Table 2** and included gynaecological and colorectal cancers. A considerable increase over time was observed for studies applying quantitative methods of imaging assessment, including measurements such as the standardized uptake value (SUV, from PET), apparent diffusion coefficient (ADC, the main quantitative measure of DWI), parameters from dynamic contrast-enhanced MRI (e.g. Ktrans), and volumetric measurements. These quantitative studies constituted 33% of the total cohort, and mainly focused on correlation between FDG-PET and MRI parameters or on use of these parameters as “biomarkers” to predict clinical outcomes. **Table 3** summarizes the main findings of this latter subgroup of papers focusing on FDG-PET/(CT) and MRI parameters used as biomarkers to predict response and/or survival, the two most investigated clinical outcomes.

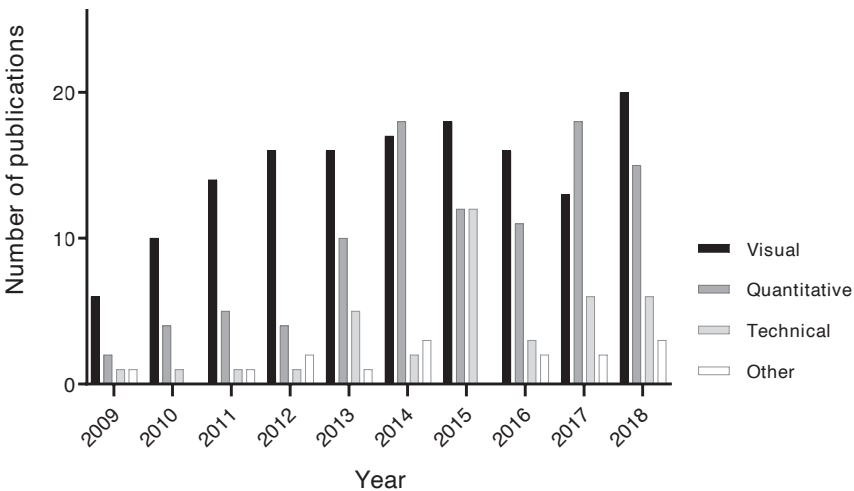


**Figure 4.** Evolution in the annual numbers of original research publications on multimodality combinations of FDG-PET/CT+MRI in abdominal oncology, specified per image evaluation approach, i.e. visual (qualitative) assessment, quantitative assessment, technical studies (i.e. protocol optimization and testing) and “other” (e.g. delineation studies for radiotherapy planning).

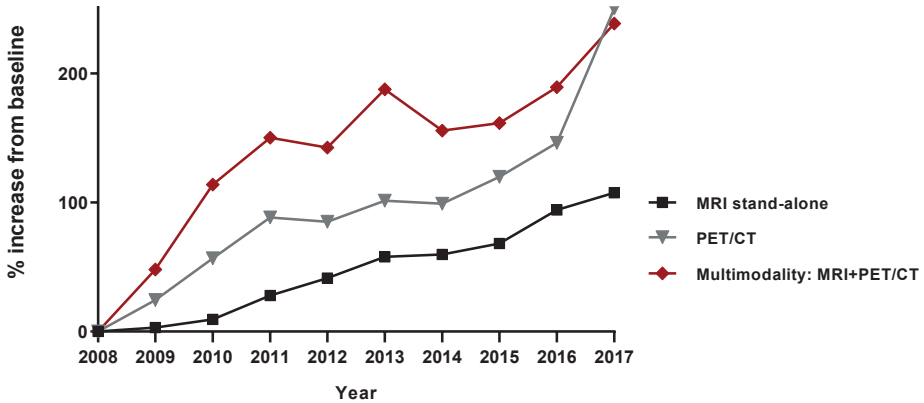


**Figure 5.** Annual growth of MR imaging studies, PET/CTs and multimodality MRI+PET/CT imaging combinations observed in our institution relative to the benchmark year 2008.

A minority (38/294, 13%) of reports concerned “technical” studies that describe the development, optimization and testing of new acquisition techniques. These studies showed a peak in the first years after the introduction of the first hybrid PET/MRI systems, and included mostly studies on MRI-based attenuation correction techniques<sup>51-57</sup> and quality of image co-registration.<sup>58-65</sup> There was a final small subgroup (16/294, 5%) of “other” studies, which for example included delineation studies (for radiotherapy planning).<sup>66,67</sup>

#### Institutional data

During the ten-year study interval, 53,537 MRIs, 27,003 PET/CTs and 5,660 multimodality MRI+PET/CT combinations (performed within a  $\leq 14$ -day interval) were performed at our institution, of which the developments are shown in **Figure 5** (Hybrid PET/MRI is not available at our institution). The overall ten-year increase relative to the baseline year (2008) was 108% for MRI, 250% for PET/CT and 239% for the multimodality combination of MRI+PET/CT, with consistently larger proportional growth of multimodality PET/CT+MRI combinations compared to either PET/CT or MRI on their own (with the exception of the final study year). The multimodality PET/CT+MRI combinations included 698 cases where PET/CT was combined with abdominal MRI examinations, and in line with our literature findings gynaecological and colorectal cancer were amongst the main tumour types under investigation.

## DISCUSSION

Aim of this paper was to describe main evolutions observed in a decade of published research on multimodality MRI and PET(/CT) imaging in abdominal oncology, and to see how these trends are reflected in data from our own institution. Annual numbers of published PET(/CT)+MRI research (as well as PET/CT+MRI combination studies performed at our own institution) showed a gradual and vast increase over time, with gynaecological and colorectal cancer being amongst the main tumour types under investigation. A major boost in PET(/CT)+MRI research was observed after the introduction of the first hybrid PET/MRI systems, which fully replaced earlier data on retrospective image fusion and bed system-combined (sequential) PET/MRI. Although a main focus of research throughout the study period remained combined use of PET/CT and MRI for visual diagnostic evaluations (i.e. lesion detection and tumour staging), quantitative analysis of PET- and MRI-based parameters as biomarkers of disease took flight in the second half of the study period. Another major development was the increased use of more tumour-specific tracers (other than FDG) in multimodality imaging, in specific the combination of PSMA-based PET(/CT) and MRI in prostate cancer.

# 2

### **Stand-alone versus hybrid combination of PET and MRI**

The majority (72%) of studies retrieved by our literature search concerned FDG-PET/CT and MRI examinations acquired sequentially, that is, as stand-alone modalities. The largest subgroup of these reports (65%) were studies that compared the diagnostic value of FDG-PET/CT to that of MRI, but a significant proportion (33%) evaluated the complementary value of combining FDG-PET/CT with MRI, which are essentially the studies that fall within the scope of our current paper focusing on “multimodality imaging”. In our institutional analysis, a remarkable increase was also observed during the study period in the number of multimodality PET/CT + MRI combinations performed as part of the same diagnostic work up. These findings suggest that PET and MRI offer complementary information (both anatomical and functional) that is of growing relevance for diagnostic oncologic imaging evaluations. This notion likely also led to the development of hybrid PET/MRI systems that became commercially available in 2011. Their introduction gave rise to a quickly growing number of hybrid PET/MRI reports in literature during the direct following years, including a peak in technical reports (e.g. on MR-based attenuation correction techniques and image co-registration) during the early study years up to 2015. In the same period, published research applying retrospective image fusion of separately acquired FDG-PET/CT

and MRI, as well as bed system-combined sequential MRI acquisition more or less disappeared, which is likely related to competition of these techniques with the newly available and logistically more attractive hybrid image acquisition techniques.

Although hybrid PET/MRI is considered by many to be the next state-of-the-art image modality in oncological research, its implementation is still an ongoing process that is to date mostly limited to a number of expert clinics and specialized oncological and/or dedicated research centres. Initial reasons for scepticism included concerns about the image quality as a result of technical adaptations required for PET and MR integration, and the substantially higher costs for installation and operation of these devices. Defining the clinical and research areas where there is a specific benefit of hybrid PET/MRI acquisition also remains a topic of debate. Currently, there seems to be agreement that the value of hybrid PET/MRI lies mainly in comprehensive regional evaluation of the local tumour and its direct (micro-)environment, rather than competing with PET/CT for whole-body applications.<sup>3,68</sup> In a recent scoping review, Morsing et al concluded that preliminary data suggest a superiority of PET/MRI for the detection of local recurrence in prostate cancer, local tumour invasion in cervical cancer, and liver metastases in colorectal cancer.<sup>69</sup> From the studies included in our literature study, it seems that overall the respective benefits of PET (i.e. staging of lymph nodes and distant metastases) and MRI (detailed local tumour staging) are maintained with simultaneous PET/MRI acquisition,<sup>70–72</sup> with the added benefit of improved imaging efficiency and potentially increased staging confidence.<sup>2,14,73,74</sup> There have, however, so far been no studies that directly compared hybrid PET/MRI to separately acquired PET/(CT) and MRI to validate these effects. Other emerging and more unique applications of hybrid PET/MRI acquisition include theranostic imaging<sup>75</sup> and in vivo dynamic evaluation of tumour biology, early tumour response and tracer kinetics, but these applications are still in early stages of research with only limited (pilot) data available.<sup>76,77</sup>

### **PET-tracers**

Another major development observed during the study period was the increased use of non-FDG, more tumour-specific PET- tracers, as illustrated in **Figure 2**, with studies using non-FDG tracers constituting even the majority of reports in the final study year. This disproportionate increase probably reflects some publication bias where results of novel tracer types – particularly positive results – are more likely to be published. Prostate-specific membrane antigen (PSMA)-targeted and choline tracers used in prostate cancer imaging, and octreotide analogues that target the somatostatin



receptor often overexpressed by neuro-endocrine tumours, were the most frequently reported. Their value lies primarily in the detection of lymph nodes and distant metastases from these specific malignancies that typically exhibit a heterogeneous or low glucose metabolism and are, therefore, less susceptible to detection by FDG-PET. Recent guideline updates have embraced the use of these novel tracers. For example in prostate cancer, PSMA-PET (or alternatively choline-PET) is now recommended for patients with biochemical recurrence who are considered for salvage treatment,<sup>6</sup> with growing evidence that PSMA-PET is superior to choline-PET for this purpose.<sup>78</sup> For primary staging of prostate cancer, PET is currently not recommended by the guidelines, but evidence that PSMA-PET/MRI may also be beneficial for these indications is emerging.<sup>79,80</sup>

### **Complementary value of FDG-PET and MRI for lesion detection and tumour staging**

Despite abovementioned recent advances in tumour-specific tracers, 18F-FDG remains the main workhorse used for multimodality PET(/CT)+MRI imaging in oncology. The abdominal tumour types most often assessed with FDG-PET(/CT) and MRI within our literature study (as well as in our institutional data) were gynaecological and colorectal cancers, which accounted for 32 and 21% of all studies. As summarized in **Table 2**, studies focusing on lesion detection and staging varied considerably in terms of patient numbers and use of retrospective versus hybrid combinations of FDG-PET and MRI. For the gynaecological group, most evidence is based on studies involving cervical cancer patients, with the largest study including a cohort of 493 patients. In this study, Kim et al constructed and validated a nomogram to predict lymph-node metastasis in patients with early stages of cervical cancer, which included tumour size on MRI, suspicion of lymph node metastasis on whole-body FDG-PET/CT and patient age as independent predictors, resulting in a model performance of AUC 0.825 (95% CI 0.736–0.895) in the validation set.<sup>81</sup> An earlier study already showed that fused FDG-PET and MRI images resulted in higher accuracy for detection of lymph node metastasis than FDG-PET/CT only (AUC 0.735 vs 0.690;  $p = 0.045$ ) in a cohort of 79 patients with FIGO stage Ib-IVa cervical cancer, again suggesting added value for the combination of PET and MRI in this setting.<sup>82</sup> Sarabhai et al<sup>70</sup> compared hybrid PET/MRI with only the MRI component, and found an improvement in diagnostic accuracy for PET/MRI. Not surprisingly, this benefit involved lymph node metastasis (accuracy 87% vs 77%) and distant metastasis (accuracy 91% vs 83%), but not local staging (85% vs 87% correct T-stage). Also for recurrent gynaecological malignancies, hybrid PET/MRI was shown to outperform diagnostic accuracy of the whole-body MRI component alone.<sup>83</sup> Combined use of MRI (for local staging) and PET/CT (for distant staging) has been adopted as a

recommended strategy in the most recent joined guidelines on cervical cancer from the European Society of Gynaecological Oncology (ESGO), the European Society for Radiotherapy and Oncology (ESTRO), and the European Society of Pathology (ESP), in particular for patients considered for curative intent chemoradiotherapy. Use of hybrid PET/MRI as an alternative approach is not specifically mentioned or discussed.<sup>84</sup>

In colorectal cancer, MRI is routinely used for detailed local staging in rectal cancer and has a known added benefit compared to CT for the detection of liver metastases, in particular for small lesions.<sup>85,86</sup> For primary staging in case of localized disease, PET/CT is not routinely recommended in current guidelines.<sup>87</sup> PET/CT is mainly advised as a problem solver in addition to routine staging, for the detection of extrahepatic disease (in candidates for local treatment of liver metastasis) and for the detection of recurrent disease after primary resection.<sup>88</sup> Vigano et al studied the role of FDG-PET/CT in 107 colorectal cancer patients before resection of liver metastasis. FDG-PET/CT revealed extrahepatic disease (mainly lymph nodes and peritoneal disease) in 28.8% (17/56) of the cases, which prevented futile liver resection in 20.3% (15/74) of patients deemed resectable by CT and/or MRI.<sup>89</sup> Use of PET is also increasingly being studied to assess response to chemotherapy or chemoradiotherapy in colorectal cancer and several studies have suggested a possible complementary role for FDG-PET/CT next to MRI for detection of a complete local response, detection of remaining pelvic lymph nodes and distant metastasis after treatment.<sup>90-92</sup> Catalano et al were among the first to compare the (re-)staging accuracy of FDG-PET/CT and hybrid PET/MRI in colorectal cancer. In a small series of 26 patients, assigned stage was discordant between the two hybrid modalities in 7/26 patients, and all but one patient were correctly staged using PET/MRI.<sup>93</sup> Further evidence on whether there is a potential benefit to perform hybrid PET/MRI in colorectal cancer is sparse.

Finally, there have been some reports in mixed abdominal cancer types suggesting that PET and MRI may have a complementary value to improve overall diagnostic staging confidence and for the diagnostic management of patients with peritoneal carcinomatosis. Wang et al studied 128 patients (including  $\pm$ 48% colorectal cancer patients) that were considered for cytoreductive surgery and hyperthermic intraperitoneal chemotherapy (HIPEC) and had undergone FDG-PET/CT, of which 91 in adjunct to CT and/or MRI. In the latter group, PET/CT had a complimentary role which contributed to patient management in 33/91 cases by confirming or excluding peritoneal and/or extraperitoneal disease.<sup>94</sup> In a study combining FDG-PET/CT and MRI for side-by-side-diagnostic assessment of 201 patients with different abdominal

cancer types, a net increase in diagnostic confidence was seen compared to separate assessment of either PET/CT or MRI, with potential clinical impact in 1 out of 9 study patients.<sup>14</sup>

### Quantitative studies on PET and MRI biomarkers

As shown in **Figure 5**, we observed a significant increase over time in published reports focusing on quantitative PET/(CT)+MRI assessment, eventually constituting approximately one third of all reports in the final year of our literature review. These studies look beyond lesion detection and regard the images as a dataset, which can be used to render quantifiable variables that may serve as biomarkers to predict clinical outcomes such as tumour stage, treatment outcome and survival<sup>26,28,31,32,36–39,41,43–45,49,50</sup> or correlate with other prognostic tumour markers such as histological tumour grade, hypoxia or microvascular invasion.<sup>95–99</sup> ADC and SUV were amongst the most frequently reported imaging markers, and several studies reported a significant inverse correlation between higher tumour SUV values and lower ADCs.<sup>30,46,100–107</sup> The common hypothesis is that tumours with a high cellular density (that show restricted diffusion and therefore low ADC values) will typically also exhibit an increased glucose metabolism, reflected by high SUV values. **Table 3** summarizes the main findings of studies focusing on use of PET and MRI biomarkers to predict response and/or survival, which constituted the two main investigated clinical outcomes. Methodology and results of these studies were highly variable. Despite this variation, a recurring finding was that higher tumour SUV, MTV or TLG and lower ACD values are generally associated with unfavourable outcomes (incomplete response, disease recurrence, reduced survival). It is worth mentioning that many of the studies in are preliminary reports that compare, rather than combine, the value of PET- and MRI-derived variables as predictors in univariable analysis.<sup>26,28,32,37,39,41–45,49</sup> Overall, there were fourteen studies (out of the 25 included) that combined PET and MRI parameters as potential outcome predictors in more comprehensive multivariable analyses,<sup>27,29–31,33–36,38,40,46–48,50</sup> of which 6/14 found complementary value for the two techniques.<sup>27,31,34,36,48,50</sup> In the remaining eight reports, either no complementary value was found (6/14 studies) or this was not explicitly analysed or reported (2/14 studies). Only two reports included (cross-) validation of data.<sup>27,36</sup>

Amongst the papers with positive findings on the combined use of PET and MRI parameters, Joye et al developed a model incorporating PET and MRI, but also molecular variables, to predict response to chemoradiotherapy in rectal cancer. They found that combining the multimodality information from PET and MRI resulted in

optimal predictive performance, outperforming prediction models based on either of the two imaging modalities on its own or those based on molecular markers.<sup>36</sup> In a preliminary study including a total of 102 patients (training n= 69, testing n= 33), Lucia et al evaluated the value of 92 pre-therapy PET/CT and MRI (T2-weighted, DWI and DCE-MRI) texture parameters to predict locoregional control and disease-free survival in patients treated with chemoradiotherapy for locally-advanced cervical cancer. They found a Radiomics signature based on a combination of ADC (Entropy-GLCM) and PET (GLNU-GLRLM) parameters to be highly predictive for locoregional control (AUC 1.0).<sup>27</sup> Additional large-scale research, preferably including independent validation cohorts, is required to help further establish the benefit of multimodality quantitative PET+MRI evaluation in building clinical models that predict outcome and prognosis.

Our study has some limitations. Firstly, the scope of this review, “multimodality PET/CT and MRI in abdominal oncology” is too wide (including a wide range of tumour types, study designs and studied outcomes) to provide an in-depth or systematic review of all available literature. Our primary aim was to provide a broad overview of observed trends and highlight some key developments. Secondly, our institutional data was retrieved as raw data from the PACS system, and the large numbers did not allow a detailed (per-patient) classification to be fully in line with the literature search. Our institutional data analysis was mainly intended to provide some insights into how trends observed in literature translate to evolutions in the use of multimodality imaging in an oncologic referral centre, using our institutional data as an anecdotal example.

## CONCLUSIONS

This review has shown that the field of multimodality imaging has evolved in several ways. During the study period hybrid PET/MRI systems were introduced, which gave rise to a major novel field of research, while at the same time shifting the focus away from retrospective PET/(CT)+MRI image fusion and bed system-combined PET/MRI acquisition. New PET-tracers have found their way into clinical practice. Studies focusing on combined quantitative analysis of PET and MRI data have taken flight and (multiparametric) predictive models incorporating these imaging biomarkers to predict clinical outcomes such as survival and treatment response are now being developed and tested. The next decade of research will need to further establish the true clinical potential of such prediction tools as well as define the definite role of hybrid PET/MRI for clinical research and practice.

## REFERENCES

1. National Center for Biotechnology Information MeSH Database: MeSH Unique ID: D064847; Multimodal imaging. Available from: [ncbi.nlm.nih.gov/mesh](https://ncbi.nlm.nih.gov/mesh) [May 26, 2021].
2. Hope TA, Fayad ZA, Fowler KJ, Holley D, Iagaru A, McMillan AB, et al. Summary of the first ISMRM-SNMIMI workshop on PET/MRI: applications and limitations. *J Nucl Med* 2019; 60: 1340–6. doi: 10.2967/jnumed.119.227231
3. Bailey DL, Pichler BJ, Gückel B, Antoch G, Barthel H, Bhujwalla ZM, et al. Combined PET/MRI: Global Warming-Summary report of the 6th International workshop on PET/MRI, March 27-29, 2017, Tübingen, Germany. *Mol Imaging Biol* 2018; 20: 4–20. doi: 10.1007/s11307-017-1123-5
4. Koh W-J, Abu-Rustum NR, Bean S, Bradley K, Campos SM, Cho KR, et al. Cervical cancer, version 3.2019, NCCN clinical practice guidelines in oncology. *J Natl Compr Canc Netw* 2019; 17: 64–84. doi: 10.6004/jnccn.2019.0001
5. Cibula D, Pötter R, Planchamp F, Avall-Lundqvist E, Fischerova D, Haie Meder C, Meder CH, et al. The European Society of gynaecological Oncology/European Society for radiotherapy and Oncology/European Society of pathology guidelines for the management of patients with cervical cancer. *Radiother Oncol* 2018; 127: 404–16. doi: 10.1016/j.radonc.2018.03.003
6. Cornford P, Bellmunt J, Bolla M, Briers E, De Santis M, Gross T, et al. EAU-ESTRO-SIOG guidelines on prostate cancer. Part II: treatment of relapsing, metastatic, and castration-resistant prostate cancer. *Eur Urol* 2017; 71: 630–42. doi: 10.1016/j.eururo.2016.08.002
7. Lordick F, Mariette C, Haustermans K, Obermannová R, Arnold D, ESMO Guidelines Committee. Oesophageal cancer: ESMO clinical practice guidelines for diagnosis, treatment and follow-up. *Ann Oncol* 2016; 27(suppl 5): v50–7. doi: 10.1093/annonc/mdw329
8. Glynne-Jones R, Nilsson PJ, Aschele C, Goh V, Peiffert D, Cervantes A, et al. Anal cancer: ESMO-ESSO-ESTRO clinical practice guidelines for diagnosis, treatment and follow-up. *Radiother Oncol* 2014; 111: 330–9. doi: 10.1016/j.radonc.2014.04.013
9. Öberg K, Knigge U, Kwekkeboom D, Perren A, ESMO Guidelines Working Group. Neuroendocrine gastro-entero-pancreatic tumors: ESMO clinical practice guidelines for diagnosis, treatment and follow-up. *Ann Oncol* 2012; 23(Supplement 7): vii124–30. doi: 10.1093/annonc/mds295

10. Mena E, Lindenberg ML, Shih JH, Adler S, Harmon S, Bergvall E, et al. Clinical impact of PSMA-based 18F-DCFBC PET/CT imaging in patients with biochemically recurrent prostate cancer after primary local therapy. *Eur J Nucl Med Mol Imaging* 2018; 45: 4–11. doi: 10.1007/s00259-017-3818-x
11. Lopci E, Saita A, Lazzeri M, Lughezzani G, Colombo P, Buffi NM, et al. 68Ga-PSMA Positron emission tomography/ computerized tomography for primary diagnosis of prostate cancer in men with contraindications to or negative multiparametric magnetic resonance imaging: a prospective observational study. *J Urol* 2018; 200: 95–103. doi: 10.1016/j.juro.2018.01.079
12. Afshar-Oromieh A, Babich JW, Kratochwil C, Giesel FL, Eisenhut M, Kopka K, et al. The rise of PSMA ligands for diagnosis and therapy of prostate cancer. *J Nucl Med* 2016; 57(Suppl 3): 79S–89. doi: 10.2967/jnumed.115.170720
13. Wulfert S, Kratochwil C, Choyke PL, Afshar-Oromieh A, Mier W, Kauczor H-U, et al. Multimodal imaging for early functional response assessment of (90)Y- (177) Lu-DOTATOC peptide receptor targeted radiotherapy with DW-MRI and (68)Ga-DOTATOC-PET/CT. *Mol Imaging Biol* 2014; 16: 586–94. doi: 10.1007/s11307-014-0722-7
14. Min LA, Vogel WW, Lahaye MJ, Maas M, Donswijk ML, Vegt E, et al. Integrated versus separate reading of F-18 FDG-PET/CT and MRI for abdominal malignancies - effect on staging outcomes and diagnostic confidence. *Eur Radiol* 2019; 29: 6900–10. doi: 10.1007/s00330-019-06253-1
15. Ouzzani M, Hammady H, Fedorowicz Z, Elmagarmid A. Rayyan—a web and mobile app for systematic reviews. *Syst Rev* 2016; 5: 1–10. doi: 10.1186/s13643-016-0384-4
16. Quero L, Vercellino L, de Kerviler E, Mongiat-Artus P, Culine S, Merlet P, et al. 18F-choline PET/CT and prostate MRI for staging patients with biochemical relapse after irradiation for prostate cancer. *Clin Nucl Med* 2015; 40: e492–5. doi: 10.1097/RLU.0000000000000932
17. Eiber M, Rauscher I, Souvatzoglou M, Maurer T, Schwaiger M, Holzapfel K, et al. Prospective head-to-head comparison of 11C-choline-PET/MR and 11C-choline-PET/CT for restaging of biochemical recurrent prostate cancer. *Eur J Nucl Med Mol Imaging* 2017; 44: 2179–88. doi: 10.1007/s00259-017-3797-y
18. Kranzbühler B, Nagel H, Becker AS, Müller J, Huellner M, Stolzmann P, et al. Clinical performance of 68Ga-PSMA-11 PET/MRI for the detection of recurrent prostate cancer following radical prostatectomy. *Eur J Nucl Med Mol Imaging* 2018; 45: 20–30. doi: 10.1007/s00259-017-3850-x

19. Afshar-Oromieh A, Haberkorn U, Schlemmer HP, Fenchel M, Eder M, Eisenhut M, et al. Comparison of PET/CT and PET/MRI hybrid systems using a  $^{68}\text{Ga}$ -labelled PSMA ligand for the diagnosis of recurrent prostate cancer: initial experience. *Eur J Nucl Med Mol Imaging* 2014; 41: 887–97. doi: 10.1007/s00259-013-2660-z
20. Bauman G, Martin P, Thiessen JD, Taylor R, Moussa M, Gaed M, et al.  $^{18}\text{F}$ -DCFPyL Positron Emission Tomography/Magnetic Resonance Imaging for Localization of Dominant Intraprostatic Foci: First Experience. *Eur Urol Focus* 2018; 4: 702–6. doi: 10.1016/j.euf.2016.10.002
21. Carideo L, Prosperi D, Panzuto F, Magi L, Pratesi MS, Rinzivillo M, et al. Role of combined [ $^{68}\text{Ga}$ ]Ga-DOTA-SST analogues and [ $^{18}\text{F}$ ]FDG PET/CT in the management of GEP-NENs: a systematic review. *J Clin Med* 2019; 8: 1032. doi: 10.3390/jcm8071032
22. Sadowski SM, Neychev V, Millo C, Shih J, Nilubol N, Herscovitch P, et al. Prospective study of  $^{68}\text{Ga}$ -DOTATATE positron emission tomography/computed tomography for detecting gastro-entero-pancreatic neuroendocrine tumors and unknown primary sites. *J Clin Oncol* 2016; 34: 588–96. doi: 10.1200/JCO.2015.64.0987
23. Beiderwellen KJ, Poeppel TD, Hartung-Knemeyer V, Buchbender C, Kuehl H, Bockisch A, et al. Simultaneous  $^{68}\text{Ga}$ -DOTATOC PET/MRI in patients with gastroenteropancreatic neuroendocrine tumors: initial results. *Invest Radiol* 2013; 48: 273–9. doi: 10.1097/RLI.0b013e3182871a7f
24. Frilling A, Sotiropoulos GC, Radtke A, Malago M, Bockisch A, Kuehl H, et al. The impact of  $^{68}\text{Ga}$ -DOTATOC positron emission tomography/ computed tomography on the multimodal management of patients with neuroendocrine tumors. *Ann Surg* 2010; 252: 850–6. doi: 10.1097/SLA.0b013e3181fd37e8
25. Ambrosini V, Campana D, Bodei L, Nanni C, Castellucci P, Allegri V, et al.  $^{68}\text{Ga}$ -DOTANOC PET/CT clinical impact in patients with neuroendocrine tumors. *J Nucl Med* 2010; 51: 669–73. doi: 10.2967/jnumed.109.071712
26. Bowen SR, Yuh WTC, Hippe DS, Wu W, Partridge SC, Elias S, et al. Tumor radiomic heterogeneity: multiparametric functional imaging to characterize variability and predict response following cervical cancer radiation therapy. *J Magn Reson Imaging* 2018; 47: 1388–96. doi: 10.1002/jmri.25874
27. Lucia F, Visvikis D, Desseroit M-C, Miranda O, Malhaire J-P, Robin P, et al. Prediction of outcome using pretreatment  $^{18}\text{F}$ -FDG PET/CT and MRI radiomics in locally advanced cervical cancer treated with chemoradiotherapy. *Eur J Nucl Med Mol Imaging* 2018; 45: 768–86. doi: 10.1007/s00259-017-3898-7



28. Sarabhai T, Tschischka A, Stebner V, Nensa F, Wetter A, Kimmig R, et al. Simultaneous multiparametric PET/MRI for the assessment of therapeutic response to chemotherapy or concurrent chemoradiotherapy of cervical cancer patients: preliminary results. *Clin Imaging* 2018; 49: 163–8. doi: 10.1016/j.clinimag.2018.03.009
29. Rahman T, Tsujikawa T, Yamamoto M, Chino Y, Shinagawa A, Kurokawa T. Different prognostic implications of 18F-FDG PET between histological subtypes in patients with cervical cancer. *Med* 2016; 95: 1–7. doi: 10.1097/MD.00000000000003017
30. Ho JC, Allen PK, Bhosale PR, Rauch GM, Fuller CD, Mohamed ASR. Diffusion-Weighted MRI as a predictor of outcome in cervical cancer following chemoradiation. *Int J Radiat Oncol Biol Phys* 2017; 97: 546–53. doi: 10.1016/j.ijrobp.2016.11.015
31. Ueno Y, Lisbona R, Tamada T, Alaref A, Sugimura K, Reinhold C. Comparison of FDG PET metabolic tumour volume versus ADC histogram: prognostic value of tumour treatment response and survival in patients with locally advanced uterine cervical cancer. *Br J Radiol* 2017; 90: 20170035. doi: 10.1259/bjr.20170035
32. Miccò M, Vargas HA, Burger IA, Kollmeier MA, Goldman DA, Park KJ, et al. Combined pre-treatment MRI and 18F-FDG PET/CT parameters as prognostic biomarkers in patients with cervical cancer. *Eur J Radiol* 2014; 83: 1169–76. doi: 10.1016/j.ejrad.2014.03.024
33. Nakamura K, Joja I, Nagasaka T, Haruma T, Hiramatsu Y. Maximum standardized lymph node uptake value could be an important predictor of recurrence and survival in patients with cervical cancer. *Eur J Obstet Gynecol Reprod Biol* 2014; 173: 77–82. doi: 10.1016/j.ejogrb.2013.10.030
34. Nakamura K, Joja I, Kodama J, Hongo A, Hiramatsu Y. Measurement of SUVmax plus ADCmin of the primary tumour is a predictor of prognosis in patients with cervical cancer. *Eur J Nucl Med Mol Imaging* 2012; 39: 283–90. doi: 10.1007/s00259-011-1978-7
35. Nakamura K, Joja I, Fukushima C, Haruma T, Hayashi C, Kusumoto T, et al. The preoperative SUVmax is superior to ADCmin of the primary tumour as a predictor of disease recurrence and survival in patients with endometrial cancer. *Eur J Nucl Med Mol Imaging* 2013; 40: 52–60. doi: 10.1007/s00259-012-2240-7
36. Joye I, Debucquoy A, Deroose CM, Vandecaveye V, Cutsem EV, Wolthuis A, et al. Quantitative imaging outperforms molecular markers when predicting response to chemoradiotherapy for rectal cancer. *Radiother Oncol* 2017; 124: 104–9. doi: 10.1016/j.radonc.2017.06.013

37. Nishimura J, Hasegawa J, Ogawa Y, Miwa H, Uemura M, Haraguchi N, et al. 18F-Fluorodeoxyglucose positron emission tomography ((18)F-FDG PET) for the early detection of response to neoadjuvant chemotherapy for locally advanced rectal cancer. *Surg Today* 2016; 46: 1152–8. doi: 10.1007/s00595-015-1297-x
38. Heijmen L, ter Voert EEGW, Oyen WJG, Punt CJA, van Spronsen DJ, Heerschap A, et al. Multimodality imaging to predict response to systemic treatment in patients with advanced colorectal cancer. *PLoS One* 2015; 10: e0120823–13. doi: 10.1371/journal.pone.0120823
39. Ippolito D, Fior D, Trattenero C, Ponti ED, Drago S, Guerra L, et al. Combined value of apparent diffusion coefficient-standardized uptake value max in evaluation of post- treated locally advanced rectal cancer. *World J Radiol* 2015; 7: 509. doi: 10.4329/wjr.v7.i12.509
40. Ippolito D, Monguzzi L, Guerra L, Deponti E, Gardani G, Messa C, et al. Response to neoadjuvant therapy in locally advanced rectal cancer: assessment with diffusion- weighted MR imaging and 18FDG PET/ CT. *Abdom Imaging* 2012; 37: 1032–40. doi: 10.1007/s00261-011-9839-1
41. Herrmann K, Bundschuh RA, Rosenberg R, Schmidt S, Praus C, Souvatzoglou M, et al. Comparison of different SUV- based methods for response prediction to neoadjuvant radiochemotherapy in locally advanced rectal cancer by FDG-PET and MRI. *Mol Imaging Biol* 2011; 13: 1011–9. doi: 10.1007/s11307-010- 0383-0
42. Lambrecht M, Deroose C, Roels S, Vandecaveye V, Penninckx F, Sagaert X, et al. The use of FDG-PET/CT and diffusion-weighted magnetic resonance imaging for response prediction before, during and after preoperative chemoradiotherapy for rectal cancer. *Acta Oncol* 2010; 49: 956–63. doi: 10.3109/0284186X.2010.498439
43. Fang P, Musall BC, Son JB, Moreno AC, Hobbs BP, Carter BW, et al. Multimodal imaging of pathologic response to chemoradiation in esophageal cancer. *Int J Radiat Oncol Biol Phys* 2018; 102: 996–1001. doi: 10.1016/j.ijrobp.2018.02. 029
44. Lee DH, Kim SH, Im S-A, Oh D-Y, Kim T-Y, Han JK. Multiparametric fully-integrated 18-FDG PET/MRI of advanced gastric cancer for prediction of chemotherapy response: a preliminary study. *Eur Radiol* 2016; 26: 2771–8. doi: 10. 1007/s00330-015-4105-5
45. Weber M-A, Bender K, von Gall CC, Stange A, Grünberg K, Ott K, et al. Assessment of diffusion-weighted MRI and 18F-fluoro- deoxyglucose PET/CT in monitoring early response to neoadjuvant chemotherapy in adenocarcinoma of the esophagogastric junction. *J Gastrointestin Liver Dis* 2013; 22: 45–52.

46. Hong CM, Ahn B-C, Jang Y-J, Jeong SY, Lee S-W, Lee J. Prognostic value of metabolic parameters of 18F-FDG PET/CT and apparent diffusion coefficient of MRI in hepatocellular carcinoma. *Clin Nucl Med* 2017; 42: 95–9. doi: 10.1097/RLU.0000000000001478
47. Han JH, Kim DG, Na GH, Kim EY, Lee SH, Hong TH, et al. Evaluation of prognostic factors on recurrence after curative resections for hepatocellular carcinoma. *World J Gastroenterol* 2014; 20: 17132–40. doi: 10.3748/wjg.v20.i45.17132
48. Chen B-B, Tien Y-W, Chang M-C, Cheng M-F, Chang Y-T, Yang S-H, et al. Multiparametric PET/MR imaging biomarkers are associated with overall survival in patients with pancreatic cancer. *Eur J Nucl Med Mol Imaging* 2018; 45: 1205–17. doi: 10.1007/s00259-018-3960-0
49. Wang ZJ, Behr S, Consunji MV, Yeh BM, Ohliger MA, Gao K, et al. Early response assessment in pancreatic ductal adenocarcinoma through integrated PET/ MRI. *AJR Am J Roentgenol* 2018; 211: 1010–9. doi: 10.2214/AJR.18.19602
50. Chen B-B, Tien Y-W, Chang M-C, Cheng M-F, Chang Y-T, Wu C-H, et al. PET/MRI in pancreatic and periampullary cancer: correlating diffusion-weighted imaging, MR spectroscopy and glucose metabolic activity with clinical stage and prognosis. *Eur J Nucl Med Mol Imaging* 2016; 43: 1753–64. doi: 10.1007/s00259-016-3356-y
51. Leynes AP, Yang J, Shanbhag DD, Kaushik SS, Seo Y, Hope TA, et al. Hybrid ZTE/ Dixon MR-based attenuation correction for quantitative uptake estimation of pelvic lesions in PET/MRI. *Med Phys* 2017; 44: 902–13. doi: 10.1002/mp.12122
52. Brendle C, Schmidt H, Oergel A, Bezrukov I, Mueller M, Schraml C, et al. Segmentation-based attenuation correction in positron emission tomography/magnetic resonance: erroneous tissue identification and its impact on positron emission tomography interpretation. *Invest Radiol* 2015; 50: 339–46. doi: 10.1097/RLI.0000000000000131
53. Eiber M, Martinez-Möller A, Souvatzoglou M, Holzapfel K, Pickhard A, Löffelbein D, et al. Value of a Dixon-based MR/PET attenuation correction sequence for the localization and evaluation of PET-positive lesions. *Eur J Nucl Med Mol Imaging* 2011; 38: 1691–701. doi: s00259-011-1842-9
54. Bezrukov I, Schmidt H, Gatidis S, Mantlik F, Schäfer JF, Schwenzer N, et al. Quantitative evaluation of segmentation- and atlas- based attenuation correction for PET/MR on pediatric patients. *J Nucl Med* 2015; 56: 1067–74. doi: 10.2967/jnumed.114.149476

55. Jochimsen TH, Schulz J, Busse H, Werner P, Schaudinn A, Zeisig V, et al. Lean body mass correction of standardized uptake value in simultaneous whole-body positron emission tomography and magnetic resonance imaging. *Phys Med Biol* 2015; 60: 4651–64. doi: 10.1088/0031-9155/60/ 12/4651
56. Kong E, Cho I. Clinical issues regarding misclassification by Dixon based PET/MR attenuation correction. *Hell J Nucl Med* 2015; 18: 42–7.
57. Arabi H, Rager O, Alem A, Varoquaux A, Becker M, Zaidi H. Clinical assessment of MR-guided 3-class and 4-class attenuation correction in PET/MR. *Mol Imaging Biol* 2015; 17: 264–76. doi: 10.1007/s11307-014-0777-5
58. Catalano OA, Umutlu L, Fuin N, Hibert ML, Scipioni M, Pedemonte S, et al. Comparison of the clinical performance of upper abdominal PET/DCE-MRI with and without concurrent respiratory motion correction (MoCo). *Eur J Nucl Med Mol Imaging* 2018; 45: 2147–54. doi: 10.1007/s00259-018-4084-2
59. Küstner T, Schwartz M, Martirosian P, Gatidis S, Seith F, Gilliam C, et al. MR-based respiratory and cardiac motion correction for PET imaging. *Med Image Anal* 2017; 42: 129–44. doi: 10.1016/j.media.2017.08.002
60. Grimm R, Fürst S, Souvatzoglou M, Forman C, Hutter J, Dregely I, et al. Self-gated MRI motion modeling for respiratory motion compensation in integrated PET/MRI. *Med Image Anal* 2015; 19: 110–20. doi: 10.1016/j.media.2014. 08.003
61. Fayad H, Schmidt H, Wuerslin C, Visvikis D. Reconstruction-Incorporated respiratory motion correction in clinical simultaneous PET/MR imaging for oncology applications. *J Nucl Med* 2015; 56: 884–9. doi: 10.2967/jnumed.114.153007
62. Roy P, Lee JKT, Sheikh A, Lin W. Quantitative comparison of misregistration in abdominal and pelvic organs between PET/MRI and PET/CT: effect of mode of acquisition and type of sequence on different organs. *AJR Am J Roentgenol* 2015; 205: 1295–305. doi: 10.2214/ AJR.15.14450
63. Ramalho M, Al Obaidy M, Burke LM, Dale BM, Busireddy KK, Wong TZ. MR-PET co-registration in upper abdominal imaging: quantitative comparison of two different T1-weighted gradient echo sequences: initial observations. *Abdom Imaging* 2015; 40: 1426–31. doi: 10.1007/ s00261-015-0460-6
64. Rosenkrantz AB, Balar AV, Huang WC, Jackson K, Friedman KP. Comparison of coregistration accuracy of pelvic structures between sequential and simultaneous imaging during hybrid PET/MRI in patients with bladder cancer. *Clin Nucl Med* 2015; 40: 637–41. doi: 10.1097/ RLU.0000000000000772
65. Kolbitsch C, Prieto C, Tsoumpas C, Schaeffter T. A 3D MR-acquisition scheme for non-rigid bulk motion correction in simultaneous PET-MR. *EJNMMI Phys* 2014; 1(Suppl 1): A37. doi: 10.1186/2197-7364-1-S1-A37

66. Rusten E, Rekstad BL, Undseth C, Al-Haidari G, Hanekamp B, Hernes E, et al. Target volume delineation of anal cancer based on magnetic resonance imaging or positron emission tomography. *Radiat Oncol* 2017; 12: 147. doi: 10.1186/s13014-017-0883-z
67. Han K, Croke J, Foltz W, Metser U, Xie J, Shek T, et al. A prospective study of DWI, DCE-MRI and FDG PET imaging for target delineation in brachytherapy for cervical cancer. *Radiother Oncol* 2016; 120: 519–25. doi: 10.1016/j.radonc.2016.08.002
68. Beyer T, Hacker M, Goh V. PET/MRI— knocking on the doors of the rich and famous. *Br J Radiol* 2017; 90: 20170347. doi: 10.1259/bjr.20170347
69. Morsing A, Hildebrandt MG, Vilstrup MH, Wallenius SE, Gerke O, Petersen H, et al. Hybrid PET/MRI in major cancers: a scoping review. *Eur J Nucl Med Mol Imaging* 2019; 46: 2138–51. doi: 10.1007/s00259-019-04402-8
70. Sarabhai T, Schaarschmidt BM, Wetter A, Kirchner J, Aktas B, Forsting M, et al. Comparison of 18F-FDG PET/MRI and MRI for pre-therapeutic tumor staging of patients with primary cancer of the uterine cervix. *Eur J Nucl Med Mol Imaging* 2018; 45: 67–76. doi: 10.1007/s00259-017-3809-y
71. Beiderwellen K, Geraldo L, Ruhlmann V, Heusch P, Gomez B, Nensa F, et al. Accuracy of [18F]FDG PET/MRI for the Detection of Liver Metastases. *PLoS One* 2015; 10: e0137285–3. doi: 10.1371/journal.pone.0137285
72. Kirchner J, Sawicki LM, Suntharalingam S, Grueneisen J, Ruhlmann V, Aktas B, et al. Whole-Body staging of female patients with recurrent pelvic malignancies: ultra-fast 18F-FDG PET/MRI compared to 18F-FDG PET/CT and CT. *PLoS One* 2017; 12: e0172553–11. doi: 10.1371/journal.pone.0172553
73. Grueneisen J, Beiderwellen K, Heusch P, Gratz M, Schulze-Hagen A, Heubner M, et al. Simultaneous positron emission tomography/magnetic resonance imaging for whole-body staging in patients with recurrent gynecological malignancies of the pelvis: a comparison to whole-body magnetic resonance imaging alone. *Invest Radiol* 2014; 49: 808–15. doi: 10.1097/RLI.0000000000000086
74. Beiderwellen K, Gomez B, Buchbender C, Hartung V, Poeppel TD, Nensa F, et al. Depiction and characterization of liver lesions in whole body [18F]-FDG PET/MRI. *Eur J Radiol* 2013; 82: e669–75. doi: 10.1016/j.ejrad.2013.07.027
75. Könik A, O'Donoghue JA, Wahl RL, Graham MM, Van den Abbeele AD. Theranostics: the role of quantitative nuclear medicine imaging. *Semin Radiat Oncol* 2021; 31: 28–36. doi: 10.1016/j.semradonc.2020.07.003
76. Ward RD, Amorim B, Li W, King J, Umutlu L, Groshar D, et al. Abdominal and pelvic 18F-FDG PET/MR: a review of current and emerging oncologic applications. *Abdom Radiol* 2021; 46: 1236–48. doi: 10.1007/s00261-020-02766-2

77. Yankeelov TE, Peterson TE, Abramson RG, Izquierdo-Garcia D, Garcia-Izquierdo D, Arlinghaus LR, et al. Simultaneous PET- MRI in oncology: a solution looking for a problem? *Magn Reson Imaging* 2012; 30: 1342–56. doi: 10.1016/j.mri. 2012.06.001
78. Treglia G, Pereira Mestre R, Ferrari M, Bosetti DG, Pascale M, Oikonomou E, et al. Radiolabelled choline versus PSMA PET/ CT in prostate cancer restaging: a meta-analysis. *Am J Nucl Med Mol Imaging* 2019; 9: 127–39.
79. Wang R, Shen G, Yang R, Ma X, Tian R. 68Ga-PSMA PET/MRI for the diagnosis of primary and biochemically recurrent prostate cancer: A meta-analysis. *Eur J Radiol* 2020; 130: 109131. doi: 10.1016/j.ejrad.2020.109131
80. Evangelista L, Zattoni F, Cassarino G, Artioli P, Cecchin D, Dal Moro F, et al. PET / MRI in prostate cancer: a systematic review and meta-analysis. *Eur J Nucl Med Mol Imaging* 2021; 48: 859–73. doi: 10. 1007/s00259-020-05025-0
81. Kim D-Y, Shim S-H, Kim S-O, Lee S-W, Park J-Y, Suh D-S, et al. Preoperative nomogram for the identification of lymph node metastasis in early cervical cancer. *Br J Cancer* 2014; 110: 34–41. doi: 10.1038/bjc.2013.718
82. Kim S-K, Choi HJ, Park S-Y, Lee H-Y, Seo S-S, Yoo CW, et al. Additional value of MR/ PET fusion compared with PET/CT in the detection of lymph node metastases in cervical cancer patients. *Eur J Cancer* 2009; 45: 2103–9. doi: 10.1016/j. ejca.2009.04.006
83. Sawicki LM, Kirchner J, Grueneisen J, Ruhlmann V, Aktas B, Schaarschmidt BM, et al. Comparison of 18F-FDG PET/MRI and MRI alone for whole-body staging and potential impact on therapeutic management of women with suspected recurrent pelvic cancer: a follow-up study. *Eur J Nucl Med Mol Imaging* 2018; 45: 622–9. doi: 10.1007/s00259- 017-3881-3
84. Cibula D, Pötter R, Planchamp F, Avall-Lundqvist E, Fischerova D, Haie Meder C, et al. The European Society of gynaecological Oncology/European Society for radiotherapy and Oncology/ European Society of pathology guidelines for the management of patients with cervical cancer. *Int J Gynecol Cancer* 2018; 28: 641–55. doi: 10.1097/IGC. 0000000000001216
85. Zech CJ, Korpraphong P, Huppertz A, Denecke T, Kim MJ, Tanomkiat W, et al. Randomized multicentre trial of gadoxetic acid-enhanced MRI versus conventional MRI or CT in the staging of colorectal cancer liver metastases. *Br J Surg* 2014; 101:613–21. doi: 10.1002/bjs. 94.9465
86. Niekel MC, Bipat S, Stoker J. Diagnostic imaging of colorectal liver metastases with CT, MR imaging, FDG PET, and/or FDG PET/CT: a meta-analysis of prospective studies including patients who have not previously undergone treatment. *Radiology* 2010; 257: 674–84. doi: 10. 1148/radiol.10100729

87. Argilés G, Tabernero J, Labianca R, Hochhauser D, Salazar R, Iveson T, et al. Localised colon cancer: ESMO clinical practice guidelines for diagnosis, treatment and follow-up. *Ann Oncol* 2020; 31: 1291–305. doi: 10.1016/j.annonc.2020.06.022
88. Van Cutsem E, Cervantes A, Nordlinger B, Arnold D, ESMO Guidelines Working Group Metastatic colorectal cancer: ESMO clinical practice guidelines for diagnosis, treatment and follow-up. *Ann Oncol* 2014; 25 Suppl 3(Supplement 3): iii1–9. doi: 10.1093/annonc/mdu260
89. Viganò L, Lopci E, Costa G, Rodari M, Poretti D, Pedicini V, et al. Positron emission tomography-computed tomography for patients with recurrent colorectal liver metastases: impact on restaging and treatment planning. *Ann Surg Oncol* 2017; 24: 1029–36. doi: 10.1245/s10434-016-5644-y
90. Ishihara S, Kawai K, Tanaka T, Kiyomatsu T, Hata K, Nozawa H, et al. Diagnostic value of FDG-PET/CT for lateral pelvic lymph node metastasis in rectal cancer treated with preoperative chemoradiotherapy. *Tech Coloproctol* 2018; 22: 347–54. doi: 10.1007/s10151-018-1779-0
91. Schneider DA, Akhurst TJ, Ngan SY, Warriar SK, Michael M, Lynch AC, et al. Relative value of restaging MRI, CT, and FDG-PET scan after preoperative chemoradiation for rectal cancer. *Dis Colon Rectum* 2016; 59:179–86. doi: 10.1097/DCR.0000000000000557
92. Cho YB, Chun H-K, Kim MJ, Choi JY, Park C-M, Kim B-T, et al. Accuracy of MRI and 18F-FDG PET/CT for restaging after preoperative concurrent chemoradiotherapy for rectal cancer. *World J Surg* 2009; 33: 2688–94. doi: 10.1007/s00268-009-0248-3
93. Catalano OA, Coutinho AM, Sahani DV, Vangel MG, Gee MS, Hahn PF, et al. Colorectal cancer staging: comparison of whole-body PET/CT and PET/MR. *Abdom Radiol* 2017; 42: 1141–51. doi: 10.1007/s00261-016-0985-3
94. Wang W, Tan GHC, Chia CS, Skanthakumar T, Soo KC, Teo MCC. Are positron emission tomography-computed tomography (PET- CT) scans useful in preoperative assessment of patients with peritoneal disease before cytoreductive surgery (CRS) and hyperthermic intraperitoneal chemotherapy (HIPEC)? *Int J Hyperthermia* 2018; 34: 524–31. doi: 10.1080/02656736.2017.1366554
95. Berg A, Gulati A, Ytre-Hauge S, Fasmer KE, Mauland KK, Hoivik EA, et al. Preoperative imaging markers and PDZ-binding kinase tissue expression predict low-risk disease in endometrial hyperplasias and low grade cancers. *Oncotarget* 2017; 8: 68530–41. doi: 10.18632/oncotarget.19708
96. Brown AM, Lindenberg ML, Sankineni S, Shih JH, Johnson LM, Pruthy S, et al. Does focal incidental 18F-FDG PET/CT uptake in the prostate have significance? *Abdom Imaging* 2015; 40: 3222–9. doi: 10.1007/s00261-015-0520-y

97. Tsuboyama T, Tatsumi M, Onishi H, Nakamoto A, Kim T, Hori M, et al. Assessment of combination of contrast-enhanced magnetic resonance imaging and positron emission tomography/computed tomography for evaluation of ovarian masses. *Invest Radiol* 2014; 49: 524–31. doi: 10.1097/RLI.0000000000000050
98. Armbruster M, Sourbron S, Haug A, Zech CJ, Ingrisich M, Auernhammer CJ, et al. Evaluation of neuroendocrine liver metastases: a comparison of dynamic contrast-enhanced magnetic resonance imaging and positron emission tomography/computed tomography. *Invest Radiol* 2014; 49: 7–14. doi: 10.1097/RLI.0b013e3182a4eb4a
99. Ahn SY, Lee JM, Joo I, Lee ES, Lee SJ, Cheon GJ, et al. Prediction of microvascular invasion of hepatocellular carcinoma using gadoteric acid-enhanced MR and 18F-FDG PET/CT. *Abdom Imaging* 2015; 40: 843–51. doi: 10.1007/s00261-014-0256-0
100. Floberg JM, Fowler KJ, Fuser D, DeWees TA, Dehdashti F, Siegel BA, et al. Spatial relationship of 2-deoxy-2-[18F]-fluoro-D-glucose positron emission tomography and magnetic resonance diffusion imaging metrics in cervical cancer. *EJNMMI Res* 2018; 8: 52. doi: 10.1186/s13550-018-0403-7
101. Goense L, Heethuis SE, van Rossum PSN, Voncken FEM, Lagendijk JJW, Lam MGEH, Lam M, et al. Correlation between functional imaging markers derived from diffusion-weighted MRI and 18F-FDG PET/CT in esophageal cancer. *Nucl Med Commun* 2018; 39: 60–7. doi: 10.1097/MNM.0000000000000771
102. Ahn SJ, Kim JH, Park SJ, Han JK, Joa Ahn S, Hoon Kim J, Joon Park S, Koo Han J. Prediction of the therapeutic response after FOLFOX and FOLFIRI treatment for patients with liver metastasis from colorectal cancer using computerized CT texture analysis. *Eur J Radiol* 2016; 85: 1867–74. doi: 10.1016/j.ejrad.2016.08.014
103. Sakane M, Tatsumi M, Kim T, Hori M, Onishi H, Nakamoto A, et al. Correlation between apparent diffusion coefficients on diffusion-weighted MRI and standardized uptake value on FDG-PET/CT in pancreatic adenocarcinoma. *Acta radiol* 2015; 56: 1034–41. doi: 10.1177/0284185114549825
104. hih I-L, Yen R-F, Chen C-A, Chen B-B, Wei S-Y, Chang W-C, et al. Standardized uptake value and apparent diffusion coefficient of endometrial cancer evaluated with integrated whole-body PET/MR: correlation with pathological prognostic factors. *J. Magn. Reson. Imaging* 2015; 42: 1723–32. doi: 10.1002/jmri.24932
105. Grueneisen J, Beiderwellen K, Heusch P, Buderath P, Aktas B, Gratz M, et al. Correlation of standardized uptake value and apparent diffusion coefficient in integrated whole-body PET/MRI of primary and recurrent cervical cancer. *PLoS One* 2014; 9: e96751–7. doi: 10.1371/journal.pone.0096751



106. Yu X, Lee EYP, Lai V, Chan Q. Correlation between tissue metabolism and cellularity assessed by standardized uptake value and apparent diffusion coefficient in peritoneal metastasis. *J Magn Reson Imaging* 2014; 40: 99–105. doi: 10.1002/jmri.24361
107. Gu J, Khong P-L, Wang S, Chan Q, Law W, Zhang J. Quantitative assessment of diffusion-weighted MR imaging in patients with primary rectal cancer: correlation with FDG-PET/CT. *Mol Imaging Biol* 2011; 13: 1020–8. doi: 10.1007/s11307-010-0433-7

Supplementary Table 1. literature search PubMed query			
Search	Items found	Search component	Search terms
#1	189992	PET	Tomography, Emission-Computed [Mesh] OR petscan* [tiab] OR pet [tiab] OR radionuclid* [tiab] OR (emission [tiab] AND tomograph* [tiab])
#2	738390	MRI	Magnetic Resonance Imaging [Mesh] OR (magnetic resonance [tiab] AND (image [tiab] OR images [tiab])) OR mri [tiab] OR mris [tiab] OR nmr [tiab] OR mra [tiab] OR mras [tiab] OR mr tomography [tiab] OR mr tomographies [tiab] OR mr tomographic [tiab] OR proton spin [tiab] OR fmri [tiab] OR fmris [tiab] OR zeugmatograph* [tiab] OR ((magneti* [tiab] OR chemical shift [tiab]) AND imaging [tiab])
#3	1486105	Abdominal Oncology	Abdominal Neoplasms [Mesh] OR Digestive System Neoplasms [Mesh] OR Prostatic Neoplasms [Mesh] OR Urinary Bladder Neoplasms [Mesh] OR Uterine Neoplasms [Mesh] OR Ovarian Neoplasms [Mesh] OR Splenic Neoplasms [Mesh] OR ((Neoplasms [Mesh] OR cancer [tiab] OR cancer* [tiab] OR carcinom* [tiab] OR tumor* [tiab] OR tumour* [tiab] OR neoplas* [tiab] OR metasta* [tiab] OR adenoma* [tiab] OR carcinosarcoma* [tiab] OR hepatoblastoma* [tiab] OR lymphangioma* [tiab] OR lymphangiomyoma* [tiab] OR sarcoma* OR chordoma* [tiab] OR germinoma [tiab] OR gonadoblastoma* [tiab] OR blastoma* [tiab] OR teratoma* [tiab] OR teratocarcinoma* [tiab] OR mesenchymoma* [tiab] OR mesonephroma* [tiab] OR carcinogen* [tiab] OR anticarcinogen* [tiab] OR precancerous [tiab] OR oncolog* [tiab] OR paraneoplastic [tiab] OR precancerous [tiab]) AND abdominal [tiab] OR abdomen [tiab] OR peritoneal [tiab] OR retroperitoneal [tiab] OR digestive [tiab] OR biliary tract [tiab] OR bile duct* [tiab] OR gallbladder [tiab] OR gall bladder [tiab] OR gastrointestinal [tiab] OR esophageal [tiab] OR esophagus [tiab] OR oesophageal [tiab] OR oesophagus [tiab] OR intestinal [tiab] OR intestine* [tiab] OR cecal [tiab] OR cecum [tiab] OR appendix [tiab] OR appendiceal [tiab] OR colorectal [tiab] OR colon [tiab] OR colonic [tiab] OR sigmoid* [tiab] OR rectum [tiab] OR rectal [tiab] OR anus [tiab] OR anal [tiab] OR duodoneal [tiab] OR duodenum [tiab] OR ileal [tiab] OR ileum [tiab] OR jejunal [tiab] OR jejunum [tiab] OR stomach [tiab] OR gastric [tiab] OR liver [tiab] OR hepatic [tiab] OR hepatocellular [tiab] OR pancreatic [tiab] OR pancreas [tiab] OR splenic [tiab] OR spleen [tiab] OR prostatic [tiab] OR prostate [tiab] OR bladder [tiab] OR urothelial [tiab] OR transitional cell* [tiab] OR adnes* [tiab] OR fallopian tumb* [tiab] OR salpin* [tab] OR ovary [tiab] OR ovaries [tiab] OR ovarial [tiab] OR ovarys [tiab] OR ovarian [tiab] OR uterus [tiab] OR uterine [tiab] OR uteral [tiab] OR uteri [tiab] OR cervix [tiab] OR cervical [tiab] OOR myometri* [tiab] OR endometri* [tiab] OR decidu* [tiab] OR gynaecolog* [tiab] OR gynecolog* [tiab]
#4	5469	Combine search #1 and #2 and #3	#1 AND #2 AND #3
#5	4032	Dated 2009 - 2018	AND (2009:2018 [dp] OR 2009:2018 [edat])
#6	3970	No animals	NOT (Animals [Mesh] NOT Humans [Mesh])
#7	36795	Original research only	NOT (systematic [sb] OR protocol [ti] OR Letter [ti] OR review* [ti] OR meta-analys* [ti] OR consensus [ti] OR reply to [ti])

2

The background is a deep blue color with several overlapping, organic, wave-like shapes. A prominent feature is a large, curved area filled with a fine halftone dot pattern, which is darker than the surrounding blue. The overall effect is a textured, layered composition.

## Chapter 3

# INTEGRATED VERSUS SEPARATE READING OF F-18 FDG-PET/CT AND MRI FOR ABDOMINAL MALIGNANCIES – EFFECT ON STAGING OUTCOMES AND DIAGNOSTIC CONFIDENCE

Lisa A. Min, Wouter V. Vogel, Max J. Lahaye Monique Maas, Maarten L. Donswijk, Erik Vegt, Miranda Kusters, Henry J. Zijlmans, Katarzyna Józwiak, Sander Roberti, Regina G. H. Beets-Tan, Doenja M. J. Lambregts

*European Radiology* (2019) 29(12):6900-6910 doi: 10.1007/s00330-019-06253-1

# ABSTRACT

## Objective

Abdominal cancer patients increasingly undergo multimodality imaging. This study evaluates effects of integrated reading of PET/CT and abdominal MRI on staging outcomes and diagnostic confidence compared to 'routine' separate reading.

## Methods

In total, N= 201 patients who underwent abdominal MRI and whole-body F-18 FDG-PET/CT within 14 days were retrospectively analyzed. Original MRI and PET/CT reports were retrieved and reported findings translated into a 5-point confidence score (1 = definitely benign to 5 = definitely malignant) for 7 standardized regions (primary tumor/regional lymph nodes/distant lymph nodes/liver/lung/bone/peritoneum) per patient. Two-reader teams (radiologist + nuclear medicine physician) then performed integrated reading of the images using the same scoring system.

## Results

Integrated reading led to discrepant findings in 59 of 201 (29%) of patients, with potential clinical impact in 25 of 201 (12%). Equivocal scores decreased from 5.7% (PET/CT) and 5.4% (MRI) to 3.2% ( $p= 0.05$  and  $p= 0.14$ ). Compared to the original PET/CT reports, integrated reading led to increased diagnostic confidence in 8.9% versus decreased confidence in 6.6% ( $p= 0.26$ ). Compared with the original MRI reports, an increase in confidence occurred in 9.6% versus a decrease in 6.9% ( $p= 0.18$ ). The effect on diagnostic confidence was most pronounced in lymph nodes ( $p= 0.08$  vs. MRI), cervical cancer ( $p= 0.03$  vs. MRI), and recurrent disease staging ( $p= 0.06$  vs. PET/CT).

## Conclusions

Integrated PET/CT+MRI reading alters staging outcomes in a substantial proportion of cases with potential clinical impact in  $\pm 1$  out of 9 patients. It can also have a small positive effect on diagnostic confidence, particularly in lymph nodes and cervical cancer, and in post-treatment settings. These findings support further collaboration between radiology and nuclear medicine disciplines.

## INTRODUCTION

In oncology, increasing numbers of patients undergo multimodality imaging, i.e., a combination of two or more imaging modalities within one clinical setting. Especially the combination of (FDG-)PET and PET/CT with MRI has gained interest, as it offers the functional metabolic information from PET as well as the high soft-tissue contrast and anatomical resolution of MRI. This allows detailed local staging combined with dedicated whole-body staging of lymph nodes and distant metastases. More recently introduced functional MRI sequences like DWI contribute to a broader application of MRI. DWI is a very sensitive technique to help detect small malignant lesions that are typically difficult to detect on FDG-PET, such as sub-centimeter liver<sup>1</sup> or peritoneal metastases.<sup>2,3</sup> Furthermore, quantitative parameters such as the ADC and SUV can be derived from DWI and FDG-PET, which both have shown potential as imaging biomarkers of response and prognosis.<sup>4,5</sup>

Recently, fully integrated (hybrid) PET/MRI devices have been introduced. The first publications describing the potential benefits of these techniques are now available. Results are still mainly preliminary and hybrid PET/MRI systems are not yet widely used in clinics, partly because current first-generation systems still have some limitations.<sup>6–27</sup> Retrospective image fusion of PET and MRI is an alternative approach, but this strategy can be cumbersome<sup>28</sup> and there is little evidence supporting its benefit.<sup>29–34</sup>

A relatively simple approach to combine the strengths of PET/CT and MRI is to perform an integrated, side-by-side reading of the images by a radiologist and a nuclear medicine physician. This could help establish a more uniform conclusion early in the diagnostic process, which would benefit the efficacy of multidisciplinary team meetings. Evidence on the performance of this approach remains scarce<sup>29,35</sup> and separate assessment and reporting is still standard practice in most clinics.

The purpose of this study was therefore to investigate the effect of integrated side-by-side reading of FDG-PET/CT and abdominal MRI on staging outcomes and diagnostic confidence, compared with the current standard of separately evaluated PET/CT and MRI.

3

# METHODS

This study was approved by the institutional ethical review board. Due to its retrospective nature, informed consent was not required.

## Patients

The institutional patient database was searched (2012–2015) for all cases where a patient with abdominal malignancy underwent ‘multimodality imaging’ within one clinical setting. Multimodality imaging was defined as a combination of any sort of abdominal MRI (i.e., pelvic or liver) and whole-body FDG-PET/CT performed within a 14-day interval without any treatment or interventions between both examinations. In total, 228 cases were considered for inclusion; 27 were excluded for reasons explained in **Figure 1**. This resulted in a study cohort of n= 201 patients.

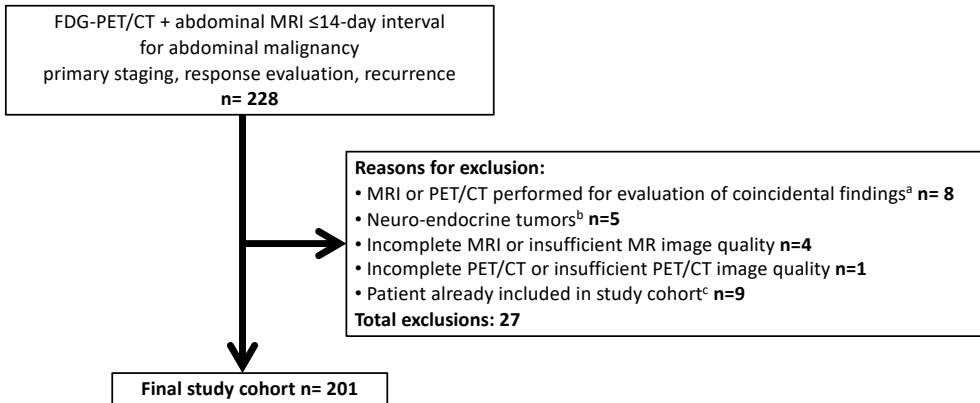


**Figure 1.** Patient in- and exclusion flowchart. <sup>a</sup> Patients were excluded if either the MRI or PET/CT was merely performed for assessment of coincidental findings (e.g., MRI of the prostate performed because of FDG-uptake in the prostate on PET/CT performed for other type of malignancy). <sup>b</sup> Neuroendocrine tumors were excluded because FDG-PETs were performed for treatment planning rather than for diagnostic purposes. <sup>c</sup> If a patient underwent multimodality FDG-PET/CT+MRI at different time points, the patient was included only once, using the earliest available imaging examinations.



### Imaging

MRIs were performed on a 1.5-tesla (n= 26) or 3.0-tesla (n= 175) scanner (Intera Achieva, Philips Healthcare) according to the routine clinical protocols employed at that time. MRIs consisted of 39 liver and 162 pelvic MRIs. Routine protocols included at least a T2-weighted sequence in one or multiple planes, typically combined with a T1-weighted sequence and/or a diffusion-weighted sequence (with at least one high b-value of b600–b1000 s/mm<sup>2</sup>). Liver MRIs also routinely included a multiple-phase contrast-enhanced sequence (gadoterate meglumine/Gd-DOTA 0.5 mmol/ml, Dotarem®, Guerbet Group; or gadoxetate disodium/Gd-EOB-DTPA 0.2 mmol/ml, Primovist®, Bayer HealthCare Pharmaceuticals).

FDG-PET/CTs (hereafter PET/CT) were performed on a Gemini TF 16 or Gemini TF Big Bore scanner (both Philips Healthcare), according to clinical standards. Patients fasted for 6h, with targeted blood-glucose level <10 mmol/l. An intravenous F-18 FDG bolus injection of 180 MBq (4.86 mCi, for BMI ≤ 28) to 240 MBq (7.56 mCi, for BMI > 28) was administered, followed by a biodistribution time of 60 ± 5 min. PET images were acquired for 2 min/bed position, and reconstructed to 4 mm isotropic voxels. An unenhanced CT (120–140 kV, 40 mAs, reconstructed to both 5 mm and 2 mm slice thicknesses and intervals) was performed for attenuation correction and anatomical correlation. The routine field of view (FOV) included the skull base to the inguinal region.

### Image evaluation

The image evaluation process is schematically illustrated in Figure 2.

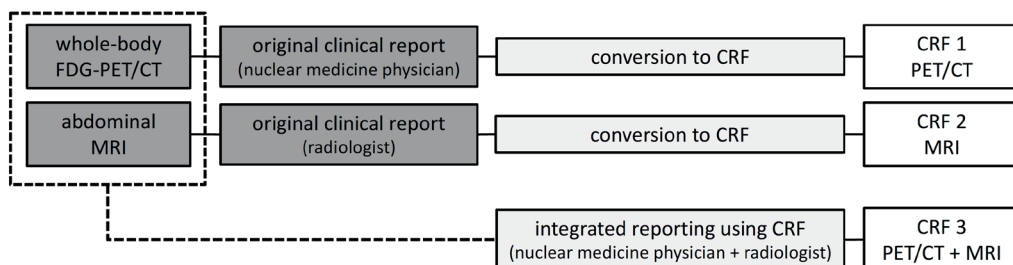


Figure 2. Schematic outline of the scoring process.



A standardized case report form (CRF) was constructed for the purpose of this study, which listed seven pre-defined anatomical regions: (1) primary tumor location, (2) loco-regional lymph nodes, (3) distant lymph nodes, (4) liver, (5) lung, (6) bone, (7) peritoneum. Each region was scored using a 5-point confidence level score reflecting the confidence of presence/absence of tumor within that particular region: 1 = definitely no tumor, 2 = probably no tumor, 3 = possible tumor/possibly no tumor (equivocal), 4 = probably tumor, 5 = definitely tumor.

### **Cases were scored in threefold and recorded in three separate CRFs:**

1. Based on the original clinical PET/CT report  
(by a nuclear medicine physician alone)
2. Based on the original clinical MRI report (by a radiologist alone)
3. Through integrated side-by-side reading of PET/CT and MRI  
(by a nuclear medicine physician and a radiologist in consensus)

### **CRFs 1 and 2: scoring of PET/CT and MRI based on original clinical reports**

Original clinical reports were collected from the electronic patient records. All MRIs were reported by board-certified radiologists and all PET/CTs (including low-dose non-enhanced CT) were reported by board-certified nuclear medicine physicians according to routine practice at our institution. An independent reader (LM) interpreted the free-text reports and converted the reported findings to a confidence score for each region. Terms expressing a high certainty of tumor ('tumor mass', 'pathologic node', 'suspicious for metastasis') were assigned a confidence score of 4 or 5, while terms indicating a benign etiology ('normal', 'benign', 'reactive') were assigned a confidence score of 1 or 2. Inconclusive terms such as 'borderline enlarged', 'differential diagnosis reactive or metastasis', and 'unable to differentiate' were assigned equivocal scores. In case of doubt, the reader could consult any of the other readers (not involved in the integrated reading of that particular case). For the MRI-CRF (CRF 2), no score was assigned for regions that were not included in the MRI-FOV.

### **CRF 3: integrated reading of PET/CT and MRI**

In a separate reading session, the MRI and PET/CT images were assessed side-by-side by a two-reader team, consisting of one board-certified radiologist (DL, ML, or MM; each with a similar experience level) and one board-certified nuclear medicine physician (WV, EV, or MD; each with a similar experience level), in randomly assigned duos. The readers were blinded to the original imaging reports and to all medical information of later date (including further follow-up imaging, multidisciplinary team

discussions, and treatment outcomes), but had access to earlier imaging exams, the clinical information and question provided with the exams, and all relevant previous medical history up to the original date of the exam. This setup was chosen to resemble the original clinical evaluation and reporting as closely as possible. The two readers together (in consensus) assigned a confidence score for each region. An independent observer (LM) was present during the scoring to ensure adherence to this protocol.

### Data analysis

Data analysis was performed using IBM-PSS Statistics 22 (IBM Corp.) and Stata Statistical Software: Release 13 (StataCorp). The confidence scores from the integrated reading (CRF 3) were compared with the scores derived from the original FDG-PET/CT and MRI reports (CRFs 1 and 2) using McNemar's test for each region. A distinction was made between regions that were within the FOV of both the MRI+PET/CT, representing a cumulative effect of combining two imaging modalities and readers from two disciplines (further referred to as 'fully integrated' reading), and regions that were outside the MRI-FOV, reflecting mainly effects of combining readers from two disciplines to assess the PET/CT images (further referred to as 'partly integrated' reading). For each region, the scores of the integrated reading (vs. the original reports) were classified as 'concordant', 'discrepant', 'increase in confidence', or 'decrease in confidence' according to the system explained in **Table 1**. The proportions of regions with an increase in confidence were compared with the proportions of regions with a decrease in confidence using  $\chi^2$  or Fisher's exact test. Agreement between the modalities/readings was quantified using weighted Kappa statistic with linear weights.

### Discussion of discrepant findings in simulated multidisciplinary team (MDT)

For cases where integrated reading led to  $\geq 1$  discrepant findings compared with the original PET/CT and/or MRI reports, full clinical patient records (clinical and imaging FU, MDT-reports, outcomes of surgery, histopathology, etc.) were analyzed and discussed in a simulated MDT. This simulated MDT included a radiologist (DL), nuclear medicine physician (WW), radiation oncologist (WW), and two oncologic surgeons (MK, gastroenterology-oncology specialist; and HZ, gynecology-oncology specialist). The MDT discussed the findings of the integrated reading and compared these with the original clinical MDT-reports, using the flowchart in **Figure 3**. Discrepant findings were defined to have clinical impact if they would have led to a change in overall disease stage (i.e., tumor vs. no tumor, node-negative vs. node-positive disease, non-metastasized vs. metastasized disease), and/or a change in clinical management (i.e., change in treatment or need for additional invasive diagnostic procedures).

**Table 1.** Comparison of scores derived from original reports vs. scores from integrated reassessment.

Score original report*	Score integrated reading					
	1	2	3	4	5	
1	=	↓	↓	≠	≠	
2	↑	=	↓	≠	≠	
3	↑	↑	=	↑	↑	
4	≠	≠	↓	=	↑	
5	≠	≠	↓	↓	=	

= indicates concordant (identical) confidence scores; ≠ indicates discrepant (contradicting) confidence scores; ↑ indicates increased diagnostic confidence with integrated re-assessment; ↓ indicates decreased diagnostic confidence with integrated re-assessment.  
 \*Scores were derived from the original clinical PET/CT or MRI report text. For the MRI report, regions that were outside the MRI field of view were recorded as such, and no score was assigned.

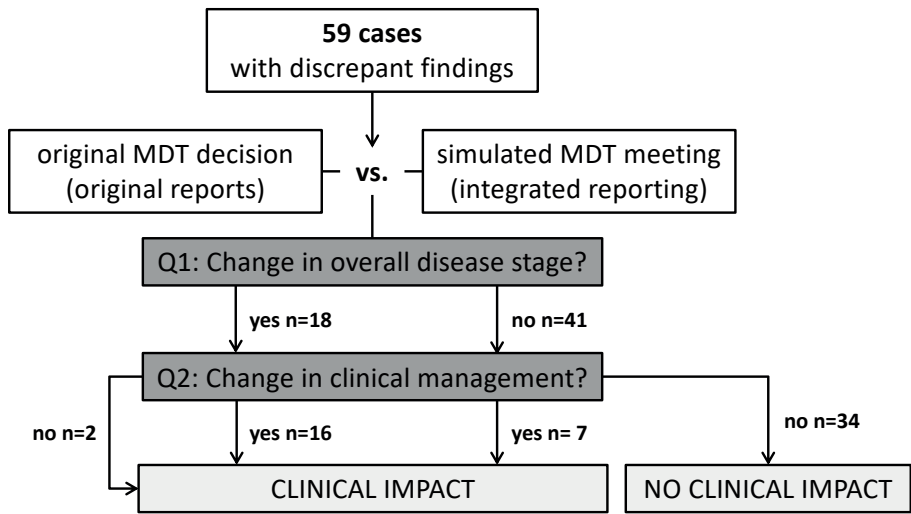


**Figure 3.** Schematic outline of the clinical impact decision process and its results. The potential clinical impact of the discrepant findings was determined by a simulated MDT, who compared the findings of the integrated reading to that of the original reports documented by the original MDT in the clinical patient records. Discrepant findings were defined to have a clinical impact if they would result in a change in the overall disease (i.e., tumor versus no tumor, node-positive versus node-negative disease, metastasized versus non-metastasized disease) and/or a change in clinical management (i.e., change in treatment or need for additional invasive diagnostic procedures such as image-guided biopsy).

## RESULTS

### Baseline characteristics

Baseline study characteristics are described in **Table 2**. The main types of malignancy were gynecological (41%), colorectal (39%), and anal carcinomas (14%). The most common imaging indication was staging of a newly diagnosed malignancy (49%). Median interval between MRI and PET/CT was 7 days (range 0–14 days). In the majority of cases (60%), MRI was performed first. In 30%, PET/CT was done first (for example to screen for suspected recurrent disease). The remaining 10% of patients underwent both studies on the same day.

### Discrepant findings and clinical impact

Integrated reading led to discrepant findings in 59 of 201 patients (29%). According to the simulated MDT meeting, these discrepancies would have had a clinical impact in 25 of 59 patients (12% of the total patient cohort). These 25 ‘clinical-impact’ cases are described in detail in **Supplementary Table 1**. Fifteen of these 25 cases concerned lymph nodes, and five concerned the differentiation of residual/recurrent disease after treatment. In total, 13 of 25 cases were upstaged and 12 were down-staged after integrated reading: in 8 cases, this led to a correct change in disease stage (based on final histopathology and/or long-term clinical follow-up data as the standard of reference); in 7 cases, integrated reading was incorrect; and in the remaining 10, no standard of reference was available to draw any conclusions. Six of the eight cases that were correctly changed after integrated reading concerned lymph nodes. In the seven incorrectly changed cases, discrepant lymph node findings also constituted the majority (4/7). Overall, discrepancies occurred more frequently in comparison to the original MRI reports than to the PET/CT reports (11.3% vs. 4.9%,  $p=0.0002$ ).

### Effects of diagnostic confidence

**Figure 4** summarizes the effects of the integrated reading on diagnostic confidence. Subgroup analyses for different types of malignancies, anatomic subsites, and imaging indications are presented in **Table 3**. A fully integrated reading was available for 407 (25%) of the total of 1607 regions scored, included in the FOV of both the MRI and PET/CT. For the remaining 1200 regions outside the MRI-FOV, a partly integrated reading of the PET/CT images was performed.

<b>Table 2. Baseline patient and imaging characteristics</b>	
<b>Variable</b>	<b>Number (%) total n= 201</b>
Median age (range)	61 (26–93)
Sex	
Male	62 (31%)
Female	139 (69%)
Primary tumor type	
Gynecological (cervix, endometrium, ovary, vagina, vulva)	83 (41%)
Colorectal	77 (39%)
Anal	29 (14%)
Urological (bladder, urethra)	7 (3%)
Upper gastrointestinal tract (stomach, esophagus)	2 (1%)
Sarcoma	2 (1%)
Indication for imaging	
Staging of primary malignancy	99 (49%)
Response evaluation	32 (16%)
Detection and/or staging of recurrent malignancy	70 (35%)
Order of imaging examinations	
MRI first (median interval)	120 (7 days)
PET/CT first (median interval)	60 (7 days)
MRI and PET/CT on the same day	21
MRI characteristics	
Field of view	
Upper abdomen/liver	36 (20%)
Lower abdomen/pelvis	144 (80%)
Diffusion-weighted sequence available	
Yes	185 (92%)
No	16 (8%)
Contrast-enhanced sequence available	
No	146 (73%)
Yes <sup>a</sup>	55 (27%)
<sup>a</sup> Contrast-enhanced abdominal MRIs were liver MRIs in 39 of 55 (71%) and pelvic MRIs in 16 of 55 (29%)	
MRI, magnetic resonance imaging; PET/CT, positron emission tomography (PET) with computer tomography (CT)	

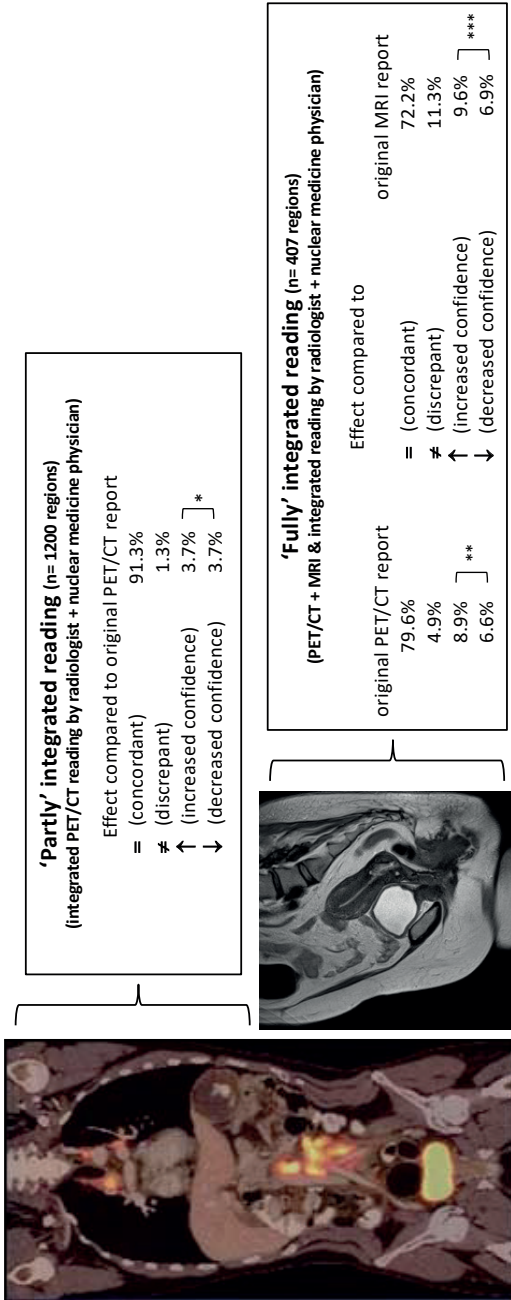


**Figure 4.** Overview of the results of the integrated reading. The 'partly' integrated reading refers to all regions that were not covered by the MRI FOV but only imaged with PET/CT; the 'fully' integrated assessment includes all regions that were included in both the PET/CT and MRI FOV. The differences in the proportion of cases with increased vs. decreased diagnostic confidence (using  $\chi^2$  comparison) were not statistically significant: \* $p= 1$ ; \*\* $p= 0.26$ ; \*\*\* $p= 0.18$

**Table 3.** Results of the subgroup analyses, comparing the percentage increase in confidence to the percentage decrease in confidence for the integrated reading vs. the original MRI and PET/CT reports, respectively.

Integrated reading	A. Anatomic subsites											
	Primary tumor region		Lymph node regions (local + distant)		Metastatic regions (liver, lung, bone, peritoneum)							
	Total no. of regions	Increase (%)	Decrease (%)	p value	Total no. of regions	Increase (%)	Decrease (%)	p value				
vs. MRI (fully integrated)	162	6.2	6.8	0.83	184	11.4	6.0	0.08	61	13.1	9.8	0.59
vs. PET (fully integrated)	162	6.2	6.2	1	184	10.3	6.0	0.14	61	11.5	9.8	0.78
vs. PET (partly integrated)	39	5.1	2.6	0.56	218	8.7	8.7	0.49	943	2.4	3.0	0.48
Integrated reading	B. Indication for imaging											
	Staging of primary malignancy (N= 99 patients)		Response evaluation after treatment (N= 32 patients)		Evaluation of recurrent tumour (N= 70 patients)							
	Total no. of regions	Increase (%)	Decrease (%)	p value	Total no. of regions	Increase (%)	Decrease (%)	p value	Total no. of regions	Increase (%)	Decrease (%)	p value
vs. MRI (fully integrated)	205	8.3	5.4	0.26	46	7.8	9.4	0.76	138	12.3	8.0	0.26
vs. PET (fully integrated)	205	7.3	5.9	0.56	46	7.8	12.5	0.41	138	11.6	5.1	0.06
vs. PET (partly integrated)	587	3.2	3.4	0.87	199	4.0	4.5	0.81	414	4.1	3.6	0.72
Integrated reading	C. Type of malignancy											
	Colorectal cancer (N= 77 patients)		Anal cancer (N= 29 patients)		Cervical cancer (N= 57 patients)							
	Total no. of regions	Increase (%)	Decrease (%)	p value	Total no. of regions	Increase (%)	Decrease (%)	p value	Total no. of regions	Increase (%)	Decrease (%)	p value
vs. MRI (fully integrated)	135	8.2	9.6	0.68	61	9.8	11.5	0.78	128	11.7	3.9	0.03
vs. PET (fully integrated)	135	8.2	9.6	0.68	61	11.5	6.6	0.37	128	7.8	5.5	0.47
vs. PET (partly integrated)	480	3.3	4.4	0.41	171	4.1	1.8	0.21	328	3.4	3.4	1

N.B. % of regions with increased vs. decreased were compared using  $\chi^2$

<sup>a</sup> Only subgroups with  $\geq 30$  patients per type of malignancy were separately analyzed MRI, magnetic resonance imaging; PET/CT, positron emission tomography (PET) with computer tomography (CT)

### Fully integrated reading (PET/CT+MRI)

The fully integrated reading was in excellent agreement with the original PET/CT reports ( $\kappa= 0.81$ ) and in good agreement with the original MRI reports ( $\kappa= 0.68$ ). After integrated reading, 3.2% of regions were assigned an inconclusive/equivocal (confidence level 3) score, compared with 5.7% for the original PET/CT ( $p= 0.05$ ) and 5.4% for the original MRI reports ( $p= 0.14$ ). Compared with the original PET/CT and MRI reports, there was an overall trend toward more increase, rather than decrease in confidence, although the results did not reach statistical significance: an increase in confidence was observed in 8.9% and 9.6% of regions, respectively, versus a decrease in confidence in 6.6% and 6.9% ( $p= 0.18$  and  $p= 0.26$ ). In the subgroup analyses, the increase in confidence was most pronounced for assessment of lymph nodes when compared with the original MRI reports (11.4% increase vs. 6.0% decrease,  $p= 0.08$ ) and for cases concerning cervical cancer (11.7% increase vs. 3.9% decrease,  $p=0.03$ ). Compared with the original PET/CT reports, the increase in confidence was most pronounced for recurrent disease cases (11.6% increase vs. 5.1% decrease;  $p= 0.06$ ). The only subgroup with an overall trend toward a decrease in confidence was response evaluation after treatment, though results did not reach statistical significance ( $p= 0.41-0.81$ ).

Agreement of the partly integrated reading with the original PET/CT reports was good ( $\kappa= 0.74$ ). There was no net effect on diagnostic confidence (3.7% increase vs. 3.7% decrease in confidence compared to the original PET/CT reports), nor was there a statistically significant change in the proportion of equivocal scores after the integrated reading (1.4% vs. 1.8%,  $p= 0.45$ ).

The chronologic order in which the imaging examinations were performed (PET/CT or MRI performed first) did not significantly affect results when comparing agreement between the integrated and original reports,  $p= 0.44-0.83$ .



## DISCUSSION

This study compared integrated side-by-side reading of F-18 FDG-PET/CT and abdominal MRI by a radiologist and a nuclear medicine physician with the conventional clinical approach of separate reading and reporting of the two exams. Our results show that, in approximately one-third of patients, this integrated reading led to discrepant findings compared to the original reports, which would have had a potential clinical impact in 12% of the total study cohort. In addition, we observed a trend toward a small relative increase in diagnostic confidence (particularly in lymph nodes, gynecological cases, and recurrent disease) and a reduction in the proportion of inconclusive outcomes in regions that were covered by both the PET/CT and MRI FOV, i.e., regions where a fully integrated reading of PET/CT and MR images could be achieved. In regions outside the MRI FOV, combined partly integrated reading of the PET and low-dose CT images by a nuclear medicine physician and a radiologist did not alter staging compared to the original PET/CT reports. In a previous report, Catalano et al compared hybrid PET/MRI to same-day PET/CT in a mixed cohort of 134 patients. They reported that the PET/MRI approach led to a potential change in clinical management in 26 of 134 (19%) of patients.<sup>7</sup> This number is similar to the 12% of patients with clinically significant discrepant findings in our current study cohort. The majority of discrepant findings in our study occurred in lymph nodes. The lymph node regions were also the regions where the most pronounced effect on diagnostic confidence was observed, particularly when compared to the original MRI-reports: an increase in confidence was observed in 11.4% (vs. a decrease in 6.0%,  $p = 0.08$ ). It is well known that staging of lymph nodes on MRI is challenging due to a lack of reliable criteria. Size is one of the main criteria used, but no optimal cutoff exists. In small nodes, metastases can easily be missed, while reactively enlarged lymph nodes are often over-staged.<sup>36</sup> In specific cancer types, such as cervical cancer, PET is known to be of value to help differentiate lymph node positive disease.<sup>37–39</sup> In these cases, a combined reading of MRI and PET/CT can be beneficial, as the soft tissue detail of MRI can aid in anatomically localizing lymph nodes, whereas the metabolic information from PET can be used to distinguish the metastatic ones. This ultimately may lead to a more confident and uniform diagnosis of the N-stage. Changes in nodal stage after integrated reading had a potential clinical impact in 15 cases. These were mainly cases where up- or downstaging of nodes would change the extension of the radiotherapy field, for example to cover para-aortic nodes in cervical cancer, or change the need for additional resection of para-iliac lymph nodes in rectal cancer. In two patients, downstaging of nodes after integrated reading could have avoided invasive

additional diagnostic procedures (Figure 5). In the cases for which histopathology (or an alternative standard of reference) was available, it was found that integrated reading correctly altered the nodal stage in six cases. However, there were also four cases in which integrated reading led to an incorrect change in nodal stage. This reflects that - despite an overall trend toward increased confidence when combining the information from PET/CT and MRI - nodal staging remains a challenging task with a risk for erroneous image interpretation.

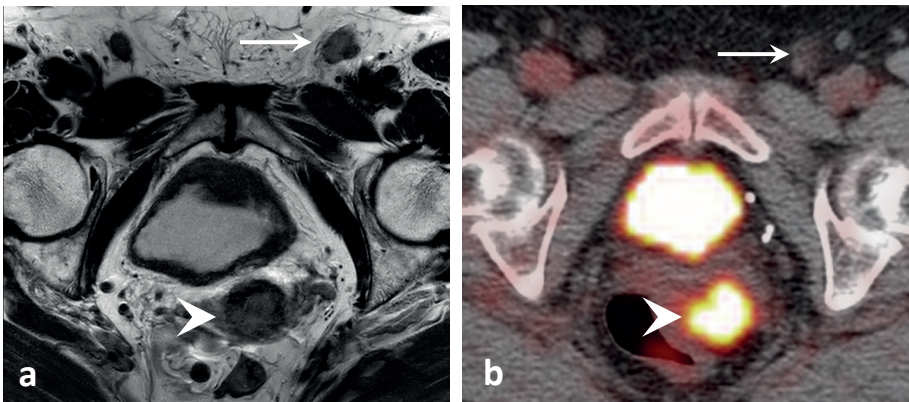


**Figure 5** Example of clinically significant discrepant case. T2-weighted MRI (a) and PET/CT fusion (b) images of a female patient staged for primary cervical carcinoma. The primary tumor in the cervix (arrowhead) was recognized in both original reports as well as after integrated reading (assigned a confidence score of 5 in all CRFs). In the original MRI report, a suspicious (confidence score 4) left inguinal lymph node was reported (arrow in a). In the original PET/CT report, the same node (arrow in b) was reported to be benign (confidence score 1). Additional ultrasound-guided fine-needle aspiration (FNA) was performed, which confirmed a benign lymph node. Integrated reading of the images resulted in the correct diagnosis of a benign node (confidence score 2). Compared to the original separate (and discrepant) reports, integrated reading would thus have led to a more uniform diagnosis, which could have prevented unnecessary FNA.

The second most observed cause of discrepancy was the post-treatment differentiation of locally recurrent (or residual) disease. Interestingly, evaluation of recurrent disease was also one of the settings where the effect on diagnostic confidence was most evident in the subgroup analyses, with a borderline significant increase in confidence compared to the original PET/CT reports (11.6% increase vs. 5.1% decrease in confidence;  $p = 0.06$ ). In these cases, the morphologic detail of MRI, combined with the expert anatomical input from a trained radiologist, can be of added value to help the nuclear medicine physician make a more confident distinction between recurrent disease and alternative causes of increased FDG accumulation such as abscesses, fistulas, or treatment-related inflammation. Incidentally, discrepant findings concerned additional detected lesions such as peritoneal (**Figure 6**) or lung metastases that were not identified in the original reports or vice versa. Interestingly, the subgroup of cases assessed for evaluation of treatment response was the only group where we observed an overall trend (albeit not statistically significant) toward a decrease in confidence after integrated reading. Although speculation should be avoided because of the small number of events in this subgroup (constituting only 64 of the total of 1607 regions analyzed), this decrease in confidence may be attributed to difficulties of anatomical MRI to differentiate vital tumor remnants in areas of post-radiation fibrosis,<sup>40</sup> and the decreased sensitivity of PET to detect small-volume residual disease after treatment.<sup>41</sup>

The overall positive trend toward a small increase in diagnostic confidence from combining PET/CT and MRI found in this study is in line with previous reports that also found a positive effect for integrated reading of PET(-CT) and MRI, either acquired sequentially or using hybrid PET/MRI systems.<sup>6,11-13,21,42-44</sup> Reduction in equivocal scores (3.2% for the integrated reading vs. 5.7% and 5.4% for the separate PET/CT and MRI reports, respectively) is similar to that previously reported. Brendle et al. compared integrated (hybrid) PET/MRI to separate PET/CT and MRI reading in a small cohort of 15 colorectal cancer patients. They showed that integrated PET/MRI reading resulted in a lower proportion of equivocal scores (2.8%) compared with PET/CT (3.9%) or MRI alone (7.8% with DWI and 10.6% without DWI), but only when the PET/MRI reading protocol included a DWI sequence.<sup>10</sup> The latter confirms the findings of several other reports that a DWI sequence benefits the MRI detection of malignant lesions (in various types of malignancies).<sup>45,46</sup> DWI is routinely performed in the majority of MRI protocols in our institute, and was available in 92% of MRI examinations of the current study cohort. In the subgroup of regions that were not included in the MRI-FOV, integrated reading merely consisted of combined assessment of the PET and low-dose CT images by a radiologist and a nuclear medicine physician. This partly integrated reading did not

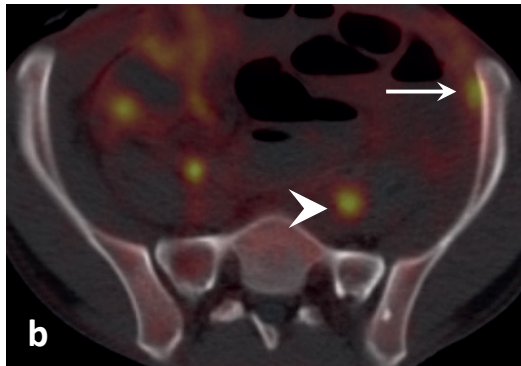
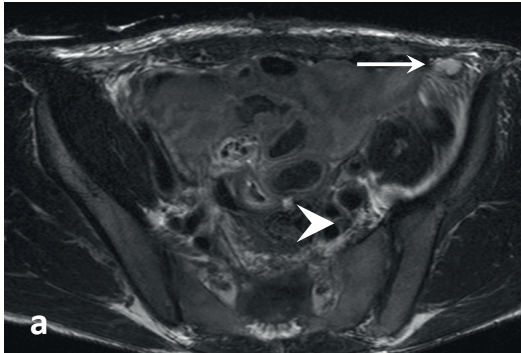


**Figure 6** Example of clinically significant discrepant case. T2-weighted MRI (a) and PET/CT fusion (b) images of a male patient 1.5 months after cytoreductive surgery with HIPEC (hyperthermic intraperitoneal chemotherapy) for metastasized mucinous-type sigmoid cancer. After integrated reading, the readers together identified two lesions (arrow and arrowhead) which they classified as recurrent peritoneal metastases (confidence score 5). In the original MRI report, the ventral lesion (arrow) was interpreted as postoperative fluid and assigned a confidence score 1 and the dorsal lesion (arrowhead) was not reported. In the original PET/CT report, the ventral lesion was not reported and the dorsal lesion was interpreted as urine activity in the left ureter (confidence score 1). On the follow-up CT performed 2.5 months later (c), both lesions progressed to large peritoneal masses (in circles), confirming recurrent disease. In this case, integrated reading would have led to a change in both disease stage and clinical management.

3

alter staging results compared to the original separate imaging reports. Apparently, the contribution provided by the radiologist in this setting is of no additional value.

There are some limitations to our study design, in addition to its retrospective nature. First, it was not possible to analyze the clinical effect of our discrepant findings in terms of diagnostic accuracy, since for most of the individual regions analyzed in this study histopathologic confirmation was not available and/or clinical follow-up was insufficient to serve as a standard of reference. This is why we chose to primarily focus on clinical impact and diagnostic confidence. Second, due to the time-consuming nature of the study, we chose to extract the scores for the separate MRI and PET/CT assessments from the original clinical reports and to perform the integrated reading by one team (of two readers) which does not account for inter-reader variations. The retrospective extraction of scores from the clinical reports may have introduced some bias, since assigning a confidence score based on free-text reports is inherently subject to some degree of subjectivity. In addition, the clinical reports originated from a multitude of readers (with varying levels of expertise), while the integrated team readings were done by a consistent group of readers with similar experience levels. Third, to represent a broad spectrum of indications for combined PET/CT and MRI (and to allow for meaningful analyses in a sufficiently large cohort), the studied population was heterogeneous in terms of primary tumor type and indication for imaging, which could make it more difficult to translate our results to specific clinical settings. We did perform additional subgroup analyses for specific tumor types/indications, but these results need to be interpreted with caution given the small and unevenly distributed size (and therefore limited statistical power) of these subgroups. Fourth, a fully integrated reading could only be achieved in the minority (25%) of anatomical regions that were included in the FOV of both the PET/CT and MRI, since the MRIs included in our study were all 'regional' and not 'whole body' examinations. Finally, the need to have two medical specialists sit together to perform an integrated reading can prove to be difficult to accomplish in busy daily clinical practice. To facilitate this, as well as the adoption of hybrid PET/MRI in the future, a change in workflow to further integrate radiology and nuclear medicine disciplines will be required.

## CONCLUSIONS

Integrated side-by-side reading of FDG-PET/CT and abdominal MRI by a multi-disciplinary team of a nuclear medicine physician and a radiologist can change staging outcomes in a substantial proportion of cases, with potential clinical impact in approximately 1 out of 9 patients in our cohort. In addition, integrated PET/MRI reading can have a small positive effect on diagnostic confidence and to help reach a more uniform diagnosis particularly in lymph nodes and in cervical cancer cases and to differentiate recurrent disease from benign post-treatment changes. These findings support further collaboration between radiology and nuclear medicine disciplines.

3

## REFERENCES

1. Löwenthal D, Zeile M, Lim WY et al (2011) Detection and characterisation of focal liver lesions in colorectal carcinoma patients: comparison of diffusion-weighted and Gd-EOB-DTPA enhanced MR imaging. *Eur Radiol* 21:832–840. doi: 10.1007/s00330-010-1977-2
2. Bozkurt M, Doganay S, Kantarci M et al (2011) Comparison of peritoneal tumor imaging using conventional MR imaging and diffusion-weighted MR imaging with different b values. *Eur J Radiol* 80:224–228. doi: 10.1016/j.ejrad.2010.06.004
3. Michielsen K, Dresen R, Vanslembrouck R et al (2017) Diagnostic value of whole body diffusion-weighted MRI compared to computed tomography for pre-operative assessment of patients suspected for ovarian cancer. *Eur J Cancer* 83:88–98. doi: 10.1016/j.ejca.2017.06.010
4. Miccò M, Vargas HA, Burger IA et al (2014) Combined pre-treatment MRI and 18F-FDG PET/CT parameters as prognostic biomarkers in patients with cervical cancer. *Eur J Radiol* 83: 1169–1176. doi: 10.1016/j.ejrad.2014.03.024
5. Joye I, Debuquoy A, Deroose CM et al (2017) Quantitative imaging outperforms molecular markers when predicting response to chemoradiotherapy for rectal cancer. *Radiother Oncol* 124:104–109. doi: 10.1016/j.radonc.2017.06.013
6. Mongula JE, Bakers FCH, Vöö S et al (2018) Positron emission tomography-magnetic resonance imaging (PET-MRI) for response assessment after radiation therapy of cervical carcinoma: a pilot study. *EJNMMI Res* 8:1. doi: 10.1186/s13550-017-0352-6
7. Catalano OA, Rosen BR, Sahani DV et al (2013) Clinical impact of PET/MR imaging in patients with cancer undergoing same-day PET/CT: initial experience in 134 patients – a hypothesis-generating exploratory study. *Radiology* 269:857–869. doi: 10.1148/radiol.13131306
8. Sotoudeh H, Sharma A, Fowler KJ, McConathy J, Dehdashti F (2016) Clinical application of PET/MRI in oncology. *J Magn Reson Imaging* 44:265–276. doi: 10.1002/jmri.25161
9. Singnurkar A, Poon R, Metser U (2017) Comparison of 18F-FDG- PET/CT and 18F-FDG-PET/MR imaging in oncology: a systematic review. *Ann Nucl Med* 31:366–378. doi: 10.1007/s12149-017-1164-5
10. Brendle C, Schwenzer NF, Rempp H et al (2016) Assessment of metastatic colorectal cancer with hybrid imaging: comparison of reading performance using different combinations of anatomical and functional imaging techniques in PET/MRI and PET/CT in a short case series. *Eur J Nucl Med Mol Imaging* 43:123–132. doi: 10.1007/s00259-015-3137-z

11. Beiderwellen K, Grueneisen J, Ruhlmann V et al (2015) [(18)F]FDG PET/MRI vs. PET/CT for whole-body staging in patients with recurrent malignancies of the female pelvis: initial results. *Eur J Nucl Med Mol Imaging* 42:56–65. doi: 10.1007/s00259-014-2902-8
12. Grueneisen J, Beiderwellen K, Heusch P et al (2014) Simultaneous positron emission tomography/magnetic resonance imaging for whole-body staging in patients with recurrent gynecological malignancies of the pelvis. *Invest Radiol* 49:808–815. doi: 10.1097/RLI.0000000000000086
13. Ruhlmann V, Ruhlmann M, Bellendorf A et al (2016) Hybrid imaging for detection of carcinoma of unknown primary: a preliminary comparison trial of whole-body PET/MRI versus PET/CT. *Eur J Radiol* 85:1941–1947. doi: 10.1016/j.ejrad.2016.08.020
14. Drzezga A, Souvatzoglou M, Eiber M et al (2012) First clinical experience with integrated whole-body PET/MR: comparison to PET/CT in patients with oncologic diagnoses. *J Nucl Med* 53: 845–855. doi: 10.2967/jnumed.111.098608.
15. Grueneisen J, Schaarschmidt BM, Beiderwellen K et al (2014) Diagnostic value of diffusion-weighted imaging in simultaneous 18F-FDG PET/MR imaging for whole-body staging of women with pelvic malignancies. *J Nucl Med* 55:1930–1935. doi: 10.2967/jnumed.114.146886
16. Grueneisen J, Schaarschmidt BM, Heubner M et al (2015) Implementation of FAST-PET/MRI for whole-body staging of female patients with recurrent pelvic malignancies: a comparison to PET/CT. *Eur J Radiol* 84:2097–2102. doi: 10.1016/j.ejrad.2015.08.010
17. Grueneisen J, Schaarschmidt BM, Heubner M et al (2015) Integrated PET/MRI for whole-body staging of patients with primary cervical cancer: preliminary results. *Eur J Nucl Med Mol Imaging* 42:1814–1824. doi: 10.1007/s00259-015-3131-5
18. Lee MS, Cho JY, Kim SY et al (2017) Diagnostic value of integrated PET/MRI for detection and localization of prostate cancer: comparative study of multiparametric MRI and PET/CT. *J Magn Reson Imaging* 45:597–609. doi: 10.1002/jmri.25384
19. Sarabhai T, Schaarschmidt BM, Wetter A et al (2018) Comparison of 18F-FDG PET/MRI and MRI for pre-therapeutic tumor staging of patients with primary cancer of the uterine cervix. *Eur J Nucl Med Mol Imaging* 45:67–76. doi: 10.1007/s00259-017-3809-y
20. Sawicki LM, Grueneisen J, Schaarschmidt BM et al (2016) Evaluation of 18 F-FDG PET/MRI, 18 F-FDG PET/CT, MRI, and CT in whole-body staging of recurrent breast cancer. *Eur J Radiol* 85:459–465. doi: 10.1016/j.ejrad.2015.12.010



21. Grueneisen J, Sawicki LM, Wetter A et al (2017) Evaluation of PET and MR datasets in integrated 18F-FDG PET/MRI: a comparison of different MR sequences for whole-body restaging of breast cancer patients. *Eur J Radiol* 89:14–19. doi: 10.1016/j.ejrad.2016.12.019
22. Pace L, Nicolai E, Luongo A et al (2014) Comparison of whole-body PET/CT and PET/MRI in breast cancer patients: lesion detection and quantitation of 18F-deoxyglucose uptake in lesions and in normal organ tissues. *Eur J Radiol* 83:289–296. doi: 10.1016/j.ejrad.2013.11.002
23. Catalano OA, Daye D, Signore A et al (2017) Staging performance of whole-body DWI, PET/CT and PET/MRI in invasive ductal carcinoma of the breast. *Int J Oncol* 51:281–288. doi: 10.3892/ijo.2017.401
24. Eiber M, Takei T, Souvatzoglou M et al (2014) Performance of whole-body integrated 18F-FDG PET/MR in comparison to PET/CT for evaluation of malignant bone lesions. *J Nucl Med* 55:191–197. doi: 10.2967/jnumed.113.12364
25. Schaarschmidt BM, Grueneisen J, Metznermacher M et al (2017) Thoracic staging with 18F-FDG PET/MR in non-small cell lung cancer - does it change therapeutic decisions in comparison to 18F-FDG PET/CT? *Eur Radiol* 27:681–688. doi: 10.1007/s00330-016-4397-0
26. Sawicki LM, Grueneisen J, Buchbender C et al (2016) Comparative performance of 18F-FDG PET/MRI and 18F-FDG PET/CT in detection and characterization of pulmonary lesions in 121 oncologic patients. *J Nucl Med* 57:582–586. doi: 10.2967/jnumed.115.167486
27. Rausch I, Quick HH, Cal-Gonzalez J, Sattler B, Boellaard R, Beyer T (2017) Technical and instrumental foundations of PET/MRI. *Eur J Radiol* 94:A3–A13. doi: 10.1016/j.ejrad.2017.04.004
28. Brendle CB, Schmidt H, Fleischer S, Braeuning UH, Pfannenberga CA, Schwenzer NF (2013) Simultaneously acquired MR/PET images compared with sequential MR/PET and PET/CT: alignment quality. *Radiology* 268:190–199. doi: 10.1148/radiol.13121838
29. Kitajima K, Suenaga Y, Ueno Y et al (2013) Value of fusion of PET and MRI for staging of endometrial cancer: comparison with 18F-FDG contrast-enhanced PET/CT and dynamic contrast-enhanced pelvic MRI. *Eur J Radiol* 82:1672–1676. doi: 10.1016/j.ejrad.2013.05.005
30. Kitajima K, Suenaga Y, Ueno Y et al (2014) Fusion of PET and MRI for staging of uterine cervical cancer: comparison with contrast-enhanced 18F-FDG PET/CT and pelvic MRI. *Clin Imaging* 38:464–469. doi: 10.1016/j.clinimag.2014.02.006

31. Stecco A, Buemi F, Cassarà A et al (2016) Comparison of retrospective PET and MRI-DWI (PET/MRI-DWI) image fusion with PET/CT and MRI-DWI in detection of cervical and endometrial cancer lymph node metastases. *Radiol Med* 121:537–545. doi: 10.1007/s11547-016-0626-5
32. Kim SK, Choi HJ, Park SY et al (2009) Additional value of MR/ PET fusion compared with PET/CT in the detection of lymph node metastases in cervical cancer patients. *Eur J Cancer* 45:2103–2109. doi: 10.1016/j.ejca.2009.04.006
33. Nakajo K, Tatsumi M, Inoue A et al (2010) Diagnostic performance of fluoro-deoxyglucose positron emission tomography/magnetic resonance imaging fusion images of gynecological malignant tumors: comparison with positron emission tomography/computed tomography. *Jpn J Radiol* 28:95–100. doi: 10.1007/s11604-009-0387-3
34. Kanda T, Kitajima K, Suenaga Y et al (2013) Value of retrospective image fusion of 18 F-FDG PET and MRI for preoperative staging of head and neck cancer: comparison with PET/CT and contrast- enhanced neck MRI. *Eur J Radiol* 82:2005–2010. doi: 10.1016/j.ejrad.2013.06.02
35. Hempel JM, Kloeckner R, Krick S et al (2016) Impact of combined FDG-PET/CT and MRI on the detection of local recurrence and nodal metastases in thyroid cancer. *Cancer Imaging* 16:37. doi: 10.1186/s40644-016-0096-y.
36. Lahaye MJ, Engelen SM, Nelemans PJ et al (2005) Imaging for predicting the risk factors –the circumferential resection margin and nodal disease– of local recurrence in rectal cancer: a meta-analysis. *Semin Ultrasound CT MR* 26:259–268. doi: 10.1053/j.sult.2005.04.005
37. Belhocine T, Thille A, Fridman V et al (2002) Contribution of whole-body 18FDG PET imaging in the management of cervical cancer. *Gynecol Oncol* 87:90–97. doi: 10.1006/gyno.2002.6769
38. Narayan K, Hicks RJ, Jobling T, Bernshaw D, McKenzie AF (2001) A comparison of MRI and PET scanning in surgically staged loco-regionally advanced cervical cancer: potential impact on treatment. *Int J Gynecol Cancer* 11:263–271. doi: 10.1046/j.1525-1438.2001.011004263.x
39. Mahmud A, Poon R, Jonker D (2017) PET imaging in anal canal cancer: a systematic review and meta-analysis. *Br J Radiol* 90: 20170370. doi: 10.1259/bjr.20170370
40. Lambregts DM, Vandecaveye V, Barbaro B et al (2011) Diffusion- weighted MRI for selection of complete responders after chemoradiation for locally advanced rectal cancer: a multicenter study. *Ann Surg Oncol* 18:2224–2231. doi: 10.1245/s10434-011-1607-5

41. Van Kessel CS, Buckens CF, van den Bosch MA et al (2012) Preoperative imaging of colorectal liver metastases after neoadjuvant chemotherapy: a meta-analysis. *Ann Surg Oncol* 19:2805–2813. doi: 10.1245/s10434-012-2300-z
42. Samarin A, Hüllner M, Queiroz MA et al (2015) 18F-FDG-PET/MR increases diagnostic confidence in detection of bone metastases compared with 18F-FDG-PET/CT. *Nucl Med Commun* 36:1165–1173. doi: 10.1097/MNM.0000000000000387.
43. Huellner MW, Appenzeller P, Kuhn FP et al (2014) Whole-body nonenhanced PET/MR versus PET/CT in the staging and restaging of cancers: preliminary observations. *Radiology* 273:859–869. doi: 10.1148/radiol.14140090
44. Kuhn FP, Hüllner M, Mader CE et al (2014) Contrast-enhanced PET/MR imaging versus contrast-enhanced PET/CT in head and neck cancer: how much MR information is needed? *J Nucl Med* 55: 551–558. doi: 10.2967/jnumed.113.125443
45. Taouli B, Beer AJ, Chenevert T et al (2016) Diffusion-weighted imaging outside the brain: consensus statement from an ISMRM- sponsored workshop. *J Magn Reson Imaging* 44:521–540. doi: 10.1002/jmri.25196
46. Charles-Edwards EM, deSouza NM (2006) Diffusion-weighted magnetic resonance imaging and its application to cancer. *Cancer Imaging* 6:135–143. doi: 10.1102/1470-7330.2006.0021

Supplementary Table 1 . Overview of individual 'major impact' discrepant cases with their staging outcomes											
N°	Case description	Discrepant region(s)	Outcome PET	Outcome MRI	Outcome integrated	Final clinical outcome	Effect of integrated scoring				
1	Colorectal ca. primary staging.	Node (iliac)	-	N/A	+	unknown	No histopathology or adequate FU available				unknown
2	Colorectal ca. primary staging.	Node (aortic bifurcation)	-	N/A	+	unknown	No histopathology or adequate FU available				unknown
3	Colorectal ca. primary staging.	Node (liver hilus)	-	+	-	-	Biopsy proven (endo-esophageal US-guided) negative lymph node				correct
4	Colorectal ca. Suspected recurrence.	Tumour (recurrence rectum) Node (iliac)	+ +	+/- -	- -	- -	Negative biopsy Negative FU (54 months)				correct
5	Colorectal ca. Suspected recurrence.	Node (iliac) Peritoneal metastases	- -	- -	+ +	unknown +	Extensive growth during FU (see Figure 5)				correct
6	Colorectal ca. Suspected recurrence.	Node (iliac)	+	-	-	unknown	No histopathology or adequate FU available				unknown
7	Colorectal ca. Suspected recurrence.	Peritoneal metastasis	-	N/A	+	-	Negative FU (30 months)				incorrect
8	Colorectal ca. M+ (liver, lung). Response evaluation after chemo and RT.	Node (lung hilus)	-	N/A	+	+	FNAC confirmed lymph node metastasis				correct
9	Colorectal ca. M+ (liver) for which previous ablation. Restaging of liver.	Liver metastasis	+	-	+	unknown	No biopsy or adequate FU available (treated with Yttrium embolization)				unknown
10	Colorectal ca., M+ (liver). Restaging prior to RFA liver.	Node (aortic bifurcation)	+	N/A	-	+	Pathology confirmed lymph node metastasis				incorrect
11	Cervical ca. primary staging.	Node (iliac)	-	-	+	-	Negative pathology after pelvic node dissection				incorrect
12	Cervical ca. primary staging.	Node (inguinal)	-	+	-	-	Negative cytology after ultrasound-guided FNA				correct

Supplementary Table 1. (continued, 2/2) Overview of individual 'major impact' discrepant cases with their staging outcomes

N°	Case description	Discrepant region(s)	Outcome PET	Outcome MRI	Outcome integrated	Final clinical outcome	Effect of integrated scoring
13	Cervical ca. primary staging.	Node (inguinal, iliac)	-	+	-	-	Negative cytology after ultrasound guided FNA correct
14	Cervical ca. primary staging.	Node (para-aortic)	-	N/A	+	unknown	No histopathology or adequate FU available unknown
15	Cervical ca. after CRT. Suspected recurrence.	Tumour (recurrence cervix)	+	+/-	-	+	Pathology confirmed recurrence incorrect
16	Cervical ca. after CRT. Suspected recurrence.	Lung metastasis	+	N/A	-	-	Negative FU (48 months) correct
17	Cervical ca after CRT. Suspected recurrence.	Bone metastasis (sacrum)	+/-	+	-	unknown	No histopathology or adequate FU available unknown
18	Cervical ca. after CRT. Response evaluation.	Tumour (residue cervix)	-	+	-	unknown	No histopathology or adequate FU available unknown
19	Cervical ca. Response evaluation.	Lung metastasis	-	N/A	+	unknown	No histopathology or adequate FU available unknown
20	Anal ca. after CRT. Response evaluation.	Tumour (residue anus)	+	+	-	-	Negative FU (24 months) correct
21	Anal ca. after CRT. Response evaluation.	Node (iliac)	-	-	+	-	Negative FU (60 months) incorrect
22	Vulva ca. primary staging.	Node (inguinal, iliac)	+/-	-	+	-	Negative pathology after pelvic node dissection incorrect
23	Vaginal ca. primary staging.	Node (obturator)	-	+	+	unknown	No histopathology or adequate FU available unknown
24	Perineal squamous cell ca. recurrence, for which CRT. Response evaluation.	Lung metastasis	+	N/A	-	unknown	No histopathology or adequate FU available unknown
25	Urethral ca. Suspected residue post-surgery.	Tumour (residue urethra)	-	-	+	-	Negative FU (43 months) incorrect

N/A indicates that the discrepant region was not within the MRI field of view. M+: metastasized disease; CRT: chemo-radiotherapy; FU: follow-up; US: ultrasound; FNA: fine-needle aspiration;





The background is a complex, abstract composition of various shades of blue. It features large, overlapping, organic shapes that resemble crumpled paper or liquid droplets. A prominent feature is a large, curved, semi-transparent area with a fine halftone dot pattern, which frames the central text. The overall effect is a sense of depth and movement, with light and shadow playing across the different layers and textures.

## Chapter 4

# VALUE OF COMBINED MULTIPARAMETRIC MRI AND FDG-PET/CT TO IDENTIFY WELL-RESPONDING RECTAL CANCER PATIENTS BEFORE THE START OF NEOADJUVANT CHEMORADIATION

Niels W. Schurink\*, Lisa A. Min\*, Maaike Berbee, Wouter van Elmpt,  
Joost J. M. van Griethuysen, Frans C. H. Bakers, Sander Roberti,  
Simon R. van Kranen, Max J. Lahaye, Monique Maas, Geerard L. Beets,  
Regina G. H. Beets-Tan, Doenja M. J. Lambregts

\* these authors contributed equally to this work

*European Radiology* (2020) 30(5):2945–2954 doi: 10.1007/s00330-019-06638-2



# ABSTRACT

## Objectives

To explore the value of multiparametric MRI combined with FDG-PET/CT to identify well-responding rectal cancer patients before the start of neoadjuvant chemoradiation.

## Methods

Sixty-one locally advanced rectal cancer patients who underwent a baseline FDG-PET/CT and MRI (T2W + DWI) and received long-course neoadjuvant chemoradiotherapy were retrospectively analysed. Tumours were delineated on MRI and PET/CT from which the following quantitative parameters were calculated: T2W volume and entropy, ADC mean and entropy, CT density (mean-HU), SUV maximum and mean, metabolic tumour volume (MTV<sub>42%</sub>) and total lesion glycolysis (TLG). These features, together with sex, age, mrTN-stage ("baseline parameters") and the CRT-surgery interval were analysed using multivariable stepwise logistic regression. Outcome was a good (TRG 1–2) versus poor histopathological response. Performance (AUC) to predict response was compared for different combinations of baseline ± quantitative imaging parameters and performance in an 'independent' dataset was estimated using bootstrapped leave-one-out cross-validation (LOOCV).

## Results

The optimal multivariable prediction model consisted of a combination of baseline + quantitative imaging parameters and included mrT-stage (OR 0.004,  $p < 0.001$ ), T2W-signal entropy (OR 7.81,  $p = 0.0079$ ) and T2W volume (OR 1.028,  $p = 0.0389$ ) as the selected predictors. AUC in the study dataset was 0.88 and 0.83 after LOOCV. No PET/CT features were selected as predictors.

## Conclusions

A multivariable model incorporating mrT-stage and quantitative parameters from baseline MRI can aid in identifying well-responding patients before the start of treatment. Addition of FDG-PET/CT is not beneficial.

## INTRODUCTION

Current standard treatment for locally advanced rectal cancer (LARC) consists of long-course neoadjuvant chemoradiotherapy (CRT) followed by surgery. In 15–25% of these patients, no residual tumour is found in the resection specimen.<sup>1,2</sup> This has raised the question whether for this group surgery may be avoided.<sup>3,4</sup> Organ-preserving treatments like the ‘watch-and-wait’ approach (W&W) are nowadays increasingly considered as an alternative to surgery, with good reported functional outcome, disease-free and overall survival.<sup>5–9</sup>

At this point, there is no pre-therapy classification method to predict how patients will respond to CRT. Although this information would currently not likely impact treatment, predicting response before the start of therapy could have a clinical impact in the future: in patients likely to respond well, neoadjuvant treatment may be further intensified to increase the chance of organ preservation, while in predicted non-responders futile CRT may be avoided. Pre-treatment response prediction may furthermore help create opportunities to select small and low-risk tumours (now typically managed with surgery without neoadjuvant treatment) to undergo CRT in case of a predicted good response, with the specific aim to achieve organ preservation.<sup>10</sup> These developments urge the need for accurate predictive biomarkers.

There is a growing interest in the value of imaging as a potential source for these biomarkers, with numerous reports exploring the potential of metabolic imaging (FDG-PET/CT)<sup>11–14</sup> and MRI with the addition of functional imaging sequences such as diffusion-weighted imaging (DWI).<sup>15–20</sup> Most studies so far have focused on single-modality imaging and included only one or a few imaging markers. Linking multiparametric data from PET and MRI may be beneficial to provide a more comprehensive insight into underlying tumour biology. The few reports that have investigated such a multimodality PET/CT + MRI assessment in rectal cancer, suggested its potential, in particular when applying sequential imaging (pre- and post-CRT) and for higher-order (radiomics) imaging variables.<sup>15,20</sup>

This study aims to further explore the value of combining baseline FDG-PET/CT and multiparametric MRI to identify before onset of treatment those patients that will respond well to neoadjuvant chemoradiation.

# METHODS

This study was approved by the local institutional review board. Informed consent was not required due to the retrospective nature of this study.

## *Patients*

From 2008 to 2015, a cohort of 104 locally advanced ( $\geq T3$  and/or N+) rectal cancer patients was identified from the local institutional database of the department of Radiation Oncology of Maastricht University Medical Center (Maastricht Clinic), that underwent both routine MRI for primary tumour staging and an additional FDG-PET/CT at baseline (prior to any treatment), either as part of a previous study protocol (trial number NCT00969657) or for standard of care radiotherapy planning. From this cohort, 61 patients were selected based on the following inclusion criteria: (1) treatment consisting of long-course CRT followed by surgery or W&W, and (2) sufficient information to establish the treatment response outcome (histopathology or  $\geq 2$  years of clinical follow-up in case of W&W-surveillance). The standard CRT protocol consisted of 50.4 Gy with concurrent capecitabine-based chemotherapy. Patients who received a non-standardised treatment, had insufficient quality imaging or mucinous tumour histology were excluded (see **Figure 1**).

## **MRI**

MRIs were performed at 1.5 Tesla (Intera (Achieva)  $n = 43$  or Ingenia  $n = 18$ , Philips Healthcare) and included a T2W-sequence in 3 orthogonal directions, and an axial DWI-sequence including b-values  $b = 0$  and  $b = 1000 \text{ s/mm}^2$ . Apparent diffusion coefficient (ADC) maps were calculated by fitting a mono-exponential decay function to the  $b = 0$  and  $b = 1000 \text{ s/mm}^2$  images. The axial T2W-MRI and DWI were angled in identical planes, perpendicular to the tumour axis. Further protocol details are given in **Table 1**. Patients received no spasmolytic or bowel preparation/filling.

## **FDG-PET/CT**

$^{18}\text{F}$ -FDG-PET/CT was performed on a Siemens Biograph 40 TruePoint PET/CT scanner (SIEMENS medical). A bolus of 2-deoxy-2-[ $^{18}\text{F}$ ]fluoro-D-glucose ( $^{18}\text{F}$  FDG, from here on: FDG) of 2.5 MBq/kg ( $n = 52$ ) or 4.0 MBq/kg ( $n = 9$ ) was administered intravenously, after a 6-h fast (blood glucose level  $< 10 \text{ mmol/L}$ ). Scanning started after an incubation time of  $60 (\pm 5) \text{ min}$ , with 5 min per bed position, and ran from the skull base to upper-thighs (reconstructed to 3 mm slice thickness, 4.07 mm in-plane resolution). A non-enhanced CT scan (120 kVp, 113–297 mAs with automatic dose modulation) was

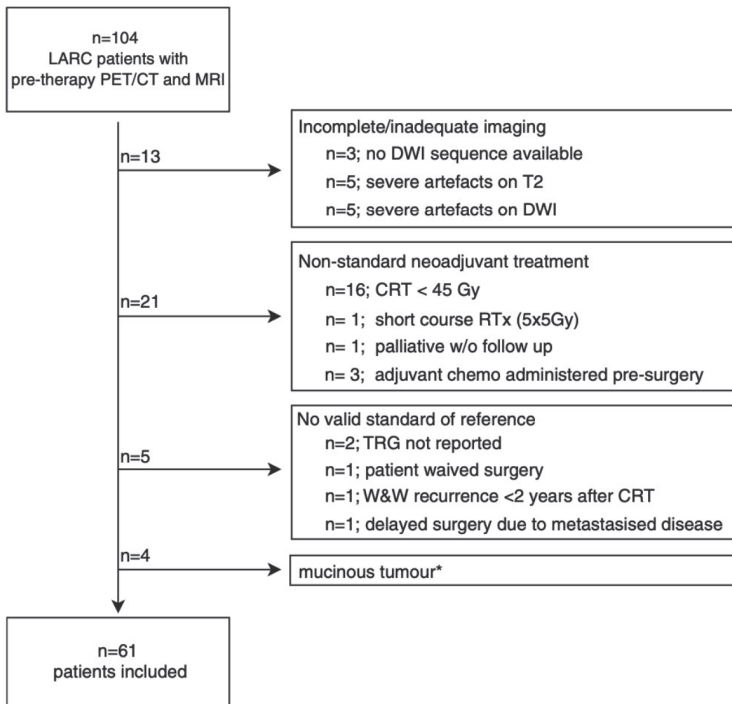


**Figure 1.** Patient in- and exclusion flowchart.

CRT chemoradiotherapy, LARC locally advanced rectal cancer ( $\geq T3$  and/or N+), RTx radiotherapy, TRG tumour regression grade (Mandard's), W&W watch-and-wait. \* Predominantly mucinous tumours were excluded because these typically exhibit distinctly different characteristics on PET and MRI and show a different response to CRT.

acquired for attenuation correction, anatomical correlation and radiotherapy planning (reconstructed to 3 mm slice thickness, 0.98 mm in-plane resolution).

### Quantitative MRI and PET/CT parameters

The image analysis workflow is illustrated in **Figure 2**. PET/ CT and MR images were transferred to an offline workstation for tumour segmentation, performed using dedicated software (3D Slicer, version 4.8.1). Feature extraction was performed using the open-source software PyRadiomics (version 2.1.2).<sup>21</sup>

**Table 1. MRI protocol**

	T2-weighted	Diffusion-weighted
Echo time (ms)	130–150	65.74–84.88
Repetition time (ms)	3427–16,738	2480–5545
Echo train length	25–28	53–87
Slice thickness (mm)	3–5 <sup>a</sup>	5
Slice gap (mm)	3.3–7.03	4–6.02
In-plane resolution (mm)	0.78125	1.25–1.71875
Number of averages	2–6	3–10
b-values (s/mm <sup>2</sup> )	-	0, 1000 <sup>b</sup>
Fat suppression	-	STIR (n= 32), SPIR (n= 7), SPAIR (n= 22)

STIR short-TI inversion recovery, SPIR spectral presaturation with inversion recovery, SPAIR spectral attenuated inversion recovery

<sup>a</sup> n= 23 patients were scanned with 5 mm and n= 38 with 3 mm axial slice thickness

<sup>b</sup> Protocols included 3–7 b-values ranging from b0 to b2000 s/mm<sup>2</sup>, but for the purpose of this study only the b= 0 and b= 1000 s/mm<sup>2</sup> series were used for analyses and to calculate the ADC map

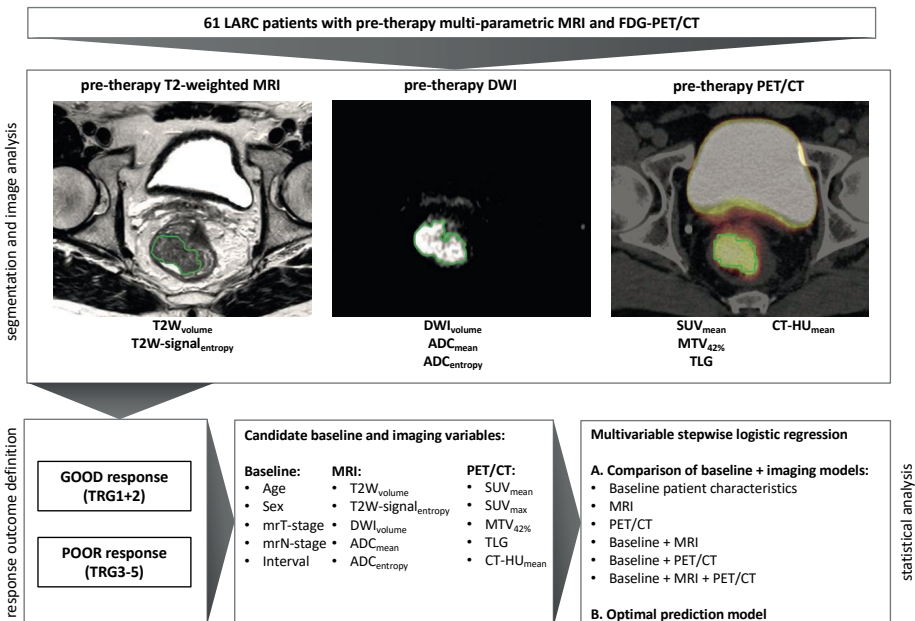


Figure 2. Schematic study outline

A board-certified radiologist (D.L., >9 years of rectal MRI experience) manually delineated whole-tumour volumes on the axial T2W-MRI and b1000-DWI, respectively, to calculate the following features: volume on T2W (T2Wvolume, mesh-volume in PyRadiomics), entropy of the T2W signal intensity histogram (T2W-signal<sub>entropy</sub>), volume on DWI (DWIvolume, mesh-volume in PyRadiomics), mean ADC (ADCmean) and entropy of the ADC intensity histogram (ADC<sub>entropy</sub>).

Metabolic tumour volumes (MTV<sub>42%</sub>) on PET/CT were semi-automatically segmented by one of the researchers experienced in PET segmentation (NS) by placing a volume of interest (VOI) over the tumour while taking care to avoid inclusion of physiologic uptake in the bladder. From this VOI, the metabolic tumour volume was calculated using a threshold of 42% of the maximum standardised uptake value (SUV<sub>max</sub>), according to methods previously described.<sup>22-24</sup> The MTV<sub>42%</sub> was used to calculate the mean standardised uptake value (SUV<sub>mean</sub>) and total lesion glycolysis (TLG; defined as SUV<sub>mean</sub> × MTV<sub>42%</sub>). The MTV<sub>42%</sub> segmentation was transferred to CT to calculate the mean Hounsfield unit (HU) (CT-HU<sub>mean</sub>).

The specific MRI and PET features described above were chosen as they represent relatively straightforward (first order) variables reflecting tumour size, heterogeneity, cellularity and metabolism, which have all shown potential in previous reports and which are relatively simple to reproduce.<sup>16,25-29</sup>

### Baseline patient characteristics

The following clinical baseline patient characteristics were documented: sex, age and T- and N-stage derived from routine clinical staging with MRI (further referred to as mrT-stage and mrN-stage). The latter were dichotomised as mrT3c-4 vs. mrT1-3b and mrN+ vs. mrN0, respectively.

### Response to chemoradiotherapy (standard of reference)

The primary outcome was the histopathological tumour regression grade (TRG) by Mandard.<sup>30</sup> Patients were classified as good responders (TRG1-2) or poor responders (TRG3-5). For W&W patients, a recurrence-free follow-up of ≥2 years was used as a surrogate endpoint of a complete response. For the purpose of this study, these patients were considered complete responders (TRG1) and classified in the good responders group.

### Statistical analysis

Statistical analysis was performed using R software (version 3.4.3; R Foundation for Statistical Computing).

The value of the quantitative MRI and PET/CT features and baseline patient characteristics to predict a good response was analysed by multivariable logistic regression, consisting of a forward stepwise feature selection method based on the Akaike Information Criterion (AIC). The AIC describes model quality as a tradeoff between model fit and model complexity (i.e. the number of variables). A lower AIC indicates a better model, and is achieved by a better goodness of fit or fewer variables.<sup>31,32</sup> The analysis workflow is summarised as follows:

- As described above, only a limited number of parameters (T2Wvolume, T2W-signal<sub>entropy</sub>, DWI<sub>volume</sub>, ADC<sub>mean</sub>, ADC<sub>entropy</sub>, MTV<sub>42%</sub>, SUV<sub>max</sub>, SUV<sub>mean</sub>, TLG, CT-HU, mrT-stage, mrN-stage, age, sex) were assessed to limit overfitting. These parameters were defined before the onset of the study based on previous literature showing their potential promise as predictors of response.<sup>16,25–28</sup> The interval between the last radiotherapy fraction and the final response evaluation (dichotomised as  $\leq 10$  vs.  $> 10$  weeks) was added as an additional variable, as longer intervals have been reported to result in higher response rates and could thus act as a potential confounder.<sup>33</sup>
- When two features showed a strong correlation (Pearson's correlation coefficient  $\rho \geq 0.8$ ), only one was entered in the feature selection process to reduce effects of multicollinearity.
- The multivariable modelling process was repeated separately for different subsets and combinations of baseline and/or imaging variables (baseline only, MRI only, PET/CT only, baseline + MRI, baseline + PET/CT, baseline + PET/CT + MRI). To limit effects of overfitting, the number of variables selected for each model was set to a maximum of 1 feature per 10 patients in the smallest outcome group (3 features in total).
- Predictive performance of each model was assessed by calculating the area under the receiver operating curve (AUC). Since our cohort size did not allow splitting of the data in a test and validation set, performance in an 'independent' dataset was estimated by performing leave-one-out cross-validation (LOOCV) with 500 bootstrap samples (to calculate confidence intervals). LOOCV involves building a model using the original dataset multiple times, while excluding one different patient each time to predict the

outcome. The cross-validated AUC is determined on the collective of these different predictions, and approximates the AUC in independent data.

To provide a complete overview of all investigated features, additional univariable logistic regression analysis was performed for each baseline and quantitative imaging variable. This was done independent of the multivariable analysis. P values <0.05 were considered statistically significant.

## RESULTS

### Patient characteristics

Baseline patient characteristics are reported in **Table 2**. In total, 54/61 patients underwent surgery: 6 (10%) had a TRG1, 18 (30%) TRG2, 19 (31%) TRG3, 11 (18%) TRG4 and 0 (0%) TRG5. The remaining seven patients (12%) were monitored with W&W and had a sustained clinical complete response (median follow-up of 59 months, range 26–89). This resulted in 31 good responders (51%, TRG 1–2) and 30 poor responders (49%, TRG 3–5).

### Comparison of different baseline and imaging models and their combinations

Results of the stepwise feature selection process including the different combinations of baseline patient characteristics, MRI and PET/CT variables are shown in **Table 3A**. The best fitting model (based on the smallest AIC) was the baseline + MRI model. The PET/CT-only model had the poorest fit and addition of PET/CT features to the 'baseline-only' or 'baseline + MRI' model was not beneficial. AUCs were 0.81 (baseline-only), 0.70 (MRI-only), 0.50 (PET/CT-only), 0.88 (baseline + MRI), 0.81 (baseline + PET/CT) and 0.88 (baseline + MRI + PET/CT), respectively.

### Optimised multivariable model

The optimised baseline + MRI model is summarised in **Table 3B**, and included mrT-stage (OR 0.004; 95% CI 0.00–0.09 for cT3c-4 vs. cT1-3b), T2W-signal<sub>entropy</sub> (OR per IQR 4.33; 95% CI 1.47–12.77) and T2W<sub>volume</sub> (OR 1.028 per cm<sup>3</sup>; 95% CI 1.00–1.05). The model had an AUC of 0.88 to predict good responders within our dataset, with a sensitivity of 0.68 (95% CI 0.49–0.83) when the ROC threshold was set at a specificity of 0.90. With leave-one-out cross-validation the found AUC was 0.83 (95% CI 0.70–0.96) with a sensitivity of 0.61 (95% CI 0.42–0.78) at a specificity of 0.90.



**Table 2.** Baseline characteristics of study population

<b>Baseline + staging</b>	Male / female	47 (77%) / 14 (23%)
	Age mean (sd)	68 (9)
	MRI-based T-stage (mrT-stage)	
	Early stage (mrT1-3b)	
	mrT1-2	5 (8%)
	mrT3a	0 (0%)
	mrT3b	34 (56%)
	Advanced stage (mrT3c-4b)	
	mrT3c	15 (25%)
	mrT3d	1 (2%)
	mrT4a	2 (3%)
	mrT4b	4 (7%)
	MR-based N-stage (mrN-stage)	
	mrN0	16 (26%)
	mrN1	30 (49%)
	mrN2	15 (25%)
	Treatment post-CRT	
Surgery	54 (88%)	
W&W	7 (12%)	
<b>Outcome</b>	TRG (Mandard)	
	1	13 (21%)
	2	18 (30%)
	3	19 (31%)
	4	11 (18%)
	5 <sup>a</sup>	0 (0%)
	Good response (= TRG1–2) / Poor response (= TRG3–5)	31% (51%) / 30% (49%)
<b>Treatment intervals (Median no. days and interquartile range)</b>	RT treatment duration	37 (36–51)
	Time from MRI to start CRT	27 (9)
	Time from PET to start CRT	7 (2)
	Time between PET and MRI	20 (9)
	Time from last RT fraction to surgery (n= 54 patients)	71 (8)
	Time from last RT fraction to W&W inclusion (n= 7 patients)	56 (4)
<p>CRT chemoradiotherapy, W&amp;W watch-and-wait follow-up, TRG tumour regression grade, RT radiotherapy</p> <p><sup>a</sup> 7/13 patients were followed up according to a watch-and-wait program and had a sustained clinical complete response for at least 2 years (median follow-up 59 months, range 26–89). This was used as a surrogate endpoint for a pathological complete response (TRG1)</p>		

Table 3. Multivariable stepwise logistic regression analysis			
A. Comparison of baseline + imaging models			
Candidate variable subset	AIC	AUC (training dataset)	Selected variables
I. Baseline patient characteristics	67.9	0.81	mrT-stage (mrT1-3b vs. mrT3c-4d), time to surgery ( $\leq 10$ vs. $>10$ weeks)
II. MRI	83.7	0.70	T2W-signal <sub>entropy</sub> (per unit), ADC <sub>entropy</sub> (per unit)
III. PET/CT	86.5	0.50	— <sup>a</sup>
IV. Baseline + MRI	58.0	0.88	mrT-stage (mrT1-3b vs. mrT3c-4d) T2W-signal <sub>entropy</sub> (per unit), T2W <sub>volume</sub> (per cm <sup>3</sup> )
V. Baseline + MRI + PET/CT	67.9	0.81	mrT-stage (mrT1-3b vs. mrT3c-4d), time to surgery ( $\leq 10$ vs. $>10$ weeks)
VI. Baseline + MRI + PET/CT	58.0	0.88	mrT-stage (mrT1-3b vs. mrT3c-4d), T2W-signal <sub>entropy</sub> (per unit), T2W <sub>volume</sub> (per cm <sup>3</sup> )
B. Optimal prediction model (baseline + MRI model)			
Modality	Selected variable	Odds ratio (95% CI)	p value
Baseline	mrT-stage (mrT1-3b vs. mrT3c-4d)	0.004 (0.00017–0.092)	<0.001
MRI	T2W-signal <sub>entropy</sub> (per unit)	7.810 (1.713–35.612)	0.0079
	T2W <sub>volume</sub> (per cm <sup>3</sup> )	1.028 (1.001–1.054)	0.0389
AUC (training dataset)	0.88		
AUC (LOOCV)	0.83 (bootstrap 95% CI: 0.70–0.96)		
<p>AIC Akaike Information Criterion, which reflects the relative efficiency of a statistical model compared to other models, with a lower value indicating a more efficient model, AUC area under the receiver operating characteristic curve, LOOCV leave-one-out cross-validation, CI confidence interval</p> <p><sup>a</sup> No variables were selected as predictors when only PET/CT variables were offered to the model.</p>			

**Supplementary Table 1** illustrates the results of the univariable analysis (which was performed independently of the multivariable feature selection process) and correlation analysis for all baseline and imaging variables. Since there was a strong correlation between  $DWI_{\text{volume}}$  and  $T2W_{\text{volume}}$  ( $\rho = 0.96$ ),  $SUV_{\text{max}}$  and  $SUV_{\text{mean}}$  ( $\rho = 0.99$ ) and  $MTV_{42\%}$  and  $TLG$  ( $\rho = 0.80$ ), only  $T2W_{\text{volume}}$ ,  $SUV_{\text{mean}}$  and  $TLG$  were entered in the multivariable selection process described above.

## DISCUSSION

This study explores the value of combining quantitative imaging features from baseline, pre-treatment FDG-PET/CT and MRI with common baseline patient characteristics to predict response to neoadjuvant CRT in rectal cancer. Our findings demonstrate that a multivariable model incorporating mrT-stage, combined with (semi-) quantitative MRI features (T2W-signal entropy and tumour volume) can aid in identifying good responders before the start of treatment, with an estimated predictive performance of AUC 0.83. Addition of FDG-PET/CT variables was not beneficial.

Our results indicated mrT-stage as the strongest baseline predictor of response, with a higher mrT-stage resulting in a lower probability of achieving a good response. This is in line with previous studies, including a pooled analysis of >3000 patients that showed that higher T-stage is negatively associated with complete response rates after CRT.<sup>1</sup> More recent large retrospective cohort studies by Joye et al. and Al-Sukhni et al. confirmed T-stage to be amongst the main baseline predictors of response.<sup>34,35</sup> In these two previous works, contradictory results were reported for the predictive value of N-stage: while Joye et al. reported higher N-stage to be associated with a favourable response, Al-Sukhni reported the opposite. mrN-stage was not identified as a significant predictor in our study. These conflicting findings are likely related to the known inaccuracies of imaging for lymph node staging.<sup>36,37</sup> Al-Sukhni et al. also found a longer interval between CRT and surgery to be associated with a higher probability of response, which is consistent with several other reports.<sup>33,38-42</sup> For this reason, we chose to include time to surgery as a potential confounder in our analyses (although it can clearly not be used as a pre-therapy predictor). While it was indeed associated with response, it was not amongst the strongest parameters ultimately included in the optimal predictive model.

In addition to mrT-stage, only the MRI-based quantitative features significantly contributed to the optimal prediction model. A positive predictive effect was observed for T2W-signal<sub>entropy'</sub> indicating that tumours with a higher entropy (i.e. a more heterogeneous texture) have a higher probability of achieving a good response. Similarly, a recent prospective study by Shu et al. found entropy on pre-CRT T2W MRI to be higher in patients who achieved a complete response after CRT.<sup>25</sup> In contrast, Meng et al. found lower pre-treatment T2W entropy to be associated with complete response,<sup>43</sup> while a third report by De Cecco et al found no significant differences at all in baseline tumour entropy between response groups.<sup>44</sup> Although in literature tumour heterogeneity is generally regarded as a factor associated with tumour aggressiveness, the precise relation between heterogeneity (as assessed on imaging) and response to treatment is not well understood. In addition, variations in methodology concerning patient selection, image processing, outcome definition and statistics may have contributed to inconsistent findings between reports. The baseline tumour volume (T2W<sub>volume</sub>) was the third independent predictor included in the model, though its effect was relatively small. This is in line with data from previous studies that reported suboptimal performance for pre-therapy tumour volumetry to predict response.<sup>45-53</sup>

Interestingly, our study showed limited predictive value for baseline PET and DWI variables. This confirms previous evidence showing disappointing or conflicting results for pre-treatment response prediction based on DWI (using mainly ADC) and PET (SUV<sub>mean</sub> and SUV<sub>max</sub>).<sup>16,17</sup> In a systematic review by Joye et al., suboptimal pooled predictive performance was reported in the pre-treatment setting for both PET (SUV<sub>max</sub> pooled sensitivity 0.78; pooled specificity 0.35) and DWI (ADC<sub>mean</sub> pooled sensitivity 0.69; pooled specificity 0.68).<sup>17</sup> More positive results for PET or DWI were mainly reported when (sequential) imaging data acquired during and/or after completion of CRT, rather than at baseline was used.<sup>16,17,19</sup> To our knowledge, only two other groups have performed a multivariable analysis combining pre-treatment PET/CT and MRI to predict rectal tumour response. Joye et al. combined PET/CT and DWI features measured before, during and after CRT, together with volume on T2W-MRI. Their multivariable model reached an AUC of 0.83 to predict a good response (ypT0-1N0). However, only features dependent on post-treatment measurements (post-CRT and ΔCRT) were selected as predictors and no pre-treatment features were included, again indicating the limited value of PET and DWI in the pretherapy setting.<sup>15</sup> The second study, by Giannini et al. specifically focused on image texture and combined first-order and second-order texture features derived from pre-treatment PET, DWI and T2W-MRI together with PET volume. Their multivariable model reached an AUC

of 0.86 in which notably 5 out of 6 selected variables were based on PET. However, this good result was achieved in a test dataset without further (cross-)validation.<sup>20</sup> Validation is required to estimate the performance of a model in actual clinical practice (unseen data), since the accuracy as established in a test dataset will likely be an overestimation. Unfortunately, our current dataset was too small to allow splitting of the data into a test and validation set. Therefore, we chose to simulate validation on an 'independent' dataset by performing leave-one-out cross-validation (LOOCV), which resulted in an AUC of 0.83. Apart from the relatively small size, our study is limited by its retrospective nature. As a consequence, variations in scanning protocols (in particular MRI) and hardware used over time may have introduced heterogeneity not related to the treatment outcome. The study further used a single-reader design for image segmentation, which does not account for inter-observer variations, particularly for the manual (MRI) delineations. These effects are expected to be limited, however, based on previously reported excellent inter-reader reproducibility.<sup>45,46,48</sup> Along the same line, some of the baseline characteristics included in the analyses were based on radiological staging (mrT-stage and mrN-stage) which are also known to be subject to inter-observer variations. An in-depth analysis of such effects, however, was beyond the scope of the current study. Histopathologic response evaluation was not available for all patients due to the inclusion of W&W patients, for which the surrogate endpoint to establish the treatment outcome was a recurrence-free follow-up of at least 2-years (median 59 months). Since locoregional regrowths indicating incomplete response occur almost exclusively within these first 2 years, we believe this can be considered an acceptable endpoint in these cases.<sup>5</sup> Future validation and replication of this work may be limited by the fact that PET/CT is typically not routinely performed as a first-line staging modality. Finally, for this study we deliberately chose to explore the predictive value of only a selective number of relatively well-known and reproducible variables (reported to be of potential value in previous literature), to prevent overfitting of a large number of features to a small sample size. As a result, alternative useful predictors may have been neglected. This would be an interesting area for further research in larger datasets (using radiomics or deep learning approaches) and should also include a more comprehensive integration of imaging features with other clinical, immunological, histological and genetic variables.

### **Conclusion and clinical outlook**

Prediction of response to neoadjuvant treatment is an increasingly relevant issue in rectal cancer, especially given the growing interest in organ-preserving treatment programs. Our findings demonstrate that a model incorporating (semi-)quantitative

imaging features from routine staging MRI combined with mrT-stage can aid in identifying patients likely to show a good response to neoadjuvant chemoradiation. Addition of PET/CT variables was not beneficial, indicating that pre-treatment PET/CT (which is currently not typically used as a first-line modality for rectal cancer staging) probably has a limited added value for pre-therapy response prediction. These results are an encouragement for further development of clinical response prediction models incorporating routine pre-therapy MR imaging in rectal cancer, which will need to be further studied and validated in large prospective patient cohorts.

## REFERENCES

1. Maas M, Nelemans PJ, Valentini V et al (2010) Long-term outcome in patients with a pathological complete response after chemoradiation for rectal cancer: a pooled analysis of individual patient data. *Lancet Oncol* 11:835–844. doi: 10.1016/S1470-2045(10)70172-8
2. Habr-Gama A, Perez RO, Wynn G, Marks J, Kessler H, Gama-Rodrigues J (2010) Complete clinical response after neoadjuvant chemoradiation therapy for distal rectal cancer: characterization of clinical and endoscopic findings for standardization. *Dis Colon Rectum* 53:1692–1698. doi: 10.1007/DCR.0b013e3181f42b89
3. Paun BC, Cassie S, MacLean AR, Dixon E, Buie WD (2010) Postoperative complications following surgery for rectal cancer. *Ann Surg* 251:807–818. doi: 10.1097/SLA.0b013e3181dae4ed
4. Hendren SK, O'Connor BI, Liu M et al (2005) Prevalence of male and female sexual dysfunction is high following surgery for rectal cancer. *Ann Surg* 242:212–223. doi: 10.1097/01.sla.0000171299.43954.ce
5. van der Valk MJM, Hilling DE, Bastiaannet E et al (2018) Long-term outcomes of clinical complete responders after neoadjuvant treatment for rectal cancer in the International Watch & Wait Database (IWWD): an international multicentre registry study. *Lancet* 391:2537–2545. doi: 10.1016/S0140-6736(18)31078-X
6. Maas M, Beets-Tan RGH, Lambregts DMJ et al (2011) Wait-and-see policy for clinical complete responders after chemoradiation for rectal cancer. *J Clin Oncol* 29:4633–4640. doi: 10.1200/JCO.2011.37.7176
7. Habr-Gama A, Gama-Rodrigues J, São Julião GP et al (2014) Local recurrence after complete clinical response and watch and wait in rectal cancer after neoadjuvant chemoradiation: impact of salvage therapy on local disease control. *Int J Radiat Oncol Biol Phys* 88: 822–828. doi: 10.1016/j.ijrobp.2013.12.012
8. Mith JD, Ruby JA, Goodman KA et al (2012) Nonoperative management of rectal cancer with complete clinical response after neoadjuvant therapy. *Ann Surg* 256:965–972. doi: 10.1097/SLA.0b013e3182759f1c
9. Appelt AL, Pløen J, Harling H et al (2015) High-dose chemoradiotherapy and watchful waiting for distal rectal cancer: a prospective observational study. *Lancet Oncol* 16:919–927. doi: 10.1016/S1470-2045(15)00120-5

10. Rombouts AJM, Al-Najami I, Abbott NL et al (2017) Can we Save the rectum by watchful waiting or TransAnal microsurgery following (chemo) Radiotherapy versus Total mesorectal excision for early REctal Cancer (STAR-TREC study)?: protocol for a multicentre, randomised feasibility study. *BMJ Open* 7:e019474. doi: 10.1136/bmjopen-2017-019474
11. Van Stiphout RGPM, Valentini V, Buijsen J et al (2014) Nomogram predicting response after chemoradiotherapy in rectal cancer using sequential PETCT imaging: a multicentric prospective study with external validation. *Radiother Oncol* 113:215–222. doi: 10.1016/j.radonc.2014.11.002
12. Janssen MHM, Öllers MC, Van Stiphout RGPM et al (2012) PET- based treatment response evaluation in rectal cancer: prediction and validation. *Int J Radiat Oncol Biol Phys* 82:871–876. doi: 10.1016/j.ijrobp.2010.11.038
13. Maffione AM, Marzola MC, Capirci C, Colletti PM, Rubello D (2015) Value of 18 F-FDG PET for predicting response to neoadjuvant therapy in rectal cancer: systematic review and meta-analysis. *AJR Am J Roentgenol* 204:1261–1268. doi: 10.2214/AJR.14.13210
14. Cliffe H, Patel C, Prestwich R, Scarsbrook A (2017) Radiotherapy response evaluation using FDG PET-CT—established and emerging applications. *Br J Radiol* 90:20160764. doi: 10.1259/bjr.20160764
15. Joye I, Debuquoy A, Deroose CM et al (2017) Quantitative imaging outperforms molecular markers when predicting response to chemoradiotherapy for rectal cancer. *Radiother Oncol* 124:104–109
16. Schurink NW, Lambregts DM, Beets-Tan RG (2019) Diffusion- weighted imaging in rectal cancer: current applications and future perspectives. *Br J Radiol* 92:20180655. doi: 10.1016/j.radonc.2017.06.013
16. Joye I, Deroose CM, Vandecaveye V, Haustermans K (2014) The role of diffusion-weighted MRI and 18F-FDG PET/CT in the prediction of pathologic complete response after radiochemotherapy for rectal cancer: a systematic review. *Radiother Oncol* 113:158–165. doi: 10.1016/j.radonc.2014.11.026.
17. Mahadevan LS, Zhong J, Venkatesulu BP et al (2018) Imaging predictors of treatment outcomes in rectal cancer: an overview. *Crit Rev Oncol Hematol* 129:153–162. doi: 10.1016/j.critrevonc.2018.06.009
18. Meng X, Huang Z, Wang R, Yu J (2014) Prediction of response to inpreoperative chemoradiotherapy in patients with locally advanced rectal cancer. *Biosci Trends* 8:11–23. doi: 10.5582/bst.8.11



19. Giannini V, Mazzetti S, Bertotto I et al (2019) Predicting locally advanced rectal cancer response to neoadjuvant therapy with 18 F- FDG PET and MRI radiomics features. *Eur J Nucl Med Mol Imaging* 46:878–888. doi: 10.1007/s00259-018-4250-6
20. Van Griethuysen JJM, Fedorov A, Parmar C et al (2017) Computational radiomics system to decode the radiographic phenotype. *Cancer Res* 77:e104–e107. doi: 10.1158/0008-5472.CAN-17-0339
21. Erdi YE, Mawlawi O, Larson SM et al (1997) Segmentation of lung lesion volume by adaptive positron emission tomography image thresholding. *Cancer* 80:2505–2509. doi: 10.1002/(sici)1097-0142(19971215)80:12+<2505::aid-cnrcr24>3.3.co;2-b
22. Miccò M, Vargas HA, Burger IA et al (2014) Combined pre-treatment MRI and 18F-FDG PET/CT parameters as prognostic biomarkers in patients with cervical cancer. *Eur J Radiol* 83: 1169–1176. doi: 10.1016/j.ejrad.2014.03.024
23. Ueno Y, Lisbona R, Tamada T, Alaref A, Sugimura K, Reinhold C (2017) Comparison of FDG PET metabolic tumour volume versus ADC histogram: prognostic value of tumour treatment response and survival in patients with locally advanced uterine cervical cancer. *Br J Radiol* 90:20170035. doi: 10.1259/bjr.20170035
24. Shu Z, Fang S, Ye Q et al (2019) Prediction of efficacy of neoadjuvant chemoradiotherapy for rectal cancer: the value of texture analysis of magnetic resonance images. *Abdom Radiol (NY)* 21: 1051–1058. doi: 10.1007/s00261-019-01971-y
25. Greenbaum A, Martin DR, Bocklage T, Lee JH, Ness SA, Rajput A (2019) Tumor heterogeneity as a predictor of response to neoadjuvant chemotherapy in locally advanced rectal cancer. *Clin Colorectal Cancer* 18:102–109. doi: 10.1016/j.clcc.2019.02.003
26. Bozkaya Y, Özdemir NY, Erdem GU et al (2018) Clinical predictive factors associated with pathologic complete response in locally advanced rectal cancer. *J Oncol Sci* 4:5–10. doi: 10.1016/j.jons.2017.12.004
27. Deantonio L, Caroli A, Puta E et al (2018) Does baseline [18F] FDG-PET/CT correlate with tumor staging, response after neoadjuvant chemoradiotherapy, and prognosis in patients with rectal cancer? *Radiat Oncol* 13:211. doi: 10.1186/s13014-018-1154-3
28. Traverso A, Wee L, Dekker A, Gillies R (2018) Repeatability and reproducibility of radiomic features: a systematic review. *Int J Radiat Oncol Biol Phys* 102:1143–1158. doi: 10.1016/j.ijrobp.2018.05.053
29. Mandard A-M, Dalibard F, Mandard J-C et al (1994) Pathologic assessment of tumor regression after preoperative chemoradiotherapy of esophageal carcinoma. Clinicopathologic correlations. *Cancer* 73:2680–2686. doi: 10.1002/1097-0142(19940601)73:11<2680::aid-cnrcr2820731105>3.0.co;2-c

30. Akaike H (1974) A new look at the statistical model identification. *IEEE Trans Autom Control* 19:716–723. doi: 10.1109/TAC.1974.1100705
31. Burnham KP, Anderson DR (2004) Multimodel Inference: Understanding AIC and BIC in Model Selection. *Sociol Methods Res* 33:261–304. doi: 10.1177/0049124104268644
32. Akgun E, Caliskan C, Bozbiyik O et al (2018) Randomized clinical trial of short or long interval between neoadjuvant chemoradiotherapy and surgery for rectal cancer. *Br J Surg* 105:1417–1425. doi: 10.1002/bjs.10984
33. oye I, Debucquoy A, Fieuws S et al (2016) Can clinical factors be used as a selection tool for an organ-preserving strategy in rectal cancer? *Acta Oncol* 55:1047–1052. doi: 10.3109/0284186X.2016.1167954
34. Al-Sukhni E, Attwood K, Mattson DM, Gabriel E, Nurkin SJ (2016) Predictors of pathologic complete response following neo- adjuvant chemoradiotherapy for rectal cancer. *Ann Surg Oncol* 23: 1177–1186. doi: 10.1245/s10434-015-5017-y
35. Lahaye MJ, Engelen SME, Nelemans PJ et al (2005) Imaging for predicting the risk factors—the circumferential resection margin and nodal disease—of local recurrence in rectal cancer: a meta- analysis. *Semin Ultrasound CT MR* 26:259–268. doi: 10.1053/j.sult.2005.04.005
36. Gröne J, Loch FN, Taupitz M, Schmidt C, Kreis ME (2018) Accuracy of various lymph node staging criteria in rectal cancer with magnetic resonance imaging. *J Gastrointest Surg* 22:146–153. doi: 10.1007/s11605-017-3568-x
37. Francois Y, Nemoz CJ, Baulieux J et al (1999) Influence of the interval between preoperative radiation therapy and surgery on downstaging and on the rate of sphincter-sparing surgery for rectal cancer: the Lyon R90-01 randomized trial. *J Clin Oncol* 17:2396– 2396. doi: 10.1200/JCO.1999.17.8.2396
38. Kalady MF, de Campos-Lobato LF, Stocchi L et al (2009) Predictive factors of pathologic complete response after neoadjuvant chemoradiation for rectal cancer. *Trans Meet Am Surg Assoc* 127:213–220. doi: 10.1097/SLA.0b013e3181b91e63
39. Foster JD, Jones EL, Falk S, Cooper EJ, Francis NK (2013) Timing of surgery after long-course neoadjuvant chemoradiotherapy for rectal cancer: a systematic review of the literature. *Dis Colon Rectum* 56:921–930. doi: 10.1097/DCR.0b013e31828aedcb
40. Probst CP, Becerra AZ, Aquina CT et al (2015) Extended intervals after neoadjuvant therapy in locally advanced rectal cancer: the key to improved tumor response and potential organ preservation. *J Am Coll Surg* 221:430–440. doi: 10.1016/j.jamcollsurg.2015.04.010
41. etrelli F, SgROI G, Sarti E, Barni S (2016) Increasing the interval between neoadjuvant chemoradiotherapy and surgery in rectal cancer. *Ann Surg* 263:458–464. doi: 10.1097/SLA.0000000000000368

42. Meng Y, Zhang C, Zou S et al (2018) MRI texture analysis in predicting treatment response to neoadjuvant chemoradiotherapy in rectal cancer. *Oncotarget* 9:11999–12008. doi: 10.18632/oncotarget.23813
43. De Cecco CN, Rengo M, Meinel FG et al (2015) Texture analysis as imaging biomarker of tumoral response to neoadjuvant chemoradiotherapy in rectal cancer patients studied with 3-T magnetic resonance. *Invest Radiol* 50:239–245. doi: 10.1097/RLI.0000000000000116
44. Martens MH, Van Heeswijk MM, van den Broek JJ et al (2015) Prospective, multicenter validation study of magnetic resonance volumetry for response assessment after preoperative chemoradiation in rectal cancer: can the results in the literature be reproduced? *Int J Radiat Oncol Biol Phys* 93:1005–1014. doi: 10.1016/j.ijrobp.2015.09.008
45. Lambregts DMJ, Rao S-X, Sassen S et al (2015) MRI and diffusion-weighted MRI volumetry for identification of complete tumor responders after preoperative chemoradiotherapy in patients with rectal cancer. *Ann Surg* 262:1034–1039. doi: 10.1097/SLA.0000000000000909
46. Curvo-Semedo L, Lambregts DMJ, Maas M et al (2011) Rectal cancer: assessment of complete response to preoperative combined radiation therapy with chemotherapy—conventional MR volumetry versus diffusion-weighted MR imaging. *Radiology* 260:734–743. doi: 10.1148/radiol.11102467
47. Quايا E, Gennari AG, Ricciardi MC et al (2016) Value of percent change in tumoral volume measured at T2-weighted and diffusion-weighted MRI to identify responders after neoadjuvant chemoradiation therapy in patients with locally advanced rectal carcinoma. *J Magn Reson Imaging* 44:1415–1424. doi: 10.1002/jmri.25310
48. Ha HI, Kim AY, Yu CS, Park SH, Ha HK (2013) Locally advanced rectal cancer: diffusion-weighted MR tumour volumetry and the apparent diffusion coefficient for evaluating complete remission after preoperative chemoradiation therapy. *Eur Radiol* 23:3345–3353. doi: 10.1007/s00330-013-2936-5.
49. Young HK, Dae YK, Tae HK et al (2005) Usefulness of magnetic resonance volumetric evaluation in predicting response to preoperative concurrent chemoradiotherapy in patients with resectable rectal cancer. *Int J Radiat Oncol Biol Phys* 62:761–768. doi: 10.1016/j.ijrobp.2004.11.005
50. Okuno T, Kawai K, Koyama K et al (2018) Value of FDG-PET/CT volumetry after chemoradiotherapy in rectal cancer. *Dis Colon Rectum* 61:320–327. doi: 10.1097/DCR.0000000000000959

51. Dos Anjos DA, Perez RO, Habr-Gama A et al (2016) Semiquantitative volumetry by sequential PET/CT may improve prediction of complete response to neoadjuvant chemoradiation in patients with distal rectal cancer. *Dis Colon Rectum* 59:805–812. doi: 10.1097/DCR.0000000000000655
52. Park J, Chang KJ, Seo YS et al (2014) Tumor SUVmax normalized to liver uptake on 18 F-FDG PET/CT predicts the pathologic complete response after neoadjuvant chemoradiotherapy in locally advanced rectal cancer. *Nucl Med Mol Imaging* 48:295–302. doi: 10.1007/s13139-014-0289-x

<b>Supplementary Table 1.</b> Univariable logistic regression analysis for predicting good response			
<b>Modality</b>	<b>Variable</b>	<b>Odds Ratio (95% CI)</b>	<b>P-value</b>
Baseline patient characteristics	Age (per year)	1.10 (0.63 – 1.91)	0.731
	Sex (female vs. male)	0.66 (0.20 – 2.20)	0.499
	mrT-stage (mrT1-3b vs. mrT3c-4d)	0.06 (0.02 – 0.25)	<0.001
	mrN-stage (mrN0 vs. mrN+)	1.05 (0.33 – 3.27)	0.939
	Time to surgery/W&W inclusion ( $\leq 10$ vs. $>10$ weeks)	0.55 (0.20 – 1.53)	0.254
MRI	T2W <sub>volume</sub> (per cm <sup>3</sup> ) <sup>a</sup>	0.99 (0.98 – 1.01)	0.485
	T2W-signal <sub>entropy</sub> (per unit)	1.84 (0.92 – 3.70)	0.085
	DWI <sub>volume</sub> (per cm <sup>3</sup> ) <sup>a</sup>	0.99 (0.98 – 1.01)	0.425
	ADC <sub>mean</sub> (per 10 <sup>-3</sup> mm <sup>2</sup> /s)	0.57 (0.01 – 22.57)	0.766
	ADC <sub>entropy</sub> (per unit)	3.99 (0.98 – 16.30)	0.054
PET/CT	MTV <sub>42%</sub> (per cm <sup>3</sup> ) <sup>b</sup>	0.98 (0.95 – 1.01)	0.243
	SUV <sub>max</sub> (per unit) <sup>c</sup>	0.96 (0.90 – 1.02)	0.219
	SUV <sub>mean</sub> (per unit) <sup>c</sup>	0.93 (0.83 – 1.05)	0.242
	TLG (per unit) <sup>b</sup>	0.99 (0.98 – 1.01)	0.403
	CT-HU <sub>mean</sub> (per HU)	0.98 (0.96 – 1.01)	0.207
W&W: watch-and-wait follow-up; HU: Hounsfield Unit; CI: confidence interval.			
<sup>a</sup> T2W <sub>volume</sub> and DWI <sub>volume</sub> correlated with Pearson's rho $\rho=0.96$ . Since T2W imaging is more readily available and less susceptible to geometric distortions, DWI <sub>volume</sub> was excluded from multivariable analysis.			
<sup>b</sup> MTV <sub>42%</sub> and TLG correlated with Pearson's rho $\rho=0.80$ . Since MTV <sub>42%</sub> describes tumour volume and T2W <sub>volume</sub> was also included as a variable, MTV <sub>42%</sub> was excluded from multivariable analysis.			
<sup>c</sup> SUV <sub>max</sub> and SUV <sub>mean</sub> correlated with Pearson's rho $\rho=0.99$ . Since the SUV <sub>max</sub> value is derived from a single pixel and therefore is more susceptible to noise than the mean SUV value, SUV <sub>max</sub> was excluded from multivariable analysis.			
Between all other variables Pearson's rho was $\rho<0.80$ .			





The background is a vibrant blue with a halftone dot pattern. A dark blue, ribbon-like shape curves across the center, partially overlapping the text. The text 'Chapter 5' is centered within this dark blue shape.

# Chapter 5

# PRE-TREATMENT PREDICTION OF EARLY RESPONSE TO CHEMORADIOOTHERAPY BY QUANTITATIVE ANALYSIS OF BASELINE STAGING FDG-PET/ CT AND MRI IN LOCALLY ADVANCED CERVICAL CANCER

Lisa A Min, Leanne LGC Ackermans, Marlies E Nowee  
Joost JM van Griethuysen, Sander Roberti, Monique Maas, Wouter V Vogel,  
Regina GH Beets-Tan, Doenja MJ Lambregts

*Acta Radiologica* (2021) 62(7):940-948 doi: 10.1177/0284185120943046



# ABSTRACT

## Background

Early prediction of response to concurrent chemoradiotherapy (cCRT) could aid to further optimize treatment regimens for locally advanced cervical cancer (LACC) in the future.

## Purpose

To explore whether quantitative parameters from baseline (pre-therapy) magnetic resonance imaging (MRI) and FDG-PET/computed tomography (CT) have potential as predictors of early response to cCRT.

## Material and Methods

Forty-six patients with LACC undergoing cCRT after staging with FDG-PET/CT and MRI were retrospectively analyzed. Primary tumor volumes were delineated on FDG-PET/CT, T2-weighted (T2W)-MRI and diffusion-weighted MRI (DWI) to extract the following quantitative parameters: T2W volume; T2W signal<sub>mean</sub>; DWI volume; ADC<sub>mean</sub>; ADC<sub>SD</sub>; MTV<sub>42%</sub>; and SUV<sub>max</sub>. Outcome was the early treatment response, defined as the residual tumor volume on MRI 3–4 weeks after start of external beam radiotherapy with chemotherapy (before the start of brachytherapy): patients with a residual tumor volume <10 cm<sup>3</sup> were classified as early responders. Imaging parameters were analyzed together with FIGO stage to assess their performance to predict early response, using multivariable logistic regression analysis with bi-directional variable selection. Leave-one-out cross-validation with bootstrapping was used to simulate performance in a new, independent dataset.

## Results

T2W volume (OR 0.94, P= 0.003) and SUV<sub>max</sub> (OR 1.15, P= 0.18) were identified as independent predictors in multivariable analysis, rendering a model with an AUC of 0.82 in the original dataset, and AUC of 0.68 (95% CI 0.41–0.81) from cross-validation.

## Conclusion

Although the predictive performance achieved in this small exploratory dataset was limited, these preliminary data suggest that parameters from baseline MRI and FDG-PET/CT (in particular pre-therapy tumor volume) may contribute to prediction of early response to cCRT in cervical cancer.

# INTRODUCTION

In cervical cancer, disease stage is typically determined at diagnosis by a combination of clinical examination and pelvic magnetic resonance imaging (MRI), complemented with whole-body 18F-fluoro-deoxyglucose (FDG) positron emission tomography/computed tomography (PET/CT) for evaluation of lymph nodes and distant metastases in more advanced cases. Current treatment standard for locally advanced cervical cancer (LACC; International Federation of Gynecology and Obstetrics (FIGO) stage  $\geq$ B2 or node-positive) is definitive concurrent chemoradiotherapy (cCRT), consisting of weekly cisplatin in combination with external beam radiotherapy (EBRT), followed by brachytherapy.<sup>1</sup>

To date, the radiotherapy schedule is generally identical for all patients, irrespective of tumor stage or other prognostic characteristics. In the vast majority, this regime results in a complete local response,<sup>2</sup> but there is considerable variation in the course of response between individual patients. In some patients, a significant tumor residue remains after the first weeks of EBRT (before brachytherapy), while others are “early responders” that already show a (near-)complete volume reduction at this stage.<sup>3</sup> In the future, these “early responders” might benefit from an early start of the subsequent brachytherapy, aiming to reduce overall treatment time, or from dose de-escalation to limit treatment toxicity while maintaining a good oncological outcome.<sup>4</sup> To facilitate such personalized treatments, tools to predict early response will be required.

One approach could be to extract such predictive information from imaging. Studies in various cancer types have shown promising results for imaging biomarkers derived from MRI and FDG-PET/CT as predictors for response and prognosis.<sup>5-8</sup> For cervical cancer, there have been reports that markers from pre-treatment MRI or FDG-PET/CT have potential to predict “late” outcomes, including disease-free and overall survival<sup>9-16</sup> or final treatment response after completion of cCRT<sup>17-26</sup>; however, so far, no studies have focused specifically on prediction of early treatment response. Furthermore, of the existing studies, only a few combined FDG-PET/CT and MRI within one patient cohort.<sup>9,12,18,27</sup>

The aim of the present study was to determine whether quantitative imaging markers from baseline staging MRI and FDG-PET/CT have potential as predictors of early response to cCRT in LACC, and whether combining parameters from both modalities has complementary value.

# MATERIAL AND METHODS

This retrospective study was approved by the institutional ethical review board, informed consent was waived. The study workflow is illustrated in **Figure 1**.

## Patients and treatment

Patients who underwent FDG-PET/CT and MRI in our institution for pre-treatment staging of primary cervical cancer (January 2011 to March 2018) were identified. From this group, 46 patients met the inclusion criteria: (i) LACC (FIGO stage  $\geq$ B2 or node-positive<sup>26</sup>); (ii) treatment by cCRT (with curative intent) and at least four of six weekly cycles of cisplatin completed; (iii) pre-treatment MRI at 3.0 T including T2-weighted (T2W) and diffusion-weighted imaging (DWI); and (iv) available MRI at 3–4 weeks after EBRT initiation, to determine “early response.”

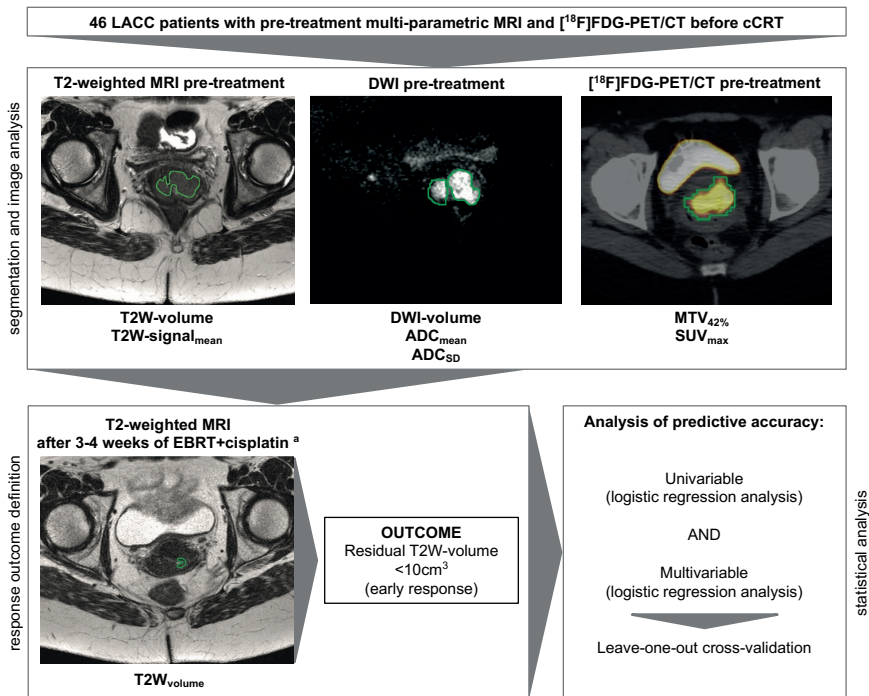


**Figure 1.** Study workflow.

<sup>a</sup> MRI acquired during cCRT for clinical brachytherapy planning. For the purpose of this study, this MRI was used for volumetric response measurement. cCRT, concurrent chemoradiotherapy; MRI, magnetic resonance imaging.

**Table 1.** MRI protocol used for primary staging and quantitative imaging evaluation

	T2W FSE	Single-shot EPI DWI
Repetition time (ms)	2515.84–4865.10	1200.0–8824.4
Echo time (ms)	110–150	54.03–97.97
Slice thickness (mm)	3–4	2.7–3
Slice gap (mm)	3–4	3.2–3.5
In-plane resolution (mm)	0.25x0.25 – 0.49x0.49	0.56x0.56 – 1.48x1.48
Echo train length	25–28	67–113
No. signal averages	1–2	1–5
b-values (used for calculation of ADC) (s/mm <sup>2</sup> )	–	0, 200, 800*
Fat suppression	–	SPAIR

\*Some changes in protocol and sequence parameters occurred during the study period: in 18 patients, ADC was calculated using slightly different b- values: 0, 188, 750. In two patients, ADC was calculated using b-values 0, 200, 1000.  
ADC, apparent diffusion coefficient; DWI, diffusion-weighted imaging; EPI, echo planar imaging; FSE, fast spin echo; MRI, magnetic resonance imaging; SPAIR, spectral attenuated inversion recovery; T2W, T2-weighted.

Routine cCRT consisted of pelvic EBRT of 46 Gy (2 Gy/fraction, five fractions/week). The radiation field was extended to the level of the renal veins in cases of suspicious para-aortic nodes. A sequential boost (14 Gy, 2 Gy/fraction, five fractions/week) was administered to suspected sites of pelvic lymph-node involvement. EBRT was followed by brachytherapy to a total dose equivalent of 90 Gy on the high-risk clinical target volume (cervix and tumor), in 3–4 fractions. Radiotherapy was accompanied by weekly cisplatin (40 mg/m<sup>2</sup> body surface area) for six weeks, starting on day 1 of EBRT.

**MRI**

Pre-therapy pelvic MRI was performed at 3.0 T (Intera Achieva (+/- dStream) or Ingenia system, Philips Healthcare) with an external surface coil. The protocol included anatomical fast spin echo (FSE) T2W sequences in three orthogonal planes and an axial single-shot echo planar imaging (ssEPI) DWI sequence, with three b-values (b 0 up to b 750–1000). Axial T2W and DWI sequences were angled in identical planes (perpendicular to the cervical canal). Protocol details are provided in **Table 1**. Spasmolytics were not administered.

### FDG-PET/CT imaging

FDG-PET/CTs were performed on a hybrid PET/CT scanner (either Gemini TF 16 or Gemini TF Big Bore, Philips Healthcare). After 6 h of fasting (target blood glucose level  $<10$  mmol/L), patients received an intravenous 2-deoxy-2-[ $^{18}\text{F}$ ]fluoro-D-glucose (FDG) bolus of 180 MBq (for body mass index (BMI)  $28$  kg/m $^2$ ) or 240 MBq (BMI  $>28$  kg/m $^2$ ), followed by an accumulation period of  $60 \pm 5$  min. Scanning ran from the skull base to upper thighs, with 2 min/bed position (reconstructed to 4-mm slices,  $4 \times 4$  mm pixels), with a non-enhanced CT (120–140 kV, target energy 40 mAs with automatic dose modulation) for attenuation correction and anatomical correlation (reconstructed to 2 mm and 5 mm slices,  $1.17 \times 1.17$  mm pixels).

### Tumor segmentation

A board-certified abdominal radiologist (DL, with  $\pm 7$  years of pelvic MRI experience) manually segmented whole-tumor volumes on the primary staging axial T2W-MRI and subsequently (in the same session) on high b-value DWI, using dedicated open-source software (3D Slicer, version 4.8.1). To assess inter-observer variation, a random subset of 15 cases was additionally segmented by a second board-certified radiologist (MM, with similar experience level), blinded for the results of the first reader.

FDG-PET/CT images were processed by a nuclear medicine physician (WV, with 13 years of experience), using the same software. The FDG-avid tumor volume was first manually segmented, while carefully excluding adjacent structures with high physiological FDG signal (e.g. urine in the bladder). The metabolic tumor volume was derived semi-automatically from this segmentation using a threshold of 42% of the  $\text{SUV}_{\text{max}}$  ( $\text{MTV}_{42\%}$  according to methods previously reported<sup>11,13,29</sup>).

### Quantitative image analysis

Using the open-source software PyRadiomics (version 2.1.0<sup>30</sup>) the following quantitative parameters were extracted from the segmented volumes: T2W volume; DWI volume; mean T2W signal ( $\text{T2W-signal}_{\text{mean}}$ ); mean apparent diffusion coefficient ( $\text{ADC}_{\text{mean}}$ ); the SD of the ADC ( $\text{ADC}_{\text{SD}}$ );  $\text{SUV}_{\text{max}}$ ; and  $\text{MTV}_{42\%}$ . These specific parameters were selected as they represent relatively simple (first-order) parameters reflecting tumor size, cellularity, heterogeneity, and metabolism, all of which have shown potential for response prediction in previous studies.<sup>10,16,17,24</sup> ADC values were calculated using a mono-exponential decay model including three b-values ( $b1/40$ ,  $b1/488/200$ ,  $b1/4750/800/1000$  s/mm $^2$ ). MRI data were resampled to account for variation in the voxel dimensions, and signal intensity was normalized (by subtracting the image mean value and dividing it by the SD).

### Outcome definition (early response)

The primary study outcome was the early response to cCRT, defined as the residual tumor volume on MRI (routinely performed for the purpose of brachytherapy planning) after 3–4 weeks of cCRT. This outcome was chosen as the residual tumor volume after EBRT but before brachytherapy has previously been described to correlate with final local control after completion of treatment.<sup>19,31,32</sup> The volume threshold was set at  $<10 \text{ cm}^3$ , based on a previously reported cut-off.<sup>19</sup> The tumor volume after EBRT was segmented on T2W-MRI by the same reader and using the same procedure and segmentation methods as for the initial tumor segmentations. In 29/46 patients, response evaluation was performed on a 1.5-T scanner (Intera Achieva, Philips Healthcare) using similar protocols as the standard 3.0-T protocol described above and in **Table 1**.

### Statistical analysis

Inter-observer variability was determined with the intraclass coefficient (ICC) in a two-way random effects model. The predictive value of the different imaging parameters (T2W volume, T2W signal<sub>mean</sub>, DWI volume, ADC<sub>mean</sub>, ADC<sub>SD</sub>, SUV<sub>max</sub>, MTV<sub>42%</sub>), together with clinical FIGO stage, to predict early response to cCRT was assessed using multivariable logistic regression analysis with bi-directional stepwise selection based on the Akaike Information Criterion (AIC).<sup>33</sup> FIGO stage was derived from the patients' electronic medical records (according to the 2009 FIGO staging system, routinely used during the inclusion period of the present study).<sup>28</sup> In case of strong correlation between different imaging parameters (Pearson's correlation coefficient  $\rho \geq 0.8$ ), only one of these parameters was used in the variable selection process to avoid effects of multicollinearity. Model performance was determined by calculating the area under the receiver operating characteristic (ROC) curve (AUC), and odds ratios (ORs) were calculated for all parameters selected in the model. To assess model performance in new, "independent" data, leave-one-out cross-validation (LOOCV) was performed. For LOOCV, each patient is left out of the dataset once and a prediction model is generated on the remaining cases (46 iterations for this study). Probability of early response is calculated by the model for the left-out patient. The cross-validated AUC is determined on the total of these predictions. A 95% bootstrap confidence interval for the cross-validated AUC was obtained by repeating the cross-validation process using 1000 bootstrapped samples. Univariable logistic regression analysis for the individual variables was performed independent of the multivariable analysis. Baseline variables were compared between outcome groups using Wilcoxon Mann–Whitney U test for independent samples or Fisher's exact test. Statistical analyses were performed using R version 3.4.3 (R Foundation for Statistical Computing, Vienna, Austria).

## RESULTS

**Baseline characteristics**

Baseline patient characteristics are given in **Table 2**. The median age was 51 years (age range: 27–75 years). Most patients had FIGO stage IIB: 34/46 (74%). In total 30/46 (65%) patients were classified as early responders (residual T2W volume <10 cm<sup>3</sup>). Total treatment time (EBRT+brachytherapy) was in the range of 5.3–8.3 weeks (median 6.3 weeks).

		Residual T2W volume <10 cm <sup>3</sup> (good early response)	Residual T2W volume ≥10 cm <sup>3</sup>	P value*
Patients (n)		30	16	n/a
Age (years)		49 (28–61)	52 (27–75)	0.188
FIGO stage†	IB2	2 (6.7)	1 (6.3)	
	IIA–IIB	23 (76.7)	11 (68.8)	
	IIIA–IIIB	4 (13.3)	3 (18.8)	
	IV	1 (3)	1 (6.3)	0.549
Node-positive disease		20 (66.7)	13 (81.3)	0.493‡
Tumor histology	Squamous cell carcinoma	27 (90)	11 (68.8)	
	Adenocarcinoma	1 (3)	4 (25)	
	Other (adenosquamous, undefined)	2 (6)	1 (6.3)	0.079‡
Median interval between start of EBRT and second MRI (days)		23 (16–25)	23 (16–24)	0.228

Values are given as n (%) or median (range). \*P>0.05 was considered statistically significant. †Stage according to the FIGO staging system of 2009. ‡Fisher's exact test, others: Wilcoxon Mann-Whitney U test (independent samples). EBRT, external beam radiotherapy; FIGO, International Federation of Gynecology and Obstetrics; MRI, magnetic resonance imaging; T2W, T2-weighted.

**Table 3.** ICC for MRI parameters

Variable	ICC (95% CI)
T2W volume	0.972 (0.920 – 0.990)
DWI volume	0.916 (0.772 – 0.971)
T2W-signalmean	0.995 (0.985 – 0.998)
ADCmean	0.992 (0.976 – 0.997)
ADCSD	0.944 (0.845 – 0.981)
Post-EBRT T2Wvolume	0.932 (0.769 – 0.978)

ADC, apparent diffusion coefficient; CI, confidence interval; DWI, diffusion-weighted imaging; EBRT, external beam radiotherapy; ICC, intraclass correlation coefficient; MRI, magnetic resonance imaging; T2W, T2- weighted.

**Inter-observer variability**

Inter-observer agreement was excellent for all quantitative image parameters, with ICCs in the range of 0.916–0.995 (Table 3).

**Univariable analysis**

Results of the univariable analysis are provided in Table 4. Among the quantitative imaging parameters, all parameters related to the pre-therapy primary tumor volume (T2W volume, DWI volume, and MTV<sub>42%</sub>) were significantly associated with early response, with ORs in the range of 0.94–0.95 (per cm<sup>3</sup>), indicating that a smaller tumor volume is associated with early response to cCRT. Of the other parameters, only ADC<sub>SD</sub> and T2W-signal<sub>mean</sub> showed borderline significant associations (OR 1.06, P= 0.07 and OR 0.98, P= 0.09, respectively). FIGO stage category was not significantly associated with early response (OR 0.60, P= 0.50).

**Multivariable prediction model**

Multivariable analysis was performed independently of the univariate results. Since a strong correlation (P= 0.8–0.9, P <0.01) was found between the three volume parameters (T2W volume, DWI volume, and MTV<sub>42%</sub>), T2W volume was chosen as the only volume-based parameter entered in the variable selection process because it corresponds best with the outcome definition (volume on T2W-MRI after EBRT).



Variable	OR (95% CI)	P value
FIGO stage (III-IV vs. I-II)	0.60 (0.14 – 2.65)	0.50
T2W volume (cm <sup>3</sup> )	0.94 (0.91 – 0.98)	<0.01*
T2W-signal <sub>mean</sub> (unit; normalized)	0.98 (0.96 – 1.00)	0.09
DWI volume (cm <sup>3</sup> )	0.95 (0.91 – 0.98)	<0.01*
ADC <sub>mean</sub> (unit; normalized)	1.01 (0.99 – 1.04)	0.38
ADC <sub>SD</sub> (unit; normalized)	1.06 (1.00 – 1.12)	0.07
MTV <sub>42%</sub> (cm <sup>3</sup> )	0.94 (0.90 – 0.98)	<0.01*
SUV <sub>max</sub> (unit)	0.96 (0.86 – 1.07)	0.44

\*P values <0.05 were considered statistically significant.  
 ADC, apparent diffusion coefficient; CI, confidence interval; DWI, diffusion-weighted imaging; EBRT, external beam radiotherapy; FIGO, International Federation of Gynecology and Obstetrics; MTV, metabolic tumor volume; OR, odds ratio; T2W, T2-weighted.

Variable	OR (95% CI)	P value
T2W volume (cm <sup>3</sup> )*	0.93 (0.89-0.98)	<0.01
SUV <sub>max</sub>	1.15 (0.94-1.40)	0.18
AUC	0.82	
AUC LOOCV†	0.68 (0.41-0.81)	

\*There was a strong correlation ( $r = 0.8-0.9$ ,  $P < 0.01$ ) between T2W volume, DWI volume, and MTV<sub>42%</sub>. Therefore, only T2W volume was used in the variable selection process.  
 †LOOCV with bootstrapping was used to account for overfitting and to estimate how the model would perform on new, independent data. ADC, apparent diffusion coefficient; AUC, area under the receiver operating characteristic curve; CI, confidence interval; LOOCV, leave-one-out cross-validation; OR, odds ratio; T2W, T2-weighted.

Results are summarized in **Table 5**. The multivariate prediction model included T2W volume (OR 0.94,  $P = 0.003$ ) and SUV<sub>max</sub> (OR 1.15,  $P = 0.18$ ) as the selected predictors. Median pre-CRT T2W volume was 24.8 cm<sup>3</sup> (range 7.2–53.7 cm<sup>3</sup>) for the early responders versus 64.1 cm<sup>3</sup> (range 21.2–134.9 cm<sup>3</sup>) for the remaining patients. Median SUV<sub>max</sub> for the early responders was 15.3 (range 6.7–26.1) versus 15.9 (range 4.8–33.6) for the remaining patients. The model's performance to predict early response was AUC 0.82 within the current dataset. AUC by cross-validation (LOOCV) was 0.68 (95% CI 0.41–0.81).

## DISCUSSION

Previous studies have shown that pre-therapy quantitative imaging markers from FDG-PET/CT and MRI have potential to predict “late” outcomes including the final treatment response<sup>17–22,24–26</sup> and survival<sup>9–15</sup> in patients with LACC. In addition to these previous works, the present study specifically assessed whether quantitative imaging parameters from baseline staging MRI (including DWI) and FDG-PET/CT may also have potential as predictors of early response to cCRT and could thus play a possible role in future optimization of treatment regimens. Our exploratory results indicate that the pre-therapy tumor volume is the best predictor (with similar results for volumes derived from T2W-MRI, DWI, and FDG-PET/CT in univariable analysis) for early response to EBRT (i.e. response before onset of brachytherapy), with smaller baseline volumes (median 24.8 vs. 64.1 cm<sup>3</sup>) for the early responders. Of the other parameters, only  $SUV_{max}$  may have some complementary value, though the  $SUV_{max}$  values between both outcome groups overlapped considerably. FIGO stage was not identified as a significant predictor for early response, nor were any of the DWI-related parameters ( $ADC_{mean}$  and  $ADC_{SD}$ ). Overall, the estimated predictive performance achieved with cross-validation was only moderate (AUC ~ 0.7) and ORs of the selected parameters were in the range of 0.94–1.15, indicating a limited predictive value, which is typically not considered sufficient for clinical decision-making. The present study was exploratory, however, and further and more in-depth research is obviously required to investigate if other (combinations of) imaging and clinical parameters yield higher predictive potential.

It is difficult to directly compare our current results with those reported by previous authors, because their studies were aimed at later endpoints (disease-free and overall survival) or final response after cCRT, while the current study focuses specifically on predicting early response to EBRT. Furthermore, few studies have combined MRI and FDG-PET/CT parameters for prediction of outcome in cervical cancer. Studies that did, in most cases found FDG-PET-based pre-therapy parameters were associated with the final outcome, including a smaller baseline metabolic tumor volume<sup>11</sup> and higher  $SUV_{max}$ <sup>18</sup> corresponding to a favourable outcome. In contrast, high pre-therapy  $SUV_{max}$  was reported to predict a poor final treatment response by Kidd et al.<sup>16,22</sup> looking at PET parameters only, yet others were unable to confirm an association.<sup>10,34</sup> In three MRI-based studies that included the tumor volume on pre-treatment T2W-MRI to predict final treatment response, this parameter was not found to be a significant predictor.<sup>15,25,35</sup> However, a study by Schernberg et al.<sup>31</sup> did show a significant association between pre-treatment tumor volumes and survival.

We were unable to detect a significant association between the DWI-derived parameters and early treatment response. Although association of  $ADC_{SD}$  nearly reached significance in univariable analysis, this parameter was not identified as an independent predictor in the multivariable analysis. Previous reports on ADC-based parameters to predict response to cCRT in cervical cancer have so far shown conflicting results. Some studies found low pre-treatment  $ADC_{mean}$  to be associated with a good final response to cCRT,<sup>17,20,24</sup> while others found no significant results.<sup>11,15,21,25,35</sup> The role of DWI to predict treatment response in cervical cancer thus remains unclear but appears to be relatively limited.

When tested within our original dataset, the multivariable model (including T2W volume and  $SUV_{max}$  as predictors) yielded an AUC of 0.82. This is likely an overestimation of its actual performance in hypothetical clinical application. Because our limited cohort size did not allow splitting of the dataset into separate training and validation sets, cross-validation of the bi-directional stepwise modelling process was used to simulate model performance on a new independent dataset (i.e. to estimate its clinical potential). This resulted in an AUC of 0.68, which is likely a more realistic approximation of the model's actual performance. As mentioned, this is certainly not sufficient for clinical decision-making, and further optimization (and larger scale validation) will obviously be required. While FIGO stage—though specifically developed for prognostication—did not contribute to the current model, it will be worthwhile to further explore the added value of clinical factors, as well as additional histological, immunohistochemical, or genetic factors to generate stronger and more comprehensive clinical prediction models. It would also be worthwhile to see if the recently updated FIGO staging system would render different results than the 2009 FIGO staging system routinely used during the clinical inclusion period of the current study. Finally, sophisticated methods of image analysis and postprocessing such as Radiomics or deep learning, often used to assess large sets of variables, may prove to be of added value as the first available publications on these relatively novel methods have shown some promising preliminary results.<sup>9,18,36</sup> In the present study, we consciously limited the number of variables to prevent overfitting in a small dataset and identified a small set of relatively intuitive (first-order) features based on previous works. We acknowledge, however, that with this approach other potentially valuable imaging biomarkers may have been overlooked.

The present study has some limitations, in addition to the aforementioned small patient cohort. First, some variations in MR acquisition protocols occurred over time, which are

difficult to avoid during retrospective analysis of clinical data. We aimed to account for this by normalizing the MRI signal intensity (T2W and ADC). Second, a validated reference standard to classify early response during cCRT does not exist. We therefore chose the residual volume on T2W-MRI after 3–4 weeks of EBRT as a measure of early response, using a volume threshold of  $<10 \text{ cm}^3$  derived from a study by Mongula et al.,<sup>19</sup> who reported this as a cut-off that correlates with local control after brachytherapy. Finally, part of the MRIs used for response classification were acquired at 1.5 T instead of 3.0 T (29/46 patients). Given the comparable visual quality and resolution, this likely had little impact on the tumor volumes used for response classification.

In conclusion, these preliminary data suggest that parameters from baseline MRI and FDG-PET/CT (particularly primary tumor volume) may contribute to prediction of early response to cCRT in LACC, although the predictive performance achieved was limited. Future larger-scale studies are required to expand this research, by combining imaging markers with other potential predictors and by exploring more sophisticated image analysis techniques, to build prediction tools that can truly aid in further treatment personalization in cervical cancer.

## REFERENCES

1. Cibula D, Pötter R, Planchamp F, et al. The European Society of Gynaecological Oncology/European Society for Radiotherapy and Oncology/European Society of Pathology guidelines for the management of patients with cervical cancer. *Radiother Oncol* 2018;127:404–416. doi: 10.1016/j.radonc.2018.03.003
2. Ranjan Datta N, Stutz E, Liu M, et al. Concurrent chemoradiotherapy vs. radiotherapy alone in locally advanced cervix cancer: A systematic review and meta-analysis. *Gynecol Oncol* 2017;145:374–385. doi: 10.1016/j.ygyno.2017.01.033
3. Jastaniyah N, Yoshida K, Tanderup K, et al. A volumetric analysis of GTVD and CTVHR as defined by the GEC ESTRO recommendations in FIGO stage IIB and IIIB cervical cancer patients treated with IGABT in a prospective multicentric trial (EMBRACE). *Radiother Oncol* 2016;120:404–411. doi: 10.1016/j.radonc.2016.05.029
4. Pötter R, Tanderup K, Kirisits C, et al. The EMBRACE II study: The outcome and prospect of two decades of evolution within the GEC-ESTRO GYN working group and the EMBRACE studies. *Clin Transl Radiat Oncol* 2018;9:48–60. doi: 10.1016/j.ctro.2018.01.001
5. Giannini V, Mazzetti S, Bertotto I, et al. Predicting locally advanced rectal cancer response to neoadjuvant therapy with 18 F-FDG PET and MRI radiomics features. *Eur J Nucl Med Mol Imaging* 2019;46:878–888. doi: 10.1007/s00259-018-4250-6
6. van Rossum PSN, Fried DV, Zhang L, et al. The value of 18F-FDG PET before and after induction chemotherapy for the early prediction of a poor pathologic response to subsequent preoperative chemoradiotherapy in oesophageal adenocarcinoma. *Eur J Nucl Med Mol Imaging* 2017;44:71–80. doi: 10.1007/s00259-016-3478-2
7. Yoon HJ, Kim Y, Chung J, et al. Predicting neo-adjuvant chemotherapy response and progression-free survival of locally advanced breast cancer using textural features of intratumoral heterogeneity on F-18 FDG PET/CT and diffusion-weighted MR imaging. *Breast J* 2019;25:373–380. doi: 10.1111/tbj.13032
8. Min M, Lin P, Liney G, et al. A review of the predictive role of functional imaging in patients with mucosal primary head and neck cancer treated with radiation therapy. *J Med Imaging Radiat Oncol* 2017;61:99–123. doi: 10.1111/1754-9485.12496
9. Lucia F, Visvikis D, Desseroit M-C, et al. Prediction of outcome using pretreatment 18 F-FDG PET/CT and MRI radiomics in locally advanced cervical cancer treated with chemoradiotherapy. *Eur J Nucl Med Mol Imaging* 2018;45:768–786. doi: 10.1007/s00259-017-3898-7

10. Guler OC, Torun N, Yildyrym BA, et al. Pretreatment metabolic tumor volume and total lesion glycolysis are not independent prognosticators for locally advanced cervical cancer patients treated with chemoradiotherapy. *Br J Radiol* 2018;91:20170552. doi: 10.1259/bjr.20170552
11. Ueno Y, Lisbona R, Tamada T, et al. Comparison of FDG PET metabolic tumour volume versus ADC histogram: Prognostic value of tumour treatment response and survival in patients with locally advanced uterine cervical cancer. *Br J Radiol* 2017;90:20170035. doi: 10.1259/bjr.20170035
12. Park JJ, Kim CK, Park BK. Prognostic value of diffusion-weighted magnetic resonance imaging and 18 F-fluorodeoxyglucose-positron emission tomography/computed tomography after concurrent chemoradiotherapy in uterine cervical cancer. *Radiother Oncol* 2016;120:507–511. doi: 10.1016/j.radonc.2016.02.014
13. Miccò M, Vargas HA, Burger IA, et al. Combined pre-treatment MRI and 18F-FDG PET/CT parameters as prognostic biomarkers in patients with cervical cancer. *Eur J Radiol* 2014;83:1169–1176. doi: 10.1016/j.ejrad.2014.03.024
14. Nakamura K, Kajitani S, Joja I, et al. The posttreatment mean apparent diffusion coefficient of primary tumor is superior to pretreatment ADCmean of primary tumor as a predictor of prognosis with cervical cancer. *Cancer Med* 2013;2:519–525. doi: 10.1002/cam4.100
15. Somoye G, Harry V, Semple S, et al. Early diffusion weighted magnetic resonance imaging can predict survival in women with locally advanced cancer of the cervix treated with combined chemoradiation. *Eur Radiol* 2012;22:2319–2327. doi: 10.1007/s00330-012-2496-0
16. Kidd EA, Siegel BA, Dehdashti F, et al. The standardized uptake value for F-18 fluorodeoxyglucose is a sensitive predictive biomarker for cervical cancer treatment response and survival. *Cancer* 2007;110:1738–1744. doi: 10.1002/cncr.22974
17. Yang W, Qiang JW, Tian HP, et al. Multi-parametric MRI in cervical cancer: early prediction of response to concurrent chemoradiotherapy in combination with clinical prognostic factors. *Eur Radiol* 2018;28:437–445. doi: 10.1007/s00330-017-4989-3
18. Bowen SR, Yuh WTC, Hippe DS, et al. Tumor radiomic heterogeneity: Multiparametric functional imaging to characterize variability and predict response following cervical cancer radiation therapy. *J Magn Reson Imaging* 2018;47:1388–1396. doi: 10.1002/jmri.25874

19. Mongula JE, Slangen BFM, Lambregts DMJ, et al. Consecutive magnetic resonance imaging during brachytherapy for cervical carcinoma: predictive value of volume measurements with respect to persistent disease and prognosis. *Radiat Oncol* 2015;10:252. doi: 10.1186/s13014-015-0559-5
20. Liu Y, Sun H, Bai R, et al. Time-window of early detection of response to concurrent chemoradiation in cervical cancer by using diffusion-weighted MR imaging: a pilot study. *Radiat Oncol* 2015;10:185. doi: 10.1186/s13014-015-0493-6
21. Makino H, Morishige K, Kato H, et al. Predictive value of diffusion-weighted magnetic resonance imaging during chemoradiotherapy for uterine cervical cancer. *J Obstet Gynaecol Res* 2013;40:1098–1104. doi: 10.1111/jog.12276
22. Kidd EA, Thomas M, Siegel BA, et al. Changes in Cervical Cancer FDG Uptake During Chemoradiation and Association With Response Radiation Oncology. *Radiat Oncol Biol* 2013;85:116–122. doi: 10.1016/j.ijrobp.2012.02.056
23. Vandecasteele K, Delrue L, Lambert B, et al. Value of magnetic resonance and 18FDG PET-CT in predicting tumor response and resectability of primary locally advanced cervical cancer after treatment with intensity-modulated arc therapy: A prospective pathology-matched study. *Int J Gynecol Cancer* 2012;22:630–637. doi: 10.1097/IGC.0b013e3182428925
24. Liu Y, Bai R, Sun H, et al. Diffusion-weighted imaging in predicting and monitoring the response of uterine cervical cancer to combined chemoradiation. *Clin Radiol* 2009;64:1067–1074. doi: 10.1016/j.crad.2009.07.010
25. Harry VN, Semple SI, Gilbert FJ, et al. Diffusion-weighted magnetic resonance imaging in the early detection of response to chemoradiation in cervical cancer. *Gynecol Oncol* 2008;111:213–220. doi: 10.1016/j.ygyno.2008.07.048
26. Mcveigh PZ, Syed AM, Milosevic M, et al. Diffusion-weighted MRI in cervical cancer. *Eur Radiol* 2008;18:1058–1064. doi: 10.1007/s00330-007-0843-3
27. Sala E, Miccò M, Burger IA, et al. Complementary prognostic value of pelvic Magnetic Resonance Imaging and whole-body fluorodeoxyglucose Positron Emission Tomography/Computed Tomography in the pretreatment assessment of patients with cervical cancer. *Int J Gynecol Cancer* 2015;25:1461–1467. doi: 10.1097/IGC.0000000000000519
28. FIGO Committee on Gynecologic Oncology. FIGO staging for carcinoma of the vulva, cervix, and corpus uteri. *Int J Gynecol Obstet* 2014;125:97–98. doi: 10.1016/j.ijgo.2014.02.003
29. Erdi YE, Mawlawi O, Larson SM, et al. Segmentation of lung lesion volume by adaptive positron emission tomography image thresholding. *Cancer* 1997;80:2505–9. doi: 10.1002/(sici)1097-0142(19971215)80:12+<2505::aid-cnrcr24>3.3.co;2-b

30. Van Griethuysen JJM, Fedorov A, Parmar C, et al. Computational radiomics system to decode the radiographic phenotype. *Cancer Res* 2017;77:e104–e107. doi: 10.1158/0008-5472.CAN-17-0339
31. Schernberg A, Bockel S, Annede P, et al. Tumor Shrinkage During Chemoradiation in Locally Advanced Cervical Cancer Patients: Prognostic Significance, and Impact for Image-Guided Adaptive Brachytherapy. *Int J Radiat Oncol Biol Phys* 2018;102:362–372. doi: 10.1016/j.ijrobp.2018.06.014
32. Minkoff D, Gill BS, Kang J, et al. Cervical cancer outcome prediction to high-dose rate brachytherapy using quantitative magnetic resonance imaging analysis of tumor response to external beam radiotherapy. *Radiother Oncol* 2015;115:78–83. doi: 10.1016/j.radonc.2015.03.007
33. Akaike H. A New Look at the Statistical Model Identification. *IEEE Trans Automat Contr* 1974;19:716–723. doi: 10.1109/TAC.1974.1100705
34. Bjurberg M, Kjellén E, Ohlsson T, et al. Prediction of patient outcome with 2-deoxy-2-[18F]fluoro-D-Glucose- Positron Emission Tomography Early During Radiotherapy for Locally Advanced Cervical Cancer. *Int J Gynecol Cancer* 2009;19:1600–1605. doi: 10.1111/IGC.0b013e3181c00359
35. Das S, Chandramohan A, Karunya J, et al. Role of conventional and diffusion weighted MRI in predicting treatment response after low dose radiation and chemotherapy in locally advanced carcinoma cervix. *Radiother Oncol* 2015;117:288–293. doi: 10.1016/j.radonc.2015.10.006
36. Altazi BA, Fernandez DC, Zhang GG, et al. Investigating multi-radiomic models for enhancing prediction power of cervical cancer treatment outcomes. *Phys Medica* 2018;46:180–188. doi: 10.1016/j.ejmp.2017.10.009



The background is a vibrant blue with a complex, organic pattern. It features several overlapping, rounded shapes that resemble stylized leaves or petals. A prominent feature is a large, dark blue, curved shape that contains a fine halftone dot pattern. The overall effect is a layered, textured composition.

## Chapter 6

# PRE-TREATMENT FDG-PET, CLINICAL AND HIGH-RISK HUMAN PAPILLOMAVIRUS BIOMARKERS IN ANAL CANCER: WHICH CAN BEST PREDICT LOCOREGIONAL TREATMENT FAILURE AFTER CHEMORADIOOTHERAPY?

Lisa A. Min, Baukelien van Triest, Wouter V. Vogel, Younan J.L. Vacher,  
Sander Roberti, Niels W. Schurink, Pétur Snæbjörnsson, Luc Dewit,  
Monique Maas, Carmelo Sofia, Regina G.H. Beets-Tan,  
Doenja M.J. Lambregts

*In submission*

# ABSTRACT

## Purpose

To build and explore the value of a multivariable predictive model incorporating semi-quantitative variables from FDG-PET/CT and clinicopathological prognostic factors to predict locoregional treatment failure before the start of treatment in anal cancer patients treated with cCRT.

## Methods

Retrospective study of 99 patients treated with cCRT for anal cancer (squamous cell carcinoma) with a minimum follow-up of  $\geq 1$  year after completion of treatment. Pre-treatment FDG-PET/CTs were analyzed and the following parameters were extracted from the primary tumour:  $MTV_{42\%}$ , SUVmax, SUVpeak, SUVskewness, SUVentropy, SUVuniformity and TLG. Age, sex, cTN-stage, high-risk HPV (hr-HPV) status and whether patients underwent a sequential radiotherapy boost were also documented. The value of different combinations of clinical baseline, hr-HPV and PET/CT-derived variables to predict locoregional treatment failure (within  $\leq 1$  year after treatment) was analyzed using penalized multivariable logistic regression analysis, using the least absolute shrinkage and selection operator (LASSO). Leave-one-out cross validation (LOOCV) was used to estimate the performance of the resulting prediction models in an “unseen” dataset.

## Results

Nineteen patients (19%) experienced 1-year locoregional treatment failure. A “clinical” model incorporating male sex (Odds Ratio (OR) 9.41), cN+ stage (OR 1.99) and hr-HPV+ status (OR 0.17) showed the best performance to predict locoregional failure with an AUC of 0.89 (0.81 after LOOCV). Adding PET/CT-derived variables to this clinical model did not improve performance: AUC 0.90 (0.79 after LOOCV). Of the PET/CT-derived parameters only  $MTV_{42\%}$  was identified as a predictor (OR 1.22). Model performance when including only PET-variables was poor (AUC 0.64; 0.36 after LOOCV).

## Conclusions

The combination of hr-HPV-negative, node-positive tumour stage and male sex provides the strongest predictive value to estimate the risk of locoregional failure after cCRT before onset of treatment. Semi-quantitative pre-treatment PET/CT-derived parameters do not offer complementary value.

## INTRODUCTION

Squamous cell carcinoma (SCC) of the anal canal is a relatively rare malignancy,<sup>1,2</sup> which is treated with concurrent chemo-radiotherapy (cCRT) in most cases (T2-4 stage and T1 if  $\geq 1$ cm).<sup>3-6</sup> To date, there is no definitive consensus about the optimal cCRT schedule.<sup>7,8</sup> Even though up to 90% of patients achieve a complete response after cCRT, the disease recurs in 15-30% of patients, the majority (up to 85%) being locoregional treatment failures within the first two years after cCRT.<sup>9-11</sup> In case of local or locoregional failure, salvage surgery is considered the only potentially curative treatment modality, provided that a radical resection is feasible. These salvage procedures often entail extensive surgery with high morbidity, and a relatively high complication and relapse rate.<sup>12-14</sup>

Pre-treatment prediction of the risk for locoregional failure after cCRT may help to select patients for intensified treatment schedules (e.g. dose escalation) or more intensive follow-up schedules, in order to improve cure rates.<sup>15,16</sup> Known risk factors for treatment failure include larger tumour volume or length, node-positive disease, male sex and high-risk human papillomavirus (hr-HPV)-negative tumours.<sup>10,15,17-19</sup> However, individually, these parameters are insufficiently accurate to use for patient selection and comprehensive prediction models incorporating these factors are currently not available. In addition, little is known about the complementary value of imaging-derived quantitative parameters or “biomarkers” for prediction of treatment failure.

Positron-Emission Tomography/Computed Tomography (PET/CT) is increasingly used in the routine diagnostic workup (and treatment response evaluation) of anal cancer patients, in particular for the clinically more advanced tumours with higher *a priori* risk for nodal and/or distant metastases. There is growing evidence that PET/CT can have a significant impact on staging - and hence affect the radiotherapy plan or the overall treatment intent - in these cases.<sup>8,20</sup> Several studies have shown that parameters derived from PET/CT, such as the standardized uptake value (SUV) or metabolic tumour volume (MTV), may also be of value as predictors of treatment response,<sup>17,21</sup> recurrence<sup>17,21-28</sup> and survival.<sup>21,22,24,26-30</sup> However, due to the low incidence of anal carcinoma, many of these studies are limited by small and/or heterogeneous patient cohorts. Moreover, in most of these studies the PET/CT-derived parameters have not yet been compared or combined with known clinical risk factors.

6

Therefore, the aim of this study was to build and explore the value of a multivariable clinical predictive model incorporating both semi-quantitative variables derived from fluorodeoxyglucose- (FDG) PET/CT as well as known clinicopathological prognostic factors such as cTN-stage and hr-HPV status to predict locoregional treatment failure before the start of treatment in anal cancer patients treated with cCRT in a relatively large and homogenous patient cohort.

## METHODS

### Patients and treatment

This retrospective study was approved by the institutional ethical review board. We identified all patients that were treated with chemoradiotherapy at The Netherlands Cancer Institute between 2008-2018 for primary anal cancer. A cohort of 99 patients fulfilled all of the following inclusion criteria:

1. Histopathologically confirmed squamous cell carcinoma
2. Pre-treatment staging including FDG-PET/CT imaging  
(with visible primary tumour in situ)
3. Treated with curative intent with concurrent chemoradiotherapy (cCRT)
4. Post-treatment follow-up of at least 1 year

The treatment protocol consisted of intensity-modulated radiation therapy (IMRT) or volumetric-modulated arc therapy (VMAT) with a simultaneous integrated boost (SIB) of 5940 cGy to the gross tumour volume (GTV) and 4950 cGy to elective lymph node regions, combined with 825 mg/m<sup>2</sup>/BID capecitabine on radiation treatment days, or 750 mg/m<sup>2</sup> 5-fluorouracil (5-FU) for five consecutive days in the first and fifth week of radiotherapy. On the first day of treatment a single dose of Mitomycin C (12 mg/m<sup>2</sup>, max 20 mg) was administered. Patients with evidence of gross macroscopic residual tumour in the fifth week of radiotherapy (as assessed by digital rectal examination and/or MRI) received a sequential radiation boost of 3 x 1.8 Gy.

### Outcome definition

The primary outcome was first-year locoregional failure, defined as a recurrence or residual disease after completion of cCRT occurring within the radiation field; from the bifurcation of the external and internal iliac arteries to the superficial and deep inguinal lymph node areas. The presence or absence of locoregional failure was



assessed by routine three-monthly clinical examination, serum SCC antigen testing, and radiological imaging upon indication. Each suspected locoregional treatment failure was confirmed histologically by biopsy or resection.

### FDG-PET/CT imaging

Pre-treatment staging FDG-PET/CTs were performed on a Gemini TF 16 or Gemini TF Big Bore hybrid scanner (both Philips Healthcare, Best, The Netherlands) after  $\geq 6$  hours of fasting (target blood glucose level  $< 10$  mmol/L) followed by administration of a 180 MBq or 280 MBq (if body mass index  $> 28$ ) intravenous bolus of 2-deoxy-2-[ $^{18}\text{F}$ ]fluoro-D-glucose (FDG). Scanning ensued after a resting period of  $\pm 60$  minutes from the skull base to the mid-thighs, with 2 minutes per bed position. PET images were attenuation corrected using native CT-images (acquired at 120-140 kV and with 29-324 mAs using automatic dose-modulation) and reconstructed to 4 x 4 mm pixels and 4 mm slices. CT images were reconstructed to 1.17 x 1.17 mm pixels and 2 mm slices with a 2 mm slice spacing.

### Image analysis

FDG-PET/CTs were transferred to an offline workstation for tumour segmentation, which was performed semi-automatically using the open-source software 3D Slicer (version 4.8.1, slicer.org). PET parameters were subsequently extracted using PyRadiomics (version 2.2.0, pyradiomics.readthedocs.io).<sup>31</sup> A preliminary volume of interest (VOI) was manually drawn around the primary tumour region in each slice of the FDG-PET image (by LM, experienced in PET/CT segmentation), from which the metabolic tumour volume (MTV) was automatically calculated using a threshold of 42% of the maximum SUV within the VOI ( $\text{MTV}_{42\%}$ ), using methods previously reported.<sup>32-34</sup> In addition to the  $\text{MTV}_{42\%}$ , the following frequently reported (first-order) semi-quantitative PET/CT parameters were extracted from the MTV: SUVmax (maximum SUV in the tumour), SUVpeak (mean SUV of the 3 x 3 x 3 voxel region with the highest average SUV), SUVskewness (asymmetry of the SUV histogram), SUVkurtosis ('peakedness' of the histogram), SUVentropy (randomness of the histogram), SUVuniformity (homogeneity of the histogram), and total lesion glycolysis (TLG:  $\text{MTV}_{42\%} \times \text{SUVmean}$ ).

### Clinical baseline variables

The following "clinical baseline" variables were collected from the medical patient records: age at diagnosis, sex, cT-stage (dichotomized as cT1/2 vs. cT3/4) and cN-stage (dichotomized as cN+ vs. cN-). cTN-stage was retrieved from the multidisciplinary team reports and based on integrated assessment of routine staging procedures including

physical examination, MRI, FDG-PET/CT and ultrasound ±fine needle aspiration. In addition, hr-HPV status was retrieved from the institutional patient record or the national pathology database, when available.

### Statistical analysis

Statistical analysis was performed in R statistical software (version 3.6.1, R Foundation for Statistical Computing). From each pair of continuous variables with a Pearson correlation at least 0.8, the variable with the greatest average correlation with all other variables was excluded from further analyses. A schematic overview of the study and analysis workflow is provided in **Figure 1**. Penalized logistic regression models predicting 1-year locoregional failure were obtained using the least absolute shrinkage and selection operator (LASSO).<sup>35</sup> Seven different models were obtained by using seven pre-defined sets of predictor variables: (1) baseline variables (age, sex, cTN-stage), (2) tumour hr-HPV status, (3) PET/CT parameters, (4) baseline variables and tumour hr-HPV status, (5) baseline variables and PET/CT parameters (MTV<sub>42%</sub>, SUVpeak, SUVuniformity, SUVkurtosis after correlation analysis), (6) tumour hr-HPV status and PET/CT parameters, and (7) baseline variables, tumour hr-HPV status and PET/CT parameters. Whether patients underwent a radiotherapy boost in addition to the standard treatment (boost yes vs. no), was included in each of the seven models as a potential confounder. Since hr-HPV status was not available for all patients, models using this variable were obtained by averaging coefficients over 100 models estimated on 100 imputed datasets that were obtained using multiple imputation by chained equations. Predictive performance of each model was assessed using the area under the receiver-operating curve (AUC). For models without hr-HPV, DeLong confidence intervals (CIs) for the AUCs were obtained. CIs were based on the imputed datasets for models with hr-HPV. Leave-one-out cross validation (LOOCV) with bootstrapping (1000 iterations) was used for each set of variables to estimate the AUC in an independent dataset. A detailed description of the statistical procedures is provided in **Supplementary Material 1**.

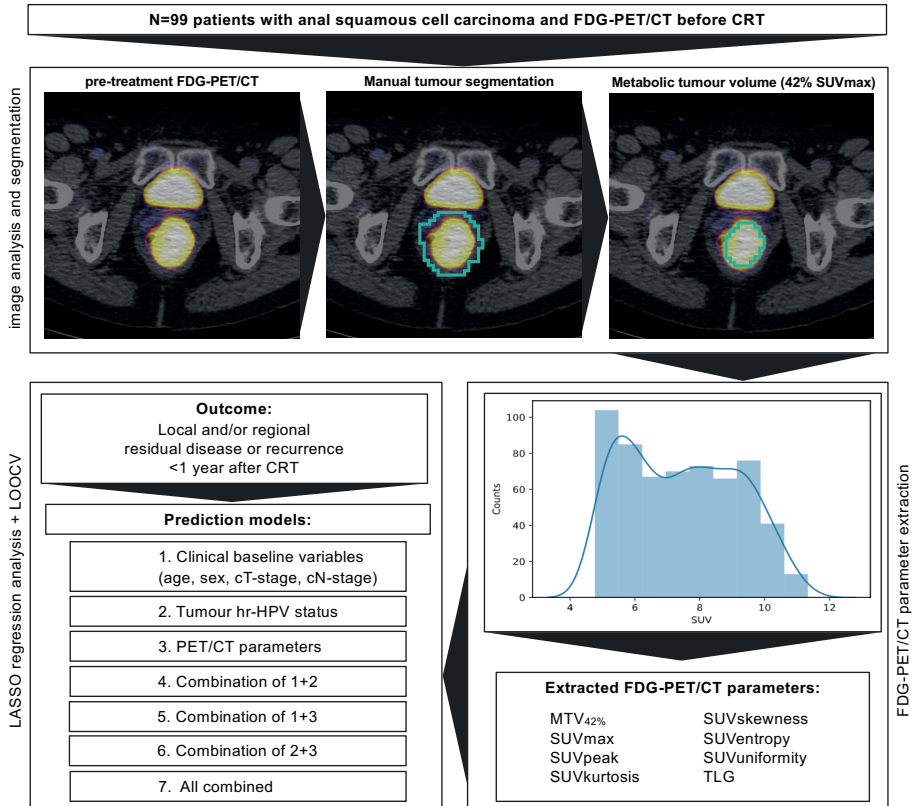


Figure 1. Schematic outline of the study and analysis workflow

## RESULTS

### Baseline characteristics

Detailed patient, tumour and treatment characteristics for the 99 study patients (43 male; median age 62 years) are given in **Table 1**. At baseline, the majority of patients had cT2 (55%) or cT3 (30%) tumours and node-positive disease (62%). Data on hr-HPV association was available for 70 patients (71%), and was positive in 62 (89%). In total, 19 patients (19%) experienced locoregional treatment failure within the first year after cCRT (12 local tumour only, 2 regional nodes only and 5 local tumour and regional nodes combined).



Table 1. Baseline patient characteristics (n= 99)		
Median age		62 years (range: 34-80)
		<b>Number of patients (%)</b>
Sex	Male	43 (43)
	Female	56 (57)
High-risk HPV	Positive*	62 (63)
	Negative	8 (8)
	Unknown	29 (29)
cT-stage <sup>†</sup>	cT1	2 (2)
	cT2	55 (54)
	cT3	30 (30)
	cT4	13 (13)
cN-stage <sup>‡</sup>	cN0	38 (38)
	cN1	36 (36)
	cN2	19 (19)
	cN3	6 (6)
Radiation therapy	IMRT	25 (25)
	VMAT	74 (75)
	Sequential boost (3 x 1.8 Gy)	
	Yes	35 (35)
No	64 (65)	
Chemotherapy regimen <sup>§</sup>	Capecitabine	92 (92)
	5-FU	7 (7)
Locoregional failure	No	80 (81)
	Yes	19 (19)
	Median time to failure	3.6 months (range 0.8 – 10.5)
Site of failure	Primary tumour site only	12 (63)
	Regional nodes only	2 (11)
	Tumour + nodes	5 (26)

Note: unless indicated differently, numbers are absolute numbers of study patients.  
 HPV: human papillomavirus; IMRT: intensity-modulated radiation therapy; VMAT: volumetric-modulated arc therapy; 5-FU: 5-fluorouracil  
 \* Tumour hr-HPV status was determined by polymerase chain reaction (PCR) in 44 cases, and by immunohistochemistry (p16 as surrogate biomarker) in 18 cases.  
<sup>†</sup> Staging was performed according to the UICC TNM Classification of Malignant Tumours 7<sup>th</sup> edition (2009). cT-stage was routinely determined using digital rectal examination and MRI.  
<sup>‡</sup> cN-stage was determined by a combination of clinical assessment, FDG-PET/CT and ultrasound with fine needle aspiration in case of suspected inguinal N+.  
<sup>§</sup> In addition to capecitabine/5-FU, a single dose of Mitomycin C was administered in all study patients. One patient switched from capecitabine to 5-FU after one week of treatment due to presumed cardiac side-effects (counted as 5-FU).

### Multivariable prediction models

The results of the multivariable regression analysis are summarized in **Table 2**. Of the initial eight PET/CT parameters, only SUV<sub>peak</sub>, SUV<sub>kurtosis</sub> and SUV<sub>uniformity</sub> were included in the multivariable analysis. The remaining parameters were excluded from further analysis because of strong correlations ( $\rho \geq 0.8$ ) (see **Figure 2**). Of the “single-modality” predictive models (PET/CT parameters only, clinical baseline variables only or hr-HPV status only), the clinical baseline model had the best predictive performance (AUC 0.84 in the original dataset, AUC 0.71 after LOOCV). Male sex was the strongest single predictor within this model (odds ratio (OR) 10.61), but node-positive disease was also associated with a higher predicted chance of locoregional failure (OR 1.50). The model with PET/CT parameters only had the weakest performance (AUC 0.64, AUC 0.36 after LOOCV), with MTV<sub>42%</sub> as the only predictive variable (OR 1.22). The hr-HPV positive tumours were associated with a lower chance of locoregional failure (OR 0.12), resulting in an AUC of 0.70 (AUC 0.55 after LOOCV) for the model based on hr-HPV status only.

Of the combined models, the model combining clinical baseline variables with hr-HPV status had the best overall performance, with an AUC of 0.89 (AUC 0.81 after LOOCV). Addition of PET/CT parameters to this model did not improve its performance (AUC 0.79 after LOOCV). The sequential radiotherapy boost that was administered in a subset of patients (and was therefore included in all analyses as a confounding factor/predictor) was associated with a higher likelihood of locoregional failure in some of the models (OR 1.00-1.64).

**Table 2.** Multivariable prediction models for locoregional failure within 1 year after cCRT

I – Separate models				
	Selected variables	OR (CI)	AUC training <sup>a</sup> (CI)	AUC LOOCV <sup>b</sup> (CI)
Clinical baseline model	Male sex (vs. female)	<b>10.61 (3.65 – 124.88)</b>	0.84 (0.76 – 0.92)	0.71 (0 – 0.81)
	Age (years)	1.00 (0.94 – 1.03)		
	T-stage 3+4 (vs. T1+2)	1.00 (0.42 – 3.55)		
	<b>N-positive (vs. negative)</b>	<b>1.50 (1.00 – 6.68)</b>		
	Boost yes (vs. no)	1.64 (1.00 – 6.50)		
hr-HPV model	<b>hr-HPV positive (vs. negative)</b>	<b>0.12 (0.02 – 0.65)</b>	0.70 (0.59 – 0.80)	0.55 (0.19 – 0.75)
	Boost yes (vs. no)	1.63 (0.51 – 5.17)		
FDG-PET/CT model	<b>MTV<sub>42%</sub> (cm<sup>3</sup>)</b>	<b>1.22 (1.00 – 2.44)</b>	0.64 (0.50 – 0.78)	0.36 (0 – 0.63)
	SUV <sub>peak</sub>	1.00 (0.61 – 2.12)		
	SUV <sub>kurtosis</sub>	1.00 (0.72 – 1.38)		
	SUV <sub>uniformity</sub>	1.00 (0.50 – 1.00)		
	Boost yes (vs. no)	1.00 (1.00 – 4.21)		
II – Combined models				
	Variables	OR (CI)	AUC training <sup>a</sup>	AUC LOOCV <sup>b</sup>
Baseline + HPV model	Male sex (vs. female)	<b>9.41 (3.70 – 110.07)</b>	0.89 (0.85 – 0.93)	0.81 (0.55 – 0.87)
	Age (years)	1.00 (0.94 – 1.03)		
	T-stage 3+4 (vs. T1+2)	1.00 (0.40 – 3.27)		
	<b>N-positive (vs. negative)</b>	<b>1.99 (1.00 – 8.27)</b>		
	<b>hr-HPV positive (vs. negative)</b>	<b>0.17 (0.05 – 0.96)</b>		
	Boost yes (vs. no)	1.32 (0.85 – 6.09)		
Baseline + FDG-PET/CT model	Male sex (vs. female)	<b>5.02 (3.24 – 73.86)</b>	0.83 (0.73 – 0.93)	0.62 (0 – 0.69)
	Age (years)	1.00 (0.94 – 1.02)		
	T-stage 3+4 (vs. T1+2)	1.00 (0.15 – 1.67)		
	N-positive (vs. negative)	1.00 (1.00 – 4.34)		
	<b>MTV<sub>42%</sub> (cm<sup>3</sup>)</b>	<b>1.09 (1.00 – 2.83)</b>		
	SUV <sub>peak</sub>	1.00 (0.62 – 2.00)		
	SUV <sub>kurtosis</sub>	1.00 (0.78 – 1.75)		
	SUV <sub>uniformity</sub>	1.00 (0.37 – 1.00)		
	Boost yes (vs. no)	1.00 (1.00 – 5.92)		
FDG-PET/CT + HPV model	hr-HPV positive (vs. negative)	0.27 (0.05 – 1.17)	0.78 (0.68 – 0.85)	0.44 (0.01 – 0.67)
	MTV <sub>42%</sub> (cm <sup>3</sup> )	1.10 (0.98 – 2.54)		
	SUV <sub>peak</sub>	1.00 (0.66 – 1.92)		
	SUV <sub>kurtosis</sub>	1.00 (0.85 – 1.37)		
	SUV <sub>uniformity</sub>	0.99 (0.56 – 1.02)		
	Boost yes (vs. no)	1.01 (0.81 – 3.72)		

PRE-TREATMENT FDG-PET, CLINICAL AND HIGH-RISK HUMAN PAPILLOMAVIRUS BIOMARKERS  
IN ANAL CANCER: WHICH CAN BEST PREDICT LOCOREGIONAL TREATMENT FAILURE AFTER  
CHEMORADIOTHERAPY?

<b>All combined</b>	<b>Male sex (vs. female)</b>	<b>7.55 (2.85 -137.17)</b>	0.90 (0.85 – 0.93)	0.79 (0.62 – 0.85)
	Age (years)	1.00 (0.94 – 1.02)		
	T-stage 3+4 (vs. T1+2)	1.00 (0.21 – 1.98)		
	N-positive (vs. negative)	1.53 (0.98 – 5.46)		
	hr-HPV positive (vs. negative)	0.21 (0.05 – 1.10)		
	MTV <sub>42%</sub> (cm <sup>3</sup> )	1.06 (0.93 – 2.95)		
	SUV <sub>peak</sub>	1.00 (0.45 – 1.59)		
	SUV <sub>kurtosis</sub>	1.00 (0.75 – 1.70)		
	<b>SUV<sub>uniformity</sub></b>	<b>0.96 (0.35 – 1.00)</b>		
	Boost yes (vs. no)	1.20 (0.76 – 6.21)		
<p>Predictive variables selected in the separate (I) and combined (II) multivariate prediction models are indicated in bold. AUC: area under the receiver-operating characteristic curve; OR: odds ratio; CI: 95% confidence interval; LOOCV: leave-one-out cross validation.  * AUC of the model when applied on the 99 patients in the actual cohort, that was used to fit the model.  † AUC after LOOCV. A detailed description of the statistical analysis including the LOOCV procedure and calculation of the CIs is provided in Supplementary Material 1.</p>				

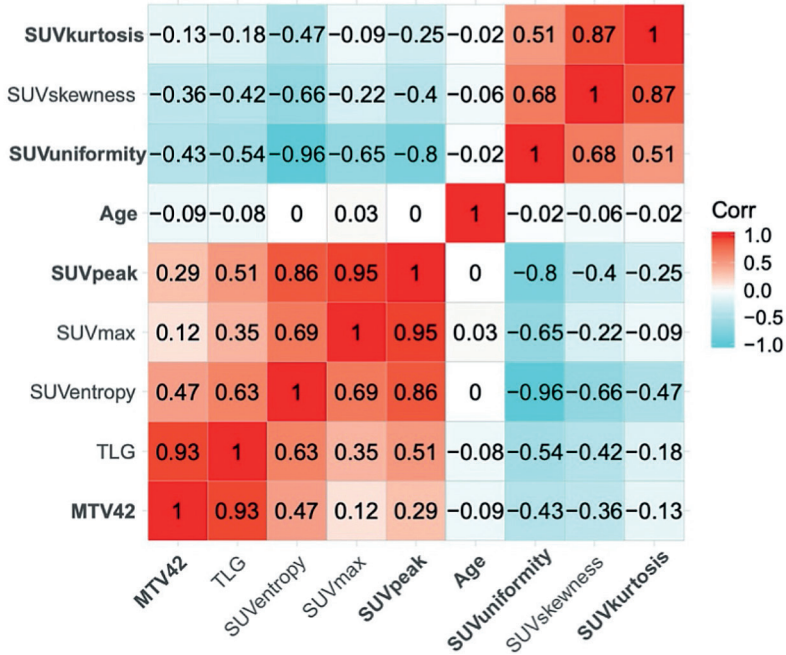


**Figure 2.** Correlation matrix with Pearson’s correlation for all pairs of continuous variables, including all FDG-PET/CT variables (MTV<sub>42%</sub>, TLG, SUV<sub>entropy</sub>, SUV<sub>max</sub>, SUV<sub>peak</sub>, SUV<sub>uniformity</sub>, SUV<sub>skewness</sub>, SUV<sub>kurtosis</sub>) and patient age. Variables included in the multivariable analyses are printed in bold italic.

## DISCUSSION

With this study we explored the value of semi-quantitative variables derived from baseline (pre-treatment) FDG-PET/CT, combined with clinical baseline variables (cTN-stage, age, sex) and tumour hr-HPV status, to build predictive models for locoregional failure within the first year after cCRT in anal cancer patients. Our results show that a combined model incorporating hr-HPV status, cN-status and the patient's sex provided the strongest clinical predictive performance (AUC 0.81 after cross-validation within our dataset), and that addition of semi-quantitative FDG-PET/CT variables did not contribute to a better predictive performance (AUC 0.79). Among the FDG-PET/CT variables, a higher metabolic tumour volume ( $MTV_{42\%}$ ) was the only potential predictor of locoregional failure, but performance of the resulting prediction model based on PET/CT only was poor (cross-validated AUC of 0.36). Based on our results, the value of pre-treatment semi-quantitative FDG-PET/CT to help predict the risk of locoregional failure after cCRT in a clinical setting thus appears to be low.

Our results are largely in line with those of a similar study by Rusten et al., who also combined FDG-PET/CT parameters and clinicopathological factors of 93 anal cancer patients to predict locoregional failure. They found a predictive role for MTV in their bivariate analysis, but – similar to our results – reported superior predictive performance for a combination of hr-HPV and N3-stage indicating that clinical parameters outperform PET parameters in this specific setting.<sup>17</sup> Two smaller studies also focused on prediction of treatment failure using FDG-PET/CT parameters, but these reports did not include clinicopathological variables. Both found an association between pre-treatment MTV and locoregional recurrence, but not for other PET/CT parameters (e.g.: SUVmax, SUVmean, TLG), results that are confirmed by our current findings.<sup>23,25</sup> In contrast, Bazan et al. found MTV to be superior to cTN-stage or patient age, sex and HIV-status, albeit to predict progression-free and overall survival rather than locoregional failure (which was not included as an outcome in their report).<sup>28</sup> A final study by Leccisotti and colleagues reported a significant association for the multivariable combination of pre-treatment SUVpeak, whole-body MTV, TLG, disease stage and patient age to predict overall survival,<sup>22</sup> but locoregional failure was again not included in their analysis, making it difficult to compare their results directly with ours. All in all, it is striking that the parameter most commonly reported as a pre-treatment predictor is the MTV, which essentially provides a reflection of the viable tumour burden or volume. For future research it would be interesting to see how MTV compares as a predictor to volumetric measures derived from other modalities, such

6

as MRI, as well as to parameters derived from (sequential) PET during and/or after treatment, as there is some preliminary evidence (in anal cancer as well as in several other tumour types) that this approach may render more valuable PET predictors.<sup>23,36-38</sup> These data were unfortunately not available in our cohort and could therefore not be included in our current study.

Tumour hr-HPV status was identified as an important predictor in our models, with a higher risk of locoregional failure in patients with hr-HPV negative tumours. Four of the eight (50%) hr-HPV-negative tumours in our cohort relapsed within the first year after cCRT, versus only six out of 62 (10%) hr-HPV positive tumours. This is consistent with literature that shows an increased chance of treatment failure after cCRT and a reduced survival for patients with hr-HPV negative tumours.<sup>18,39,40</sup> Meulendijks et al. studied a population very similar to our cohort and detected hr-HPV (both PCR- and P16 IHC-positive) in 87% of 107 patients. In their cohort of patients treated with radiotherapy with or without concurrent chemotherapy, the patients with hr-HPV-negative tumours had reduced 3-year locoregional control (LRC: 15%) and overall survival rates (OS: 35%) compared to those with hr-HPV positive tumours (LRC 82%, OS 87%). The authors suggested a role for *TP53* tumour suppressor gene disruption in inducing relative radiotherapy resistance in hr-HPV-negative tumours.<sup>18</sup> Although hr-HPV tumour status is generally acknowledged as a prognostic factor, it is to date not routinely tested in all anal cancer patients. This unfortunately hampers its availability as a predictor in (retrospectively designed) clinical prediction models like ours. In our cohort hr-HPV status was unavailable for 29% of the study patients, which was compensated for by using multiple imputation. The fact that hr-HPV status is not yet part of the standard workup for all patients is probably related to the fact that so far it did not directly impact patient management strategies. Our current results, however, confirm the status of hr-HPV as an important clinical predictive and prognostic factor, and support its further adoption in the routine clinical workup of anal cancer.

Male sex and cN-stage were the other clinical variables that were selected in our models as predictors for locoregional failure. The association between male sex and reduced prognosis in anal cancer has previously been described in literature,<sup>2,15,41-43</sup> but a clear explanation for this correlation has not been established so far. One suggested mediating factor is HIV-status. In many western countries HIV is more frequently diagnosed in men, due to a combination of higher prevalence among men who have sex with men and associated testing bias. Positive HIV status and its treatment with highly-active antiretroviral therapy (HAART) have both been associated with poorer

treatment outcomes, though not consistently.<sup>44,45</sup> In our cohort HIV-test results were only available from our institutional patient records for a limited number of patients, which did not allow meaningful analysis of this variable. As a critical note, the negative effect of male sex in our cohort (40% vs. 4% locoregional failure for male vs. female patients) appears to be disproportionate compared to previous reports, for which we could not find an explanation. Clinical N-stage has also been reported previously as predictor of both locoregional failure and survival.<sup>3,46</sup> As mentioned before, the study by Rusten et al. identified cN+ disease (N3-stage) as a major predictor for treatment failure.<sup>17</sup> This association may be attributed to the fact that positive N-stage is a sign of more aggressive and advanced stage disease. This is further suggested by our finding that in most (86%) of the cN+ patients in our cohort who experienced a locoregional failure, the site of the primary tumour was also involved in the relapse.

From a clinical perspective, one of the main reasons to predict response to cCRT would be to allow further personalisation of treatment based on the anticipated treatment outcome. Pre-therapy selection of patients with a high risk of locoregional failure, using parameters available from the baseline staging workup, could enable future selective dose escalation strategies for these patients. To date, most guidelines still advise a uniform cCRT regimen for all anal cancer patients,<sup>8</sup> but there is some evidence that boost-intensity modulated strategies may improve clinical outcomes.<sup>47</sup> In our institute an additional boost of three fractions of 1.8 Gy to the GTV is already routinely prescribed to patients with clinically detectable gross residual tumour in the fifth week of radiation therapy (after  $\pm 45$  Gy). In the current cohort, 35% of patients received this sequential boost. As this selective treatment modification was expected to interfere with the outcome of treatment failure, we included the radiotherapy boost (yes vs. no) as a variable in the modelling process to detect and correct for potential confounding. It was confirmed to be associated with locoregional failure, in particular in combination with the baseline variables and hr-HPV status. The patients receiving an additional boost in our cohort constitute the subgroup of patients that showed the poorest clinical response already after five weeks of treatment suggesting a more aggressive tumour biology, which also explains why they had a higher chance of locoregional failure (with ORs up to 1.32). The patients in our cohort routinely underwent an interim clinical response assessment during treatment. The role of such an interim response evaluation, by clinical assessment and/or imaging, is poorly documented in literature, but it may – in addition to baseline prediction models – play an important role in selecting patients for dose escalation strategies, and would form an interesting topic for future studies. As mentioned above, it would also be worthwhile to assess the

6



value of sequential PET/CT examinations during and/or after treatment, as well as to investigate the potential role of MRI, both at baseline and for response evaluation during and after cCRT, as there have been some reports that have suggested potential for MRI in these settings.<sup>41,48,49</sup> To investigate the role of MRI was unfortunately outside the scope of the current study, because MRI data was only available for a limited number of patients in our cohort.

Our study has some limitations. First, it is a retrospective analysis, in which the endpoints were not systematically determined. Second, based on the available follow-up data in our cohort, we were forced to limit our main outcome to locoregional failures occurring within the first year, which may be too short since we know that most recurrences occur in the first two years.<sup>9-11</sup> Third, even though our patient cohort was relatively large, considering the low incidence of anal cancer, the total number of events (treatment failures) remained limited. This did not allow splitting the data to create an independent validation set to test our model's performance and restricted the number of variables that could be considered without overfitting. This why we used the LASSO method for variable selection and LOOCV as an alternative method of internal validation. Finally, as discussed earlier, tumour hr-HPV status was not available for all patients in our cohort. Multiple imputation was used to allow inclusion of this known prognostic factor in our analyses.

To conclude, we found that at baseline the combination of a hr-HPV-negative, node positive tumour stage and male sex provides the strongest predictive value to estimate the risk of first-year locoregional failure after cCRT, and that semi-quantitative FDG-PET parameters do not offer complementary value. Further investigations should focus on validating these findings in an independent patient cohort and on exploring whether there is added value in including parameters from MRI, interim imaging during cCRT, and additional clinical and molecular variables to further optimize our model's predictive performance to allow future treatment personalization for anal cancer patients.

## REFERENCES

1. Islami F, Ferlay J, Lortet-Tieulent J, et al. International trends in anal cancer incidence rates. *Int. J. Epidemiol.* 2017;46:924–938. doi: 10.1093/ije/dyw27
2. Bouvier AM, Belot A, Manfredi S, et al. Trends of incidence and survival in squamous-cell carcinoma of the anal canal in France: A population-based study. *Eur. J. Cancer Prev.* 2016;25:182–187. doi: 10.1097/CEJ.0000000000000163
3. Gunderson LL, Winter KA, Ajani JA, et al. Long-term update of USGI intergroup RTOG 98-11 phase III trial for anal carcinoma: survival, relapse, and colostomy failure with concurrent chemoradiation involving fluorouracil/mitomycin versus fluorouracil/cisplatin. *J. Clin. Oncol.* 2012;30:4344–4351. doi: 10.1200/JCO.2012.43.8085
4. Ajani JA, Winter KA, Gunderson LL, et al. Fluorouracil, mitomycin, and radiotherapy vs fluorouracil, cisplatin, and radiotherapy for carcinoma of the anal canal: a randomized controlled trial. *JAMA.* 2008; 299(16):1914-1921. doi: 10.1001/jama.299.16.1914
5. Bartelink H, Roelofsen F, Eschwege F, et al. Concomitant radiotherapy and chemotherapy is superior to radiotherapy alone in the treatment of locally advanced anal cancer: results of a phase III randomized trial of the European Organization for Research and Treatment of Cancer Radiotherapy and Gastrointestinal Cooperative Groups. *J. Clin. Oncol.* 1997;15:2040–2049. doi: 10.1200/JCO.1997.15.5.2040
6. Flam M, John M, Pajak TF, et al. Role of mitomycin in combination with fluorouracil and radiotherapy, and of salvage chemoradiation in the definitive nonsurgical treatment of epidermoid carcinoma of the anal canal: results of a phase III randomized intergroup study. *J. Clin. Oncol.* 1996;14:2527–2539. doi: 10.1200/JCO.1996.14.9.252
7. Moureau-Zabotto L, Vendrely V, Abramowitz L, et al. Anal cancer: French Intergroup Clinical Practice Guidelines for diagnosis, treatment and follow-up (SNFGE, FFCD, GERCOR, UNICANCER, SFCD, SFRO, SNFCP). *Dig. Liver Dis.* 2017;49:831–840. doi: 10.1016/j.dld.2017.05.011
8. Glynne-Jones R, Nilsson PJ, Aschele C, et al. Anal cancer: ESMO-ESSO-ESTRO clinical practice guidelines for diagnosis, treatment and follow-up. *Radiother. Oncol.* 2014;111:330–339. doi: 10.1016/j.radonc.2014.04.013
9. Frazer ML, Yang G, Felder S, et al. Determining Optimal Follow-up for Patients With Anal Cancer Following Chemoradiation. *Am. J. Clin. Oncol.* 2020;43:319–324. doi: 10.1097/COC.0000000000000673



10. Shakir R, Adams R, Cooper R, et al. Patterns and Predictors of Relapse Following Radical Chemoradiation Therapy Delivered Using Intensity Modulated Radiation Therapy With a Simultaneous Integrated Boost in Anal Squamous Cell Carcinoma. *Int. J. Radiat. Oncol. Biol. Phys.* 2020;106:329–339. doi: 10.1016/j.ijrobp.2019.10.016
11. Foster CC, Lee AY, Furtado L V, et al. Treatment outcomes and HPV characteristics for an institutional cohort of patients with anal cancer receiving concurrent chemotherapy and intensity-modulated radiation therapy. *PLoS One.* 2018;13:1–10. doi: 10.1371/journal.pone.0194234
12. Hagemans JAW, Blinde SE, Nuyttens JJ, et al. Salvage Abdominoperineal Resection for Squamous Cell Anal Cancer: A 30-Year Single-Institution Experience. *Ann. Surg. Oncol.* 2018;25:1970–1979. doi: 10.1245/s10434-018-6483-9
13. Alamri Y, Buchwald P, Dixon L, et al. Salvage surgery in patients with recurrent or residual squamous cell carcinoma of the anus. *Eur. J. Surg. Oncol.* 2016;42:1687–1692. doi: 10.1016/j.ejso.2016.05.00
14. Akbari RP, Paty PB, Guillem JG, et al. Oncologic outcomes of salvage surgery for epidermoid carcinoma of the anus initially managed with combined modality therapy. *Dis. Colon Rectum.* 2004;47:1136–1144. doi: 10.1007/s10350-004-0548-5
15. Johnsson A, Leon O, Gunnlaugsson A, et al. Determinants for local tumour control probability after radiotherapy of anal cancer. *Radiother. Oncol.* 2018;128:380–386. doi: 10.1016/j.radonc.2018.06.007
16. Muirhead R, Partridge M, Hawkins MA. A tumor control probability model for anal squamous cell carcinoma. *Radiother. Oncol.* 2015;116:192–196. doi: 10.1016/j.radonc.2015.07.014
17. Rusten E, Rekstad BL, Undseth C, et al. Anal cancer chemoradiotherapy outcome prediction using 18F-fluorodexoyglucose positron emission tomography and clinicopathological factors. *Br. J. Radiol.* 2019;92:20181006. doi: 10.1259/bjr.20181006
18. Meulendijks D, Tomaso NB, Dewit L, et al. HPV-negative squamous cell carcinoma of the anal canal is unresponsive to standard treatment and frequently carries disruptive mutations in TP53. *Br. J. Cancer.* 2015;112:1358–1366. doi: 10.1038/bjc.2015.20
19. Tomaszewski JM, Link E, Leong T, et al. Twenty-five-year experience with radical chemoradiation for anal cancer. *Int. J. Radiat. Oncol. Biol. Phys.* 2012;83:552–558. doi: 10.1016/j.ijrobp.2011.07.007
20. Mahmud A, Poon R, Jonker D. PET imaging in anal canal cancer: A systematic review and meta-analysis. *Br. J. Radiol.* 2017;90:20170370. doi: 10.1259/bjr.20170370

21. Deantonio L, Milia ME, Cena T, et al. Anal cancer FDG-PET standard uptake value: correlation with tumor characteristics, treatment response and survival. *Radiol. Medica*. 2016;121:54–59. doi: 10.1007/s11547-015-0562-9
22. Leccisotti L, Manfrida S, Barone R, et al. The prognostic role of FDG PET/CT before combined radio-chemotherapy in anal cancer patients. *Ann. Nucl. Med.* 2020;34:65–73. doi: 10.1007/s12149-019-01416-y
23. Hong JC, Cui Y, Patel BN, et al. Association of Interim FDG-PET Imaging During Chemoradiation for Squamous Anal Canal Carcinoma With Recurrence. *Int. J. Radiat. Oncol. Biol. Phys.* 2018;102:1046–1051. doi: 10.1016/j.ijrobp.2018.04.062
24. Duimering A, Riauka T, Nijjar Y, et al. Prognostic utility of pre- and post-treatment FDG-PET parameters in anal squamous cell carcinoma. *Radiother. Oncol.* 2019;136:21–28. doi: 10.1016/j.radonc.2019.03.014
25. Jones MP, Hruby G, Metser U, et al. FDG-PET parameters predict for recurrence in anal cancer - Results from a prospective, multicentre clinical trial. *Radiat. Oncol.* 2019;14:1–6. doi: 10.1186/s13014-019-1342-9
26. Cardenas ML, Spencer CR, Markovina S, et al. Quantitative FDG-PET/CT predicts local recurrence and survival for squamous cell carcinoma of the anus. *Adv. Radiat. Oncol.* 2017;2:281–287. doi: 10.1016/j.adro.2017.04.007
27. Gauthé M, Richard-Molard M, Fayard J, et al. Prognostic impact of tumour burden assessed by metabolic tumour volume on FDG PET/CT in anal canal cancer. *Eur. J. Nucl. Med. Mol. Imaging.* 2017;44:63–70. doi: 10.1007/s00259-016-3475-5
28. Bazan JG, Koong AC, Kapp DS, et al. Metabolic tumor volume predicts disease progression and survival in patients with squamous cell carcinoma of the anal canal. *J. Nucl. Med.* 2013;54:27–32. doi: 10.2967/jnumed.112.109470
29. Mohammadkhani Shali S, Schmitt V, Behrendt FF, et al. Metabolic tumour volume of anal carcinoma on 18FDG PET/CT before combined radiochemotherapy is the only independent determinant of recurrence free survival. *Eur. J. Radiol.* 2016;85:1390–1394. doi: 10.1016/j.ejrad.2016.05.009
30. Kidd EA, Dehdashti F, Siegel BA, et al. Anal cancer maximum F-18fluorodeoxyglucose uptake on positron emission tomography is correlated with prognosis. *Radiother. Oncol.* 2010;95:288–291. doi: 10.1016/j.radonc.2010.02.019
31. Van Griethuysen JJM, Fedorov A, Parmar C, et al. Computational radiomics system to decode the radiographic phenotype. *Cancer Res.* 2017;77:e104–e107. doi: 10.1158/0008-5472.CAN-17-0339

32. Schurink NW, Min LA, Berbee M, et al. Value of combined multiparametric MRI and FDG-PET/CT to identify well-responding rectal cancer patients before the start of neoadjuvant chemoradiation. *Eur. Radiol.* 2020;30:2945–2954. doi: 10.1007/s00330-019-06638-2
33. Ueno Y, Lisbona R, Tamada T, et al. Comparison of FDG PET metabolic tumour volume versus ADC histogram: Prognostic value of tumour treatment response and survival in patients with locally advanced uterine cervical cancer. *Br. J. Radiol.* 2017;90:20170035. doi: 10.1259/bjr.20170035
34. Erdi YE, Mawlawi O, Larson SM, et al. Segmentation of lung lesion volume by adaptive positron emission tomography image thresholding. *Cancer.* 1997;80:2505–9. doi: 10.1002/(sici)1097-0142(19971215)80:12+<2505::aid-cnrcr24>3.3.co;2-b
35. Tibshirani R. Regression Shrinkage and Selection Via the Lasso. *J. R. Stat. Soc. Ser. B.* 1996;58:267–288. doi: 10.1111/j.2517-6161.1996.tb02080.x
36. Martens RM, Noij DP, Ali M, et al. Functional imaging early during (chemo)radiotherapy for response prediction in head and neck squamous cell carcinoma; a systematic review. *Oral Oncol.* 2019;88:75–83. doi: 10.1016/j.oraloncology.2018.11.005
37. Kidd EA, Thomas M, Siegel BA, et al. Changes in Cervical Cancer FDG Uptake During Chemoradiation and Association With Response Radiation Oncology. *Radiat. Oncol. Biol. Phys.* 2013;85:116–122. doi: 10.1016/j.ijrobp.2012.02.056
38. Oh D, Lee JE, Huh SJ, et al. Prognostic significance of tumor response as assessed by sequential 18F-fluorodeoxyglucose-positron emission tomography/computed tomography during concurrent chemoradiation therapy for cervical cancer. *Int. J. Radiat. Oncol. Biol. Phys.* 2013;87:549–554. doi: 10.1016/j.ijrobp.2013.07.009
39. Mai S, Welzel G, Ottstadt M, et al. Prognostic relevance of HPV infection and p16 overexpression in squamous cell anal cancer. *Int. J. Radiat. Oncol. Biol. Phys.* 2015;93:819–827. doi: 10.1016/j.ijrobp.2015.08.004
40. Koerber SA, Schoneweg C, Slynko A, et al. Influence of human papillomavirus and p16INK4a on treatment outcome of patients with anal cancer. *Radiother. Oncol.* 2014;113:331–336. doi: 10.1016/j.radonc.2014.11.013
41. Hocquelet A, Auriac T, Perier C, et al. Pre-treatment magnetic resonance-based texture features as potential imaging biomarkers for predicting event free survival in anal cancer treated by chemoradiotherapy. *Eur. Radiol.* 2018;28:2801–2811. doi: 10.1007/s00330-017-5284-z
42. Arora N, Gupta A, Zhu H, et al. Race- and sex-based disparities in the therapy and outcomes of squamous cell carcinoma of the anus. *JNCCN J. Natl. Compr. Cancer Netw.* 2017;15:998–1004. doi: 10.6004/jnccn.2017.0135

43. Rödel F, Wieland U, Fraunholz I, et al. Human papillomavirus DNA load and p16INK4a expression predict for local control in patients with anal squamous cell carcinoma treated with chemoradiotherapy. *Int. J. Cancer*. 2015;136:278–288. doi: 10.1002/ijc.28979
44. Camandaroba MPG, Iseas S, Oliveira C, et al. Disease-Free Survival and Time to Complete Response After Definitive Chemoradiotherapy for Squamous-Cell Carcinoma of the Anus According to HIV Infection. *Clin. Colorectal Cancer*. 2020:1–8. doi: 10.1016/j.clcc.2020.03.006
45. Pappou EP, Magruder JT, Fu T, et al. Prognostic and Predictive Clinicopathologic Factors of Squamous Anal Canal Cancer in HIV-Positive and HIV-Negative Patients: Does HAART Influence Outcomes? *World J. Surg*. 2018;42:876–883. doi: 10.1007/s00268-017-4201-6
46. Glynne-Jones R, Sebag-Montefiore D, Adams R, et al. Prognostic factors for recurrence and survival in anal cancer: Generating hypotheses from the mature outcomes of the first United Kingdom Coordinating Committee on Cancer Research Anal Cancer Trial (ACT I). *Cancer*. 2013;119:748–755. doi: 10.1002/cncr.27825
47. Tomaso NB, Meulendijks D, Nijkamp J, et al. Clinical outcome in patients treated with simultaneous integrated boost – intensity modulated radiation therapy (SIB-IMRT) with and without concurrent chemotherapy for squamous cell carcinoma of the anal canal. *Acta Oncol*. 2016;55:760–766. doi: 10.3109/0284186X.2015.1124141
48. Owczarczyk K, Prezzi D, Cascino M, et al. MRI heterogeneity analysis for prediction of recurrence and disease free survival in anal cancer. *Radiother. Oncol*. 2019;134:119–126. doi: 10.1016/j.radonc.2019.01.022
49. Kochhar R, Renehan AG, Mullan D, et al. The assessment of local response using magnetic resonance imaging at 3- and 6-month post chemoradiotherapy in patients with anal cancer. *Eur. Radiol*. 2017;27:607–617.



The background is a vibrant blue with a complex, organic pattern. It features overlapping, wavy shapes that resemble crumpled paper or liquid ripples. A prominent feature is a large, dark blue, curved shape that contains a fine halftone dot pattern. The overall effect is a sense of depth and movement.

## Chapter 7

# GENERAL DISCUSSION AND FUTURE PERSPECTIVES



# GENERAL DISCUSSION AND FUTURE PERSPECTIVES

## **Evolutions in multimodality imaging**

Reviewing the literature on combined PET/CT+MRI and hybrid PET/MRI from 2009-2018 in **Chapter 2**, we observed a tremendous increase in the number of research publications on this topic, and identified several trends and developments that occurred in the multimodality research field. The introduction of hybrid PET/MRI systems was a major stimulus for the observed growth in numbers of these publications, while at the same time studies investigating the combination of stand-alone (i.e., separately acquired) MRI and PET/CT continued to make up an important proportion of published works. Many of these reports focus on the combination of PET and MRI, or hybrid PET/MRI, for (visual) diagnostic staging. Our literature review rendered no studies that directly compared hybrid PET/MRI to separate acquisition of PET/CT and MRI in terms of diagnostic benefit. So far, it appears that the respective benefits of PET (staging of lymph nodes and distant metastases) and MRI (detailed local tumour staging) are maintained with simultaneous PET/MRI acquisition,<sup>1-3</sup> with the potential added benefits of improved imaging efficiency and increased staging confidence.<sup>4-7</sup> Another important development was the significant rise in numbers of studies with a focus on multimodality imaging using tumour-specific (non-FDG) PET tracers, in particular those targeting prostate cancer (PSMA, choline) and neuroendocrine tumours (octreotide analogues). The positive results of these studies have greatly contributed to the clinical adoption of these novel tracers and their implementation into current guideline updates.<sup>8,9</sup> A final notable observation was the gradual shift from a predominant focus on visual image assessment, to a growing proportion of studies using quantitative image analysis. This change was positively influenced by the development of functional imaging techniques, such as diffusion-weighted imaging (DWI), perfusion MRI and the aforementioned new PET-tracers, which can provide quantifiable information about the biological properties of a tissue, tumour or other region of interest within the image. During the studied decade, the concept of “imaging biomarkers” has become a hot topic in oncologic imaging research with numerous publications in this field. Nevertheless, evidence on multimodality combinations of imaging biomarkers derived from different imaging techniques has so far been limited. As a final part of this thesis we therefore explored the value of multi-modality combinations of quantitative imaging biomarkers in three pelvic malignancies, which will be addressed later in this discussion. The growing importance of multimodality imaging observed in the

literature was reflected by the institutional data we collected from The Netherlands Cancer Institute, that showed a steep increase of +239% in multimodality imaging (combinations of PET/CT and MRI performed within one diagnostic workup), and +250% for hybrid PET/CT, clearly exceeding the increase of +108% in single-modality (MRI) examinations, during a similar 10-year study period.

### **Integrated multimodality imaging assessment for clinical staging**

Given the increasing demand for multimodality imaging, the traditional workflow of separately assessing and reporting PET/CT (by a nuclear medicine physician) and MRI (by a radiologist) studies that is still common practice in many clinics, including our own, will likely become outdated and should make way for more integrated assessment of all available imaging information to allow a more comprehensive and uniform evaluation of both the local and distant extent of disease. In **Chapter 3** we investigated the potential effects of such an integrated 'side-by-side' assessment of PET/CT and MRI in a retrospective clinical study setting, focusing on the staging of different types of abdominal malignancies. We found that integrated image assessment of MRI and PET/CT, by a team consisting of a radiologist and a nuclear medicine physician, affected staging outcome with a potential impact on clinical management in 1 out of 9 patients in our studies cohort of  $n=201$ . Combined assessment also had a positive effect on reader confidence, especially in cases of cervical cancer, and on the overall staging of recurrent disease and lymph nodes.

Though previous evidence on this topic is scarce, there have been some earlier reports that show that integrated assessment of PET/CT and MRI has a positive effect on the detection of incomplete response of cervical cancer after curative intent chemoradiotherapy,<sup>10</sup> lymph node staging after neo-adjuvant treatment for rectal cancer,<sup>11</sup> detecting extrahepatic disease in candidates for local treatment of liver metastasis of colorectal cancer<sup>12</sup> and for disease burden assessment in peritoneal metastasis.<sup>13</sup>

Considering these previous and our own results, we may conclude that combined assessment and reporting of PET(/CT) and MRI can have a positive clinical impact in the form of improved diagnostic staging confidence, reduction of inconclusive findings, and improved diagnostic performance in specific clinical settings. Adopting such workflows into clinical practice requires a close collaboration and further integration of Radiology and Nuclear Medicine departments.

To date, there is no available data on direct comparisons of hybrid PET/MRI acquisition versus approaches of separate PET(/CT) and MRI acquisition with side-by-side assessment. This comparison, as well as the impact of hybrid PET/MRI acquisition on cost-effectiveness and patient comfort were not addressed in this thesis. Further research is required to answer these questions, and to determine if the advantages warrant the high costs of its implementation. Current costs and limited availability of hybrid systems suggest that in general clinical practice the focus should probably first be on adoption of an integrated PET/CT + MRI approach for the foreseeable future. Whether hybrid PET/MRI will eventually become widely accessible and if it should replace the combination of MRI and PET/CT for general staging purposes remain major questions. From the current perspective, it seems more likely that hybrid PET/MRI will have its own specific place in abdominal oncological practice, and future research should be aimed at identifying those applications where its added value is most apparent, for example for serial functional multi-parametric imaging,<sup>14</sup> response evaluation<sup>15,16</sup> and for specific (complex or complicated) diagnostic questions.

### Quantitative modelling

In the final part of this thesis we explored the potential of quantitative imaging parameters integrated in clinical prediction models of local treatment outcome in cohorts of rectal, cervical and anal cancer patients.

In our cohort of rectal cancer patients (**Chapter 4**), a model incorporating MRI-based T-stage, combined with signal entropy and tumour volume derived from T2-weighted MRI, showed good diagnostic performance to predict a good response to neoadjuvant chemoradiotherapy on baseline MRI, with a cross-validated AUC of 0.83. Tumour volume was also identified as a predictive factor of local tumour response in our cervical (**Chapter 5**) and anal cancer (**Chapter 6**) cohorts, though in the latter case volume (i.e., metabolic tumour volume derived from PET) was only significant if no other clinical variables were entered into the prediction model. Intuitively, this predictive role for volume is not very surprising, as a (near-) complete response to chemoradiotherapy will be more difficult to achieve in larger tumours. In our cervical cancer cohort in **Chapter 5**, the SUVmax from PET was the only other imaging parameter in addition to volume that was found to be independently associated with early response to chemoradiotherapy, though performance of the resulting model by cross-validation was at best moderate with an AUC of only 0.68, which will typically not be considered sufficient to guide clinical decision-making. T2W signal 'entropy', which was identified as a potential predictor in rectal cancer, is a texture parameter

reflective of tissue heterogeneity. SUVmax and entropy both have previously been associated with tumour cellularity, proliferation rate and hypoxia,<sup>17,18</sup> though the mechanism behind these associations and the relation with treatment response is not well understood. One possible hypothesis may be that both parameters (indirectly) reflect mitotic activity, and hence the tumour's relative susceptibility to anti-cancer therapies such as radiotherapy.

When considering the combined results of our three pelvic study cohorts, the overall predictive value of quantitative PET-based parameters was found to be limited, especially when combined with other imaging (MRI) or clinical baseline variables. In our literature review in **Chapter 2**, a total of fourteen previous studies combined (semi-)quantitative PET and MRI parameters in multivariable prediction models of either treatment response or survival.<sup>19–31</sup> Out of these reports, only six described a complementary value for combining PET with MRI.<sup>19, 15,21,22,26,28</sup> Based on these findings, the complementary value of PET and MRI for quantitative modelling appears to be somewhat disappointing. Interestingly, it were mainly the more 'clinical' staging variables acquired by means of simple visual (qualitative) image evaluation that rendered the best predictive results, such as cT-stage in our rectal cancer cohort and cN-stage in anal cancer. When combined with other clinical, non-imaging variables (sex and high-risk HPV status) this resulted in a cross-validated AUC of 0.81 to predict local control in our cohort of anal cancer patients described in **Chapter 6**, with no added benefit from any of the quantitative PET parameters. The few rather heterogeneous previous studies that have reported a complementary effect of combining quantitative imaging and clinical variables in outcome prediction models are listed in the overview Table 2 of the literature review in **Chapter 2**. These are mainly studies in gynaecological cancer cohorts, showing that a combination of DWI and/or PET parameters with clinical variables (FIGO-stage, node-negative disease and histological subtype) can contribute to improved prediction of disease-free and overall survival.<sup>3,26,27,32</sup> In addition, there have been some reports in hepatocellular carcinoma patients showing that recurrence or survival may be predicted by a combination of PET-based parameters, serum-biomarkers, clinical T-stage and patient sex.<sup>20, 31</sup>

To conclude, the limited added value of pre-therapy multiparametric quantitative imaging parameters, when combined with more conventional TNM-stage and size in response prediction, suggests that these conventional parameters that are mainly based on visual image assessment may make up most of the predictive potential that can be derived from these images. If this is the case, optimal visual assessment

by experienced diagnosticians is key and addition of quantitative multiparametric imaging parameters to a prediction model will not substantially improve the model's accuracy. We have to acknowledge though that for the prediction models generated as part of this thesis we tested only a small selection of parameters, and also the studies mentioned above were not exhaustive. This leaves some room for discussion about the potential role of parameters that have not been (extensively) tested including those acquired via more sophisticated artificial intelligence (AI) based methods such as Radiomics and (deep) machine learning. There have already been some promising first reports, showing that AI-based clinical prediction models may perform at a level similar to that of expert radiologists to predict response and can render whole new arrays of unexplored imaging biomarkers.<sup>33,34</sup>

## CONCLUSIONS

From the findings in this thesis we have learned that there is a growing potential for combined imaging modalities in comprehensive diagnostic oncologic assessments. Especially in dedicated oncologic centers, multimodality imaging will continue to have a growing impact on daily clinical practice. Integrated assessment and reporting of PET/CT and MRI in abdominal cancer staging has a positive impact on clinical decision-making in specific staging settings, reflected in reader confidence and reduction of inconclusive findings. The added diagnostic value of hybrid PET/MRI acquisition within this integrated workflow in the clinical setting remains to be further determined. To keep up with these developments, our existing workflows will have to be redesigned. Also, the effects of integrated assessment of PET/CT and MRI on diagnostic accuracy, patient outcomes and cost-efficiency require further research. From the clinical perspective, good quality visual evaluation of pre-therapy PET(/CT) and MRI is key for prognostication and treatment stratification, quantitative parameters from these modalities currently have limited additional predictive value.

## REFERENCES

1. Sarabhai T, Schaarschmidt BM, Wetter A, Kirchner J, Aktas B, Forsting M, et al. Comparison of 18F-FDG PET/MRI and MRI for pre-therapeutic tumor staging of patients with primary cancer of the uterine cervix. *Eur J Nucl Med Mol Imaging*. 2018;45(1):67–76. doi: 10.1007/s00259-017-3809-y
2. Beiderwellen K, Geraldo L, Ruhlmann V, Heusch P, Gomez B, Nensa F, et al. Accuracy of [18F]FDG PET/MRI for the detection of liver metastases. *PLoS One*. 2015;10(9):e0137285. doi: 10.1371/journal.pone.0137285
3. Kirchner J, Sawicki LM, Suntharalingam S, Grueneisen J, Ruhlmann V, Aktas B, et al. Whole-body staging of female patients with recurrent pelvic malignancies: Ultra-fast 18F-FDG PET/MRI compared to 18F-FDG PET/CT and CT. *PLoS One*. 2017;12(2):e0172553. doi: 10.1371/journal.pone.0172553
4. Hope TA, Fayad ZA, Fowler KJ, Holley D, Iagaru A, McMillan AB, et al. Summary of the first ISMRM-SNMMI workshop on PET/MRI: Applications and limitations. *J Nucl Med*. 2019;60(10):1340–6. doi: 10.2967/jnumed.119.227231
5. Min LA, Vogel WV, Lahaye MJ, Maas M, Donswijk ML, Vegt E, et al. Integrated versus separate reading of F-18 FDG-PET/CT and MRI for abdominal malignancies – effect on staging outcomes and diagnostic confidence. *Eur Radiol*. 2019;29(12):6900–10. doi: 10.1007/s00330-019-06253-1
6. Grueneisen J, Beiderwellen K, Heusch P, Gratz M, Schulze-Hagen A, Heubner M, et al. Simultaneous Positron Emission Tomography/Magnetic Resonance Imaging for Whole-Body Staging in Patients With Recurrent Gynecological Malignancies of the Pelvis. *Invest Radiol*. 2014;49(12):808–15. doi: 10.1097/RLI.0000000000000086
7. Beiderwellen K, Gomez B, Buchbender C, Hartung V, Poeppel TD, Nensa F, et al. Depiction and characterization of liver lesions in whole body [18F]-FDG PET/MRI. *Eur J Radiol*. 2013 Nov;82(11):e669-75. doi: 10.1016/j.ejrad.2013.07.027
8. Cornford P, van den Bergh RCN, Briers E, Van den Broeck T, Cumberbatch MG, De Santis M, et al. EAU-EANM-ESTRO-ESUR-SIOG Guidelines on Prostate Cancer. Part II—2020 Update: Treatment of Relapsing and Metastatic Prostate Cancer. *Eur Urol*. 2021;79(2):263–82. doi: 10.1016/j.eururo.2020.09.046
9. Pavel M, Öberg K, Falconi M, Krenning EP, Sundin A, Perren A, et al. Gastroenteropancreatic neuroendocrine neoplasms: ESMO Clinical Practice Guidelines for diagnosis, treatment and follow-up. *Ann Oncol*. 2020;31(7):844–60. doi: 10.1016/j.annonc.2020.03.304

10. Kalash R, Glaser SM, Rangaswamy B, Horne ZD, Kim H, Houser C, et al. Use of Functional Magnetic Resonance Imaging in Cervical Cancer Patients With Incomplete Response on Positron Emission Tomography/Computed Tomography After Image-Based High-Dose-Rate Brachytherapy. *Int J Radiat Oncol Biol Phys*. 2018 Nov;102(4):1008–13. doi: 10.1016/j.ijrobp.2018.01.092
11. Ishihara S, Kawai K, Tanaka T, Kiyomatsu T, Hata K, Nozawa H, et al. Diagnostic value of FDG-PET/CT for lateral pelvic lymph node metastasis in rectal cancer treated with preoperative chemoradiotherapy. *Tech Coloproctol*. 2018 May;22(5):347–54. doi: 10.1007/s10151-018-1779-0
12. Georgakopoulos A, Pianou N, Kelekis N, Chatziioannou S. Impact of 18F-FDG PET/CT on therapeutic decisions in patients with colorectal cancer and liver metastases. *Clin Imaging*. 2013;37(3):536–41. doi: 10.1016/j.clinimag.2012.09.011
13. Wang W, Tan GHC, Chia CS, Skanthakumar T, Soo KC, Teo MCC. Are positron emission tomography-computed tomography (PET-CT) scans useful in preoperative assessment of patients with peritoneal disease before cytoreductive surgery (CRS) and hyperthermic intraperitoneal chemotherapy (HIPEC)? *Int J Hyperth*. 2018;34(5):524–31. doi: 10.1080/02656736.2017.1366554
14. Min M, Lee MT, Lin P, Holloway L, Wijesekera DJ, Gooneratne Di, et al. Assessment of serial multi-parametric functional MRI (diffusion-weighted imaging and R2\*) with 18F-FDG-PET in patients with head and neck cancer treated with radiation therapy. *Br J Radiol*. 2016;89(1058): 20150530. doi: 10.1259/bjr.20150530
15. Ueno Y, Lisbona R, Tamada T, Alaref A, Sugimura K, Reinhold C. Comparison of FDG PET metabolic tumour volume versus ADC histogram: prognostic value of tumour treatment response and survival in patients with locally advanced uterine cervical cancer. *Br J Radiol* 2017; 90: 20170035. doi: 10.1259/bjr.20170035
16. Crimi F, Spolverato G, Lacognata C, Garieri M, Cecchin D, Urso ED, et al. 18F-FDG PET/MRI for Rectal Cancer TNM Restaging After Preoperative Chemoradiotherapy: Initial Experience. *Dis Colon Rectum*. 2020;63(3):310–8. doi: 10.1097/DCR.0000000000001568
17. Bos BR, Hoeven JJM Van Der, Wall E Van Der, Groep P Van Der, Diest PJ Van, Comans EFI, et al. Biologic Correlates of 18 Fluorodeoxyglucose Uptake in Human Breast Cancer Measured by Positron Emission. *J Clin Oncol*. 2002;20(2):379–87. doi: 10.1200/JCO.2002.20.2.379
18. Zhang H, Li W, Hu F, Sun Y, Hu T, Tong T. MR texture analysis: potential imaging biomarker for predicting the chemotherapeutic response of patients with colorectal liver metastases. *Abdom Radiol*. 2019;44(1):65–71. doi: 10.1007/s00261-018-1682-1

19. ucia F, Visvikis D, Desseroit M-C, Miranda O, Malhaire J-P, Robin P, et al. Prediction of outcome using pretreatment 18 F-FDG PET/CT and MRI radiomics in locally advanced cervical cancer treated with chemoradiotherapy. *Eur J Nucl Med Mol Imaging*. 2018;45(5):768–86. doi: 10.1007/s00259-017-3898-7
20. Han JH, Kim DG, Na GH, Kim EY, Lee SH, Hong TH, et al. Evaluation of prognostic factors on recurrence after curative resections for hepatocellular carcinoma. *World J Gastroenterol*. 2014;20(45):17132–40. doi: 10.3748/wjg.v20.i45.17132.
21. Chen B Bin, Tien YW, Chang MC, Cheng MF, Chang YT, Yang SH, et al. Multiparametric PET/MR imaging biomarkers are associated with overall survival in patients with pancreatic cancer. *Eur J Nucl Med Mol Imaging*. 2018;45(7):1205–17. doi: 10.1007/s00259-018-3960-0
22. Chen B Bin, Tien YW, Chang MC, Cheng MF, Chang YT, Wu CH, et al. PET/MRI in pancreatic and periampullary cancer: correlating diffusion-weighted imaging, MR spectroscopy and glucose metabolic activity with clinical stage and prognosis. *Eur J Nucl Med Mol Imaging*. 2016;43(10):1753–64. doi: 10.1007/s00259-016-3356-y
23. Ho JC, Allen PK, Bhosale PR, Rauch GM, Fuller CD, Mohamed ASR, et al. Diffusion-weighted MRI as a Predictor of Outcome in Cervical cancer Following Chemoradiation. *Int J Radiat Oncol Biol Phys*. 2017;97(3):546–53. doi: 10.1016/j.ijrobp.2016.11.015
24. Rahman T, Tsujikawa T, Yamamoto M, Chino Y, Shinagawa A, Kurokawa T, et al. Different prognostic implications of 1818-FDG PET between histological subtypes in patients with cervical cancer. *Medicine (Baltimore)*. 2016;95(9):1–7. doi: 10.1097/MD.0000000000003017
25. Nakamura K, Joja I, Nagasaka T, Haruma T, Hiramatsu Y. Maximum standardized lymph node uptake value could be an important predictor of recurrence and survival in patients with cervical cancer. *Eur J Obstet Gynecol Reprod Biol*. 2014;173(1):77–82. doi: 10.1016/j.ejogrb.2013.10.030
26. Nakamura K, Joja I, Kodama J, Hongo A, Hiramatsu Y. Measurement of SUVmax plus ADCmin of the primary tumour is a predictor of prognosis in patients with cervical cancer. *Eur J Nucl Med Mol Imaging*. 2012;39(2):283–90. doi: 10.1007/s00259-011-1978-7
27. Nakamura K, Joja I, Fukushima C, Haruma T, Hayashi C, Kusumoto T, et al. The preoperative SUVmax is superior to ADCmin of the primary tumour as a predictor of disease recurrence and survival in patients with endometrial cancer. *Eur J Nucl Med Mol Imaging*. 2013;40(1):52–60. doi: 10.1007/s00259-012-2240-7



28. Joye I, Debuquoy A, Deroose CM, Vandecaveye V, Cutsem E Van, Wolthuis A, et al. Quantitative imaging outperforms molecular markers when predicting response to chemoradiotherapy for rectal cancer. *Radiother Oncol.* 2017;124(1):104–9.
29. Heijmen L, Ter Voert EEGW, Oyen WJG, Punt CJA, Van Spronsen DJ, Heerschap A, et al. Multimodality imaging to predict response to systemic treatment in patients with advanced colorectal cancer. *PLoS One.* 2015;10(4):1–13. doi: 10.1016/j.radonc.2017.06.013
30. Ippolito D, Monguzzi L, Guerra L, Deponti E, Gardani G, Messa C, et al. Response to neoadjuvant therapy in locally advanced rectal cancer: Assessment with diffusion-weighted MR imaging and 18FDG PET/CT. *Abdom Imaging.* 2012;37(6):1032–40. doi: 10.1007/s00261-011-9839-1
31. Hong CM, Ahn BC, Jang YJ, Jeong SY, Lee SW, Lee J. Prognostic Value of Metabolic Parameters of 18F-FDG PET/CT and Apparent Diffusion Coefficient of MRI in Hepatocellular Carcinoma. *Clin Nucl Med.* 2017;42(2):95–9. doi: 10.1097/RLU.0000000000001478
32. Miccò M, Vargas HA, Burger IA, Kollmeier MA, Goldman DA, Park KJ, et al. Combined pre-treatment MRI and 18F-FDG PET/CT parameters as prognostic biomarkers in patients with cervical cancer. *Eur J Radiol.* 2014 Jul;83(7):1169–76. doi: 10.1016/j.ejrad.2014.03.024
33. Delli Pizzi A, Chiarelli AM, Chiacchiaretta P, d’Annibale M, Croce P, Rosa C, et al. MRI-based clinical-radiomics model predicts tumor response before treatment in locally advanced rectal cancer. *Sci Rep.* 2021;11(1):5379. doi: 10.1038/s41598-021-84816-3
34. van Griethuysen JJM, Lambregts DMJ, Trebeschi S, Lahaye MJ, Bakers FCH, Vliegen RFA, et al. Radiomics performs comparable to morphologic assessment by expert radiologists for prediction of response to neoadjuvant chemoradiotherapy on baseline staging MRI in rectal cancer. *Abdom Radiol.* 2020;45(3):632–43. doi: 10.1007/s00261-019-02321-8



The background is a vibrant blue with a complex, organic pattern. It features several overlapping, rounded shapes that resemble stylized leaves or petals. A prominent feature is a large, curved area filled with a fine halftone dot pattern, which creates a textured, grid-like appearance. The overall composition is dynamic and modern.

## Chapter 8

ON THE IMPACT OF  
THIS THESIS

SUMMARY / SAMENVATTING

LIST OF PUBLICATIONS

DANKWOORD

CURRICULUM VITAE

# ON THE IMPACT OF THIS THESIS

## **Main aims and outcomes of this thesis**

The overall aim of this thesis was to investigate how combined use of different medical imaging modalities, in specific the combination of magnetic resonance imaging (MRI) and positron emission tomography (PET), can benefit the diagnostic assessment and treatment of patients with cancer that originates from one of the abdominal organs. To investigate this, we formulated three main research questions, that together compose the different chapters of this thesis:

1. What can we learn from published literature?
2. How can we benefit from the combination of PET and MRI when visually interpreting these images to diagnose and determine the cancer stage in patients with abdominal cancers?
3. Are quantitative measurements derived from the tumour on PET and MRI useful as "markers" to help predict how well patients with abdominal cancers will respond to their anti-cancer treatment?

From our literature search described in Chapter 2 we have learned that during the last decade there has been a tremendous increase in published research involving multimodality combinations of PET(/CT) and MRI, not in the least part due to introduction of hybrid PET/MRI scanners. Hybrid PET/MRI refers to the combined acquisition of PET and MRI images using a single machine. The clinical introduction of these machines as of 2011 has greatly boosted PET/MRI research, though the clinical role and added value of hybrid PET/MRI remains to be established. Another important development has been the increase in use of new PET tracers, with the ability to more specifically target certain tumour types, such as prostate cancer or neuroendocrine tumours. Finally, we have learned that in addition to combined use of PET(/CT) and MRI for visual diagnostic evaluations, there is a rapidly growing interest for more advanced quantitative analysis of the images. We have investigated this quantitative approach ourselves in Chapters 4-6, but first performed a study with cases from our own institution to determine the benefit of combined visual assessment of PET and MRI for diagnostic staging. In Chapter 3 we reviewed 201 patients who underwent a combination of PET/CT and MRI as part of the same diagnostic staging workup. The combined imaging sets were re-assessed by a nuclear medicine physician and a radiologist together as a team, and their combined imaging findings were compared to the reports of the original, separate assessments to establish how this combined

assessment might have impacted diagnosis and treatment. We learned that integrated (side-by-side) evaluation of the images had a small positive effect on the confidence with which the diagnosticians could reach a uniform diagnosis, with a potential impact on treatment planning in approximately 1 out of 9 patients. Finally, in the last three chapters we focused on the value of “quantitative” assessment of PET and MRI data in patients with rectal cancer (Chapter 4), cervical cancer (Chapter 5) and anal cancer (Chapter 6). Quantitative imaging refers to an approach where measurable variables are extracted from the images, varying from simple measurements, such as tumour size or volume, to more specific parameters, such as the ‘maximum standardized uptake value’ (SUVmax) which describes the glucose uptake on PET, or ‘texture’ measurements that describe the spatial heterogeneity of tumour signal within an image. In chapters 4-6 we combined these variables, derived from PET and MRI scans performed before the start of treatment, with other more clinical variables such as patient age, sex and overall disease (TNM) stage, to build statistical models to predict the chance of a successful treatment outcome. We learned that, though some of these parameters – such as tumour volume, signal heterogeneity and SUV – had some predictive value, it were parameters derived from visual assessment of the images (e.g. tumour and nodal disease stage) that were valuable in the prediction of patient outcomes. This stresses the need for a good quality visual diagnostic assessment of medical imaging by experienced diagnosticians.

### **Relevance of this research**

With this thesis we have shown that integration of PET and MRI in diagnostic workflows – via hybrid acquisition and/or integrated assessment by dedicated diagnosticians – can contribute to improved reader confidence and a reduction of inconclusive or conflicting diagnostic outcomes, thereby potentially changing clinical management in a substantial number of patients with abdominal cancer. This suggests that adopting such integrated workflows into clinical practice can have a positive clinical impact, urging the need for further collaboration and integration of Radiology and Nuclear Medicine departments. Whether hybrid PET/MRI acquisition will eventually become widely accessible, if it should replace the “stand-alone” combination of MRI and PET/CT, and for which particular diagnostic indications, remain major questions to be addressed by future research. Finally, we have shown that clinical prediction models incorporating information derived from imaging via visual assessment and (to a lesser extent) quantitative measurements, can aid in predicting the outcome of anti-cancer treatments – though further studies are obviously needed. Considering that these treatments are often costly and associated with (long-term) morbidity or



disability, selecting the right patient for the right treatment based on the anticipated treatment effect is highly relevant to improve patient outcomes and more effective use of healthcare resources.

### **Target population**

There are several audiences that may benefit from the research presented in this thesis. Firstly, our findings on the evolution of multimodality PET(/CT) and MRI imaging in the literature will be of interest to radiologists and nuclear medicine physicians, as it provides valuable insights into recent developments in their workfield, and indicates likely courses for the (near) future. Our study on integrated PET/CT and MRI assessment will be of interest to the same groups, particularly those leading or working in departments where integrated reporting is currently not (yet) the norm. Our results may provide insight into what benefits can be expected, and on how to implement and evaluate the effects. Second, researchers conducting studies on response prediction or decision support models may benefit from the results of the studies presented in **Chapter 4-6**. They can compare these to their own findings, or consider using a similar strategy or method to design their own studies. Finally, the findings and recommendations formulated in this thesis could inspire further research in the proposed directions, hopefully to the benefit of more expedient use of imaging and treatment, to ultimately benefit the quality of healthcare and patient outcomes.

### **Activities**

The research presented in this thesis has been shared actively within the research community by publication in peer-reviewed journals and by presentation at multiple national and international conferences. The projects that were conducted and the presented results have contributed to the formation of a 'hybrid imaging team' at the Netherlands Cancer Institute, boosting the collaboration between the Radiology and Nuclear Medicine department in research and diagnostic reporting. Finally, our work on quantitative imaging analysis has been continued as part of an ongoing multicenter project on multiparametric imaging modelling in rectal cancer.





## SUMMARY

The aim of this thesis was to investigate the current status and possible future applications of combined PET(/CT) and MRI in abdominal cancer patients, both from a visual (qualitative) and quantitative perspective.

**Chapter 2** reviews the main trends and evolutions observed in a decade of published literature on combined PET(/CT) and MRI in abdominal oncology, which were compared to trends observed during the same time period in our own comprehensive cancer centre. A major boost in multimodality research was observed after the introduction of hybrid PET/MRI scanners, which largely replaced the earlier retrospective image fusion and bed system-combined PET/MRI studies. There was a shift from predominantly visual image evaluation towards more quantitative image analysis and image biomarker studies. New, more tumour-specific PET-tracers, such as prostate specific membrane antigen (PSMA) for prostate cancer, were introduced and made their way into clinical practice. The tremendous increase in multimodality imaging research demonstrates a growing demand for multi-parametric information to guide oncological practice, which was also reflected by our institutional data that showed a similar increase in the multimodality use of PET/CT combined with MRI during the last decade.

In **Chapter 3** we investigated the effect of integrated (side-by-side) reading of PET/CT and MRI by a radiologist and nuclear medicine physician, compared to the conventional clinical approach of separate reading and reporting, in a cohort of 201 patients with different forms of abdominal cancer. In approximately one-third of the studied cases, integrated reading led to discrepant findings compared to the original separate reports, with potential clinical impact in 12% of the total study cohort. In addition, we saw a trend towards a small relative increase in diagnostic confidence and a decrease in the number of equivocal (inconclusive) findings, in particular for the evaluation of lymph nodes, in cervical cancer cases and to differentiate recurrent disease from benign post-treatment changes.

In chapters 4, 5 and 6 we focussed on combined PET/CT and MRI for (semi-)quantitative image analysis to predict treatment outcomes in three cohorts of rectal, cervical and anal cancer patients.

In **Chapter 4** we examined the value of multiparametric MRI combined with FDG-PET/CT to identify well-responding rectal cancer patients before the start of neoadjuvant chemoradiotherapy. From the baseline tumour volume of 61 locally advanced rectal cancer patients we extracted various MRI parameters ( $T2W_{\text{volume}}$ ,  $T2W\text{-signal}_{\text{entropy}}$ ,  $DWI_{\text{volume}}$ ,  $ADC_{\text{mean}}$ ,  $ADC_{\text{entropy}}$ ) and PET parameters ( $MTV_{42\%}$ ,  $SUV_{\text{max}}$ ,  $SUV_{\text{mean}}$ , TLG, CT-HU). We combined these with baseline patient characteristics and staging variables (e.g., sex, age, T- and N-stage) to build multiparametric models to predict the final tumour regression grade (TRG) after completion of treatment. After comparing different combinations of variables, the best performing model to predict a good response to treatment (TRG1-2) had an area under the curve of 0.83 after internal cross-validation, and included baseline staging and MRI variables (T-stage,  $T2W_{\text{volume}}$  and  $T2W\text{-signal}_{\text{entropy}}$ ). PET/CT variables showed limited predictive performance and were not of added predictive value.

**Chapter 5** describes our study exploring the potential of baseline (semi-)quantitative PET/CT and MRI variables, combined with clinical FIGO stage, as predictors of early response to concurrent chemoradiotherapy in a group of 46 locally advanced cervical cancer patients. Early response was defined as a reduction in tumour volume to  $<10 \text{ cm}^3$  at interim image evaluation after 3-4 weeks of chemoradiotherapy. Multivariable analysis showed that mainly tumour volume measured on baseline MRI was a predictive variable for early response;  $SUV_{\text{max}}$  measured on PET was an additional independent predictor, albeit with less predictive power. The prediction model based on tumour volume and  $SUV_{\text{max}}$  resulted in a moderate predictive performance of AUC of 0.68 after internal cross-validation in this small exploratory dataset.

**Chapter 6** explores the value of pre-treatment semi-quantitative variables derived from baseline PET/CT combined with clinical baseline variables (T- and N-stage, age, sex) and high-risk HPV-status, to predict locoregional treatment failure before the start of chemoradiotherapy treatment with curative intent in anal cancer patients. Treatment failure was defined as an incomplete response or local recurrence occurring within the first year after completion of treatment. A combined "clinical" model incorporating male sex, positive N-stage and negative high-risk HPV status showed the strongest predictive performance, with an AUC of 0.81 after internal cross-validation. Adding semi-quantitative PET/CT variables to this clinical model did not improve its predictive performance.



## SAMENVATTING

Het doel van dit proefschrift was om de huidige status en mogelijke toekomstige toepassingen van gecombineerde PET(/CT) en MRI voor abdominale oncologie patiënten te onderzoeken, zowel vanuit een visueel (kwalitatief) als kwantitatief perspectief.

**Hoofdstuk 2** geeft een overzicht van de belangrijkste trends en ontwikkelingen die werden gezien gedurende tien jaar gepubliceerde literatuur over gecombineerde PET(/CT) en MRI in abdominale oncologie. Deze bevindingen werden vervolgens vergeleken met de trends in dezelfde periode in ons eigen gespecialiseerde oncologisch centrum. Een grote impuls voor multimodaliteitsonderzoek werd gezien na de introductie van hybride PET/MRI-scanners, die de eerdere retrospectieve beeldfusie- en bedstysteem-gecombineerde PET/MRI-onderzoeken grotendeels vervingen. Er was een verschuiving van voornamelijk visuele beeldevaluatie naar meer kwantitatieve beeldanalyse en studies naar zogenaamde 'imaging biomarkers'. Nieuwe, meer tumor-specifieke PET-tracers, zoals prostaat-specifiek membraanantigeen (PSMA) voor prostaatkanker, werden geïntroduceerd en vonden hun weg naar de klinische praktijk. De enorme toename van multimodale beeldvorming weerspiegelt een groeiende vraag naar multiparametrische informatie voor besluitvorming in de klinische oncologische praktijk. Dit bleek ook uit onze institutionele data, die een vergelijkbare toename lieten zien in het multimodaliteitsgebruik van PET/CT in combinatie met MRI gedurende het laatste decennium.

In **Hoofdstuk 3** onderzochten we het effect van geïntegreerde (side-by-side) beoordeling van PET/CT en MRI door een radioloog en nucleair geneeskundige, vergeleken met de conventionele klinische benadering van gescheiden beoordeling en verslaglegging, in een cohort van 201 patiënten met verschillende vormen van kanker in het abdomen. In ongeveer een derde van de onderzochte patiënten leidde de geïntegreerde beoordeling tot tegenstrijdige bevindingen in vergelijking met de oorspronkelijke afzonderlijke verslagen, met een klinische impact in 12% van het totale onderzoekscohort. Daarnaast zagen we een trend richting een kleine relatieve toename van diagnostisch vertrouwen en een afname van het aantal niet-conclusieve bevindingen, met name voor de evaluatie van lymfeklieren, bij baarmoederhalskanker en bij het onderscheid tussen recidief en goedaardige veranderingen als gevolg van de behandeling.

In hoofdstukken 4, 5 en 6 hebben we ons gericht op gecombineerde PET/CT en MRI voor (semi-)kwantitatieve beeldanalyse om behandeluitkomsten te voorspellen in drie cohorten van patiënten met rectum-, baarmoederhals- en anuscarcinoom.

**In Hoofdstuk 4** onderzochten we de waarde van multiparametrische MRI in combinatie met FDG-PET/CT om goed reagerende rectumcarcinoompatiënten te identificeren vóór de start van neoadjuvante chemoradiotherapie. Uit het pre-therapie tumorvolume van 61 patiënten met lokaal gevorderd rectumcarcinoom extraheerden we verschillende MRI-parameters ( $T2W_{\text{volume}}$ ,  $T2W\text{-signal}_{\text{entropy}}$ ,  $DWI_{\text{volume}}$ ,  $ADC_{\text{mean}}$ ,  $ADC_{\text{entropy}}$ ) en PET-parameters ( $MTV_{42\%}$ ,  $SUV_{\text{max}}$ ,  $SUV_{\text{mean}}$ , TLG, CT-HU). We combineerden deze met patiëntkenmerken en stadiëringsvariabelen (geslacht, leeftijd, T- en N-stadium) om multiparametrische predictiemodellen te genereren voor pathologische tumorregressiegraad (TRG) na het afronden van de behandeling. Na vergelijking van verschillende combinaties van deze variabelen, had het best voorspellende model voor een goede respons op behandeling (TRG1-2) een AUC van 0,83 na interne validatie, en omvatte stadiërings- en MRI-variabelen (T-stadium,  $T2W_{\text{volume}}$  en  $T2W\text{-signal}_{\text{entropy}}$ ). PET/CT-variabelen hadden beperkte voorspellende waarde en waren niet bijdragend voor de predictiemodel.

**Hoofdstuk 5** beschrijft onze studie waarin de waarde van pre-therapie (semi-)kwantitatieve PET/CT- en MRI-variabelen, gecombineerd met het klinische FIGO-stadium, worden onderzocht als voorspellers van vroege respons op chemoradiotherapie, in een groep van 46 patiënten met lokaal gevorderde baarmoederhalscarcinoom. Vroege respons werd gedefinieerd als een vermindering van het tumorvolume tot  $<10 \text{ cm}^3$  bij tussentijdse beeldvorming na 3-4 weken chemoradiotherapie. Multivariabele analyse wees uit dat vooral het tumorvolume gemeten op baseline MRI een voorspellende variabele was voor vroege respons.  $SUV_{\text{max}}$  gemeten op PET was daarnaast een onafhankelijke voorspeller, zij het met duidelijk minder voorspellende kracht. Het predictiemodel op basis van tumorvolume en  $SUV_{\text{max}}$  resulteerde in een matige voorspellende prestatie van de AUC van 0,68 na interne validatie in deze kleine, verkennende dataset.

Hoofdstuk 6 onderzoekt de waarde van semi-kwantitatieve variabelen die zijn afgeleid van pre-therapie PET/CT, in combinatie met klinische variabelen (T- en N-stadium, leeftijd, geslacht) en high-risk HPV-status, om locoregionaal behandelingsfalen te voorspellen vóór de start van in opzet curatieve chemoradiotherapie bij patiënten met anuscarcinoom. Falen van de behandeling werd gedefinieerd als een onvolledige



respons of lokaal recidief binnen het eerste jaar na voltooiing van de behandeling. Een gecombineerd "klinisch" model met daarin mannelijk geslacht, positief N-stadium en negatieve hoog-risico HPV-status had de beste voorspellende waarde, met een AUC van 0,81 na interne validatie. Het toevoegen van semi-kwantitatieve PET/CT-variabelen aan dit klinische model verbeterde de voorspellende prestaties niet.



## LIST OF PUBLICATIONS

This thesis

A decade of multi-modality PET and MR imaging in abdominal oncology

**Lisa A Min**, Francesca Castagnoli, Wouter V Vogel, Jisk P Vellenga, Joost JM van Griethuysen, Max J Lahaye, Monique Maas, Regina GH Beets-Tan, Doenja MJ Lambregts

*Br J Radiol.* 2021 Oct 1;94(1126):20201351. doi: 10.1259/bjr.20201351.

Pre-treatment prediction of early response to chemoradiotherapy by quantitative analysis of baseline staging FDG-PET/CT and MRI in locally advanced cervical cancer.

**Min LA**, Ackermans LL, Nowee ME, Griethuysen JJV, Roberti S, Maas M, Vogel WV, Beets-Tan RG, Lambregts DM.

*Acta Radiol.* 2021 Jul;62(7):940-948. doi: 10.1177/0284185120943046.

Value of combined multiparametric MRI and FDG-PET/CT to identify well-responding rectal cancer patients before the start of neoadjuvant chemoradiation.

Schurink NW, **Min LA**, Berbee M, van Elmpt W, van Griethuysen JJM, Bakers FCH, Roberti S, van Kranen SR, Lahaye MJ, Maas M, Beets GL, Beets-Tan RGH, Lambregts DMJ.

*Eur Radiol.* 2020 May;30(5):2945-2954. doi: 10.1007/s00330-019-06638-2.

*Awarded the European Radiology ESGAR Gold Award 2020*

Integrated versus separate reading of F-18 FDG-PET/CT and MRI for abdominal malignancies - effect on staging outcomes and diagnostic confidence.

**Min LA**, Vogel WV, Lahaye MJ, Maas M, Donswijk ML, Vegt E, Kusters M, Zijlmans HJ, Józwiak K, Roberti S, Beets-Tan RGH, Lambregts DMJ.

*Eur Radiol.* 2019 Dec;29(12):6900-6910. doi: 10.1007/s00330-019-06253-1.

## Other

Studying local tumour heterogeneity on MRI and FDG-PET/CT to predict response to neoadjuvant chemoradiotherapy in rectal cancer.

Schurink NW, van Kranen SR, Berbee M, van Elmpt W, Bakers FCH, Roberti S, van Griethuysen JJM, **Min LA**, Lahaye MJ, Maas M, Beets GL, Beets-Tan RGH, Lambregts DMJ.

*Eur Radiol.* 2021 Sep;31(9):7031-7038. doi: 10.1007/s00330-021-07724-0.

Gross tumour volume delineation in anal cancer on T2-weighted and diffusion-weighted MRI - Reproducibility between radiologists and radiation oncologists and impact of reader experience level and DWI image quality.

**Min LA**, Vacher YJL, Dewit L, Donker M, Sofia C, van Triest B, Bos P, van Griethuysen JJW, Maas M, Beets-Tan RGH, Lambregts DMJ.

*Radiother Oncol.* 2020 Sep;150:81-88. doi: 10.1016/j.radonc.2020.06.012.

Multiparametric Imaging for the Locoregional Follow-up of Rectal Cancer

Doenja M. J. Lambregts, **Lisa A. Min**, Niels Schurink, Regina G. H. Beets-Tan

*Current Colorectal Cancer Reports.* 2020 Apr;16(2):19-28. doi: 10.1007/s11888-020-00450-7

Normal hematopoietic stem cells within the AML bone marrow have a distinct and higher ALDH activity level than co-existing leukemic stem cells.

Gerrit J Schuurhuis, Michael H Meel, Floris Wouters, **Lisa A Min**, Monique Terwijn, Nick A de Jonge, Angele Kelder, Alexander N Snel, Sonja Zweegman, Gert J Ossenkoppele, Linda Smit.

*PLoS One.* 2013 Nov 11;8(11):e78897. doi: 10.1371/journal.pone.0078897.



## DANKWOORD

Zoals dat geldt voor de meeste prestaties, zou ook dit proefschrift het licht niet hebben gezien zonder de betrokkenheid en hulp van heel veel anderen. Op uiteenlopende manieren, groot en ogenschijnlijk klein, hebben veel mensen een directe of indirecte bijdrage geleverd aan dit werk. Ik hoop dat al deze mensen weten hoeveel ik dat waardeer. Een aantal van hen wil ik hier in het bijzonder bedanken.

Prof. dr. Regina Beets-Tan, mijn promotor. Dank u voor het in mij gestelde vertrouwen en de kansen die u mij hiermee hebt geboden. Het was een eer om onder u promovenda te zijn en een genoegen om deel uit te maken van het u zo dierbare researchteam. Uw passie voor onderzoek, creativiteit en analytisch vermogen waren voor mij een inspiratie, die ik voortaan meedraag en zal nastreven in mijn verdere werk. Bedankt voor wat u mij hebt geleerd.

Dr. Doenja Lambregts, mijn co-promotor. Beste Doenja, wat ik hier ook zou opschrijven zou geen recht doen aan jouw immense inzet voor het onderzoek, en voor dit proefschrift in het bijzonder. Dank je wel dat je mijn co-promotor was en voor de korte lijnen waarover we konden samenwerken. Ik kon altijd bij jou terecht en jouw drive is aanstekelijk. Op die momenten dat het voorkwam, was jouw 'tough love' precies wat ik nodig had. Of samen een biertje drinken. Dank je wel voor al deze dingen.

Dr. Monique Maas en dr. Max Lahaye, niet alleen eersteklas co-auteurs maar ook inval-begeleiders en de originele Recteam-leden. Jullie hebben mij veel geleerd, mijn projecten gesteund en verbeterd, en mijn tijd als promovenda opgefleurd met jullie aanwezigheid in het Tuinhuis en ook regelmatig daarbuiten. Daarvoor wil ik jullie heel hard bedanken.

Dr. Wouter Vogel, nog een eersteklas co-auteur en eindeloos geduldige co-segmenteur. Je was betrokken bij de meeste papers in dit proefschrift, vanwege je multidisciplinaire expertise, maar zeker niet in de laatste plaats omdat het zo prettig is om met jou samen te werken. Dank je wel dat ik op jou kon rekenen.

Bedankt aan alle verdere co-auteurs voor jullie bijdragen aan onze papers: dr. Baukelien van Triest (ooit mijn stagebegeleider en de reden dat ik ook arts wilde worden), Carmelo Sofia, dr. Erik Vegt, Frans Bakers, Prof. dr. Geerard Beets, dr. Henry Zijlmans, Jisk Vellenga, dr. Katarzyna Józwiak, dr. Maaïke Berbee, Maarten Donswijk, dr. Marlies

Nowee, dr. Miranda Kusters, dr. Luc Dewit, dr. Pétur Snæbjörnsson, statistisch redder Sander Roberti, dr. Simon van Kranen, ass Prof. dr. Wouter van Elmpt.

Niels Schurink, Joost van Griethuysen, de collega's met wie ik samen heb gezocht, gerekend, gekletst, geschreven, gereisd en gelachen. Ik heb van jullie veel geleerd. Dank jullie enorm voor jullie inzet en het plezier dat we hebben gehad.

Francesca Castagnoli, thank you so much for the good times we had sorting out the literature and eating all those cookies. You are hilarious.

Alle andere (oud) Tuinhuysgenoten: Eun Kyoung (Amy) Hong, dr. Brigit Aarts, Charlotte Rijsemus, Denise van der Reijd, Femke Staal, Hedda van der Hulst, Hester Haak, dr. Ieva Kurilova, dr. Irene van Kalleveen, Jona Shkurti, Jorrita Tuurenhout, Judith Boot, Kay van der Hoogt, Kevin Groot-Lipman, Marit van der Sande, Marjaneh Taghavi, Maurits Engbersen, Melda Yeghaian, Myrte de Boer, Najim El Khababi, Nino Bogveradze, Paula Bos, Rebecca Dijkhoff, dr. Sophie Vollenbrock, dr. Stefano Trebeschi, Sylvia Drago, PD dr. med. Thi Dan Linh Nguyen-Kim, Theresa Bucho, Zuhir Bodalal, en natuurlijk de 'Nucs': dr. Daan Hellingman, dr. Daphne Huizing en dr. Judith olde Heuvel. Altijd wat, en het was geweldig.

De studenten die ik heb mogen helpen begeleiden tijdens hun wetenschappelijke stages, en die op hun beurt mij hebben geholpen daarmee: Leanne Ackermans, Younan Vacher en Christiaan de Bloeme.

Vrienden en vriendinnen: Ester Hopstaken-Krom, Josee van der Steen-Theissling, Mariska Glorie-van der Steen, Mariska Lettinga, Joukje Deinum, De Whiskeyclub: Bob Jansen, Frank Gerritse, Marianne Vos, Mathijs Kruk, Petra Caarls, Tim Jansen, Verena de Zwart.

Mijn lieve familie: papa en mama, Nanou, Johan, Jonah, Vincent, Sarah, het Erwtje, Renate, Joyce, Marcel, Naomi, Thomas en Lucas. Oma Nanou. Dank voor jullie liefde en dat jullie in mij geloven.

Mijn lieverd, Roy Sterken. Popje, dank je wel dat ik alles met jou mag delen, hoogte- en dieptepunten, waaronder ook die van deze reis. Ik kan me geen beter maatje wensen. En dan nu samen weer lekker verder aanmodderen.



## CHAPTER 8

Dank ook aan de patiënten van Het Antoni van Leeuwenhoek en Maastru, die hun medische data beschikbaar hebben gesteld, waarmee dit onderzoek kon worden uitgevoerd.



## CURRICULUM VITAE

Lisa Anna Min was born on March 8, 1987 in Limmen (N-H), the Netherlands. She graduated in 2005 from Jac. P. Thijsse College with a major in science and health. Because she was fascinated by biology, she chose to study Biomedical Science at the Vrije Universiteit Amsterdam (VU). In 2008 she acquired her bachelor's degree and continued her scientific training at the VU with the Master's programme in Oncology. She graduated *cum laude* in 2012. Meanwhile, she had started medical training in 2010 at the University of Utrecht, via the 'Selective Utrecht Medical Master' (SUMMA) programme. After obtaining her medical degree in 2014, she first worked as a resident not in training in cardiology (Maasstad hospital, Rotterdam) and geriatric medicine (Gelre hospital, Apeldoorn), before returning to the scientific community in 2016 as a PhD student in radiology, under supervision of Prof. dr. Beets-Tan and Dr. Lambregts, at Maastricht University/the Netherlands Cancer Institute. During her PhD programme, she participated in the European Radiology Review Fellowship.

In June 2020 Lisa started her residency program in radiology and nuclear medicine at Gelre hospital/University Medical Centre Utrecht.

